Sustainable Food Packaging: Food Processing Waste Fibres for Thermoformed Moulded Pulp Food Packaging

A thesis presented in partial fulfilment of the requirements for the degree of Master of Food Technology at Massey University, Manawatu, New Zealand

YiChen Huang

2025

Abstract

There is growing demand for sustainable packaging alternatives that substitute non-recyclable plastic packaging. This thesis aimed to investigate the potential of New Zealand's food industry waste fibres for manufacturing moulded pulp trays that can reduce overall plastic consumption in the food takeaway area. Two novel and promising fibres, apple pomace and corn husk, were pulped and formed into handsheets and trays to explore their potential enhancement in mechanical and barrier properties compared to conventional wood fibres.

Handsheets were produced under standard and thermo-forming conditions, and their performance was assessed. Initially, standard sheets containing mechanically pulped apple pomace, hemp seed husk, and Bleached Chemi-Thermo-Mechanical Pulp (BCTMP) fibres were tested for mechanical performance, Cobb value (water barrier), and oil penetration to screen the best formulations. Formulation containing 50% and 25% of apple pomace and 50% corn husk were selected, standard and hot-pressed sheets composed and assessed using tensile, tearing, bursting, short-span compression, Gurley, Cobb, grease resistance testing, contact angle, as well as roughness (through OCT and fringe projection) measurements.

Sheets produced with apple pomace and BCTMP exhibited promising mechanical and barrier properties, surpassing those made from BCTMP alone. Their improved performance was due to higher density and stronger fibrous bonding from the addition of shorter fibres, with better packing of fibres. When hot-pressed at 230°C for 30 seconds using pressure of 393 kPa, the sheets displayed even greater mechanical and barrier performance, owing to denser fibrous networks and lignin flow, though reduced flexibility likely due to hornification, partial components degradation, and lignin cross-link reactions. In contrast, sheets incorporating corn husks demonstrated inferior

mechanical performance due to ineffective fibre bonding, uneven fibre distribution, and material loss during formation, but exhibited slightly improved water resistance from increased hydrophobicity and surface roughness from the material.

Moulded fibre tray prototypes were also produced at pilot scale to demonstrate commercial feasibility. A commercialisation pathway was then explored, focusing on market availability, industrial feasibility, and cost analysis of necessary equipment and energy. New Zealand food contact compliance and the composition of materials that may pose potential risks were also evaluated, revealing the restriction of some chemicals and that the moulded pulp product should meet Good Manufacturing Practice (GMP) requirements.

Acknowledgements

First and foremost, I would like to express my deepest gratitude to my supervisor at Massey University, Dr Eli-Gray Stuart, for his guidance, continuous support, and encouragement throughout the course of my research and writing of this thesis.

I am also deeply grateful to my supervisors Dr Kate Parker and Dr Kelly Wade at Scion for providing me with the source of materials, access to equipment, spending most of their time to attend meetings, to review and evaluate this thesis as well as expertise and insightful feedback.

I would especially like to thank the examiners for reviewing this thesis with his expertise, advice, patience, motivation, and so beneficial in scientific discussion to this thesis.

I would also like to wish my deepest thanks to Scion and Prof. John E. Bronlund for offering me a place to conduct this research, and colleagues at Scion, Michelle Sloane, Maxine Smith, Robin Parr and Garth Weinberg, for providing training in equipment that was necessary to perform the tests for this research; Sean Taylor for pre-treating corn husk fibres for me.

I would also like to sincerely thank my girlfriend, Kun Wu, for her unwavering companionship, assistance in my apple pomace treatment work, and constant encouragement throughout the entire year of this project.

Finally, A heartfelt thanks go to my parents Jin De Huang and Li Li Shen, for their support since my bachelor study and love throughout my life. Without their support, I definitely could not make it.

Table of Contents

List of Figures

List of Tables

List of Abbreviations

ADF	Acidic Detergent Fibre
AKD	Alkyl Ketene Dimer
AP	Apple Pomace
AP-Hp	Hot pressed Apple Pomace handsheets
ASA	Alkenyl Succinic Anhydride
BCTMP	Bleached Chemi-Thermo-Mechanical Pulp
BPA	Bioresource Processing Alliance
BPP	BCTMP Pine Pulp
CLF	Cellulose Fibre
CBF	Cardboard Fibre
CD	Cross-machine Direction
CH	Corn Husk
CHF	Corn Husk Fibre
CM	Canola Meal
CTMP	Chemi-Thermo-Mechanical Pulping
EU	European Union
F	Functional additive
FCMs	Food Contact Materials
FDA	Food and Drug Administration
FQA	Fibre Quality Analyser
GMP	Good Manufacturing Practices
GRAS	Generally Recognized As Safe
GY	Glycerol
HDPE	High-Density Polyethylene
HHP	Hemp seed Husk Powder
HL	Hemp Leaves

L&W	Lorentzen & Wettre (Brand)
MD	Machine Direction
NC	Nanocellulose
NDF	Neutral Detergent Fibre
NP	Newspaper
NSSC	Neutral Sulphite Semi-Chemical
OLP	Olive Pomace
OP	Orange Peel
OSF	Olive Stone Flour
PET	Polyethylene Terephthalate
PFAS	Per- and Poly-fluoroalkyl substances
PIP	Pineapple Pulp
QM	Quantitative migration
RMP	Refiner Mechanical Pulping
RP	Recycled Paper
RBP	Rhubarb Pomace
SC	Semi-Chemical
SCT	Short-span Compression Testing
SD	Standard Deviation
TAPPI	Technical Association of the Pulp and Paper Industry
TCR	Temperature- and humidity-Controlled Room
TEA	Tensile Energy Absorption
TMP	Thermo-Mechanical pulping
WVP	Water Vapour Permeability

Chapter 1 Introduction

1.1 Background

Food packaging is a critical aspect of the modern food industry, and a factor in preserving the benefits of food processing and ensuring safe transportation during logistics to prevent physical damage (Marsh & Bugusu, 2007). It also protects food from environmental contaminants, such as dust and microorganisms, while helping to maintain the moisture and temperature conditions of food products (Han et al., 2018). Food packaging also serves as a medium for communication and a quality indicator for the food. There is an increasing focus on sustainability and convenience, driven by increasing global awareness and consumer demand of environmentally responsible choice (Vasile & Baican, 2021).

There are various forms of food packaging materials, including plastic, glass, cardboard, and others. Among these, packaging made from compostable materials is often preferred over non-degradable plastics for single-use purposes, like food packaging, where food residue often contaminates the packaging, especially when reuse options are unavailable and recyclability is limited (Versino et al., 2023). With the growing demand for sustainable and eco-friendly products, innovation in food packaging has been spurred across the food industry. Sustainable food packaging focuses on designing and using materials that reduce environmental impact throughout their entire lifecycle, while ensuring food safety and quality (Branca et al., 2024; Versino et al., 2023). According to a report by "Precedence Research," the market for sustainable food packaging is projected to grow significantly, with its value expected to double over the next decade, from US$ 225.1 billion to US$ 505.41 billion, as shown in **Figure 1**, and the Asia-Pacific region is expected to account for the largest share of this market (PrecedenceResearch, 2024). The report states that this growth will be driven by

innovative food packaging technologies, such as moulded fibre packaging and active packaging with optimal use of renewable and readily available natural materials.

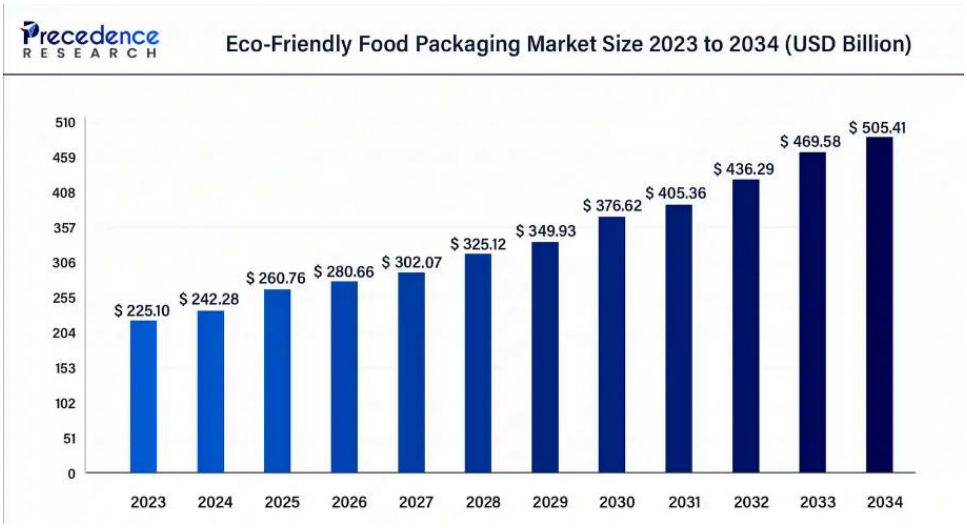

Figure 1. The market size estimation of sustainable food packaging in the next decade, from 2023 to 2034. Reported by Precedence Research in 2024.

The global takeaway food container market is substantial, valued at US$ 104.8 billion in 2023, with projections to reach US$ 150 billion over the next decade, according to a report by "Future Market Insights Inc." (FMI, 2023). Conventional takeaway containers are typically made for single use with non-recyclable plastics or styrofoam due to their low cost, high production efficiency, and great performance, such as strong tensile strength and resistance to contamination from the external environment. However, these containers represent a major source of plastic waste, especially given the rising demand for single-use takeaway containers since the COVID-19 pandemic in the food service industry (Zhuo et al., 2023). Thus, there is a pressing need to develop takeaway containers using degradable and sustainable materials.

Moulded fibre is a renewable and sustainable material that can enable a reduction in single-use plastics in many packaging applications. It can be produced from wood fibres or from other fibrous agricultural by-products and recycled fibre (Didone et al., 2017). However, due to potential contamination, this material may have limited use in food

contact applications. The global moulded fibre packaging market is expected to grow at a CAGR (compound annual growth rate) of 5.2 % from 2024 to 2030, with an estimated value of US$ 8.23 billion in 2023 (Grand View Research, 2023). Contributing to this growth is the increased interest in using moulded fibre for food packaging. Moulded fibre packaging is widely used in applications like egg trays, but its use has now expanded to other forms of food packaging, including takeaway containers, fruit and vegetable packaging, drink packaging, and so on, driven by the need for alternatives to plastic packaging.

New Zealand is known for its large food sector, and the residues produced during secondary processing of produce represents not only an environmental burden but also a missed opportunity for resource recovery. A report by "WasteMINZ" integrated food waste data from various sources, including the BPA (Bioresource Processing Alliance), personal publications, and government documents, proposed that the NZ food industry generates approximately 40,800 tonnes of organic waste annually. Of this, 28% (11,424 tonnes) ends up in landfills and 47% of the waste is collected for feedstock, which is a significant portion of which could be repurposed for food packaging materials (WasteMINZ, 2018). Meanwhile, fibres make up 60% of the total organic waste from the food industry, with 26% of these fibres being sent to landfills (Macdonald, 2022). Therefore, it is worth exploring whether these food residues materials could be utilised in moulded pulp food packaging. While several studies have investigated different biodegradable materials derived from food waste as packaging material, research on integrating New Zealand-specific waste streams into functional food container designs remains limited, and the potential for commercialisation and the comprehensive practical functions of such products have not yet been fully explored.

1.2 Objectives

The aim of this thesis focuses on discovering one or two locally available food residues from the New Zealand food manufacturing sector that can be effectively blended with Bleached Chemi-Thermo-Mechanical Pulp (BCTMP) to produce moulded fibre products. These products were characterised in terms of the mechanical and barrier properties to assess their potential as a good packaging solution. The goal is to develop a New Zealand fibre based takeaway food tray that meets both technical and regulatory requirements while being suitable for commercialisation. This would offer businesses a sustainable and cost-effective packaging option. The main objectives of this study are as follows:

Laboratory-scale prototyping:

- To assess the availability of local food processing residues in New Zealand and evaluate their potential for producing pulp to make handsheets with improved mechanical and barrier properties.
- To create prototype handsheets using the selected food processing residues blended with BCTMP, or varying blend ratios and analyse their mechanical and barrier properties to identify one or two promising formulations. The handsheet used as the prototype for the moulded fibre tray should enable the tray to be utilised for a minimum of four hours.
- Produce standard handsheets using the optimal formulations at Scion, applying both standard pressing and hot-pressing techniques.
- Compare the mechanical and barrier properties of handsheets made from BCTMP and BCTMP-food processing residue blends, including the hot-pressed ones.
- Mould the takeaway trays for the blend giving best performance using Scion's pilot scale moulded fibre thermo-former and assess their performance.

Commercialisation considerations:

- To design a process flow for an industrial plant.
- To estimate the costs of equipment and energy needed for the mass production and compare to the incumbent products.
- To assess the food contact compliance standards of different countries for moulded fibre materials.

Chapter 2 Literature Review

2.1 Introduction

Food packaging plays an essential role in preserving the added value of products by minimising waste and loss in the supply chain. The worldwide demand for packaged food is increasing by 5% each year, with 40% of this food now being packaged in plastics, much of which is difficult to recycle (Kan & Miller, 2022). This raises challenges for New Zealand as noticed by the report by Office of the Prime Minister's Chief Science Advisor (2023), which outlined that 150,000 tonnes of imported plastics are utilised in the packaging field and 40% of these imported plastics used for food packaging. Takeaway food packaging significantly contributes to plastic and this has increased since the outbreak of COVID-19 pandemic (Zhuo et al., 2023). New Zealand's capacity to manage these non-degradable plastics has been exceeded, leading to the export of 90% of collected plastic waste overseas for processing (Ministry of Environment, 2020). Therefore, the importance of developing sustainable packaging is increasingly raised in environmental discussions. In response to these circumstances, New Zealand has implemented a variety of initiatives such as bans on single-use and hard-to-recycle plastic due to their environmental and health risks since 2020. Moulded fibre packaging is becoming popular due to its recyclability, sustainability, and biodegradability (Zhang et al., 2022). A forecast by Preceden Research in the "Moulded Pulp" report in 2025 anticipates that the global market for moulded pulp packaging is expected to grow from US$13.44 billion in the next decade by 2034 (Preceden Research, 2025).

New Zealand has a lot of food/fibre processing waste from its large food/forestry sector which is underutilised. This presents a significant opportunity where it could be used as a fibre source or additive for moulded fibre products and potentially create packaging with superior mechanical and barrier properties. Therefore, identifying the available NZ food processing fibre waste residues, and obtaining a thorough understanding of the properties of those fibres in the term of mechanic and barrier properties for moulded fibre applications is a major focus of this literature review. Enhancement additives and suitable pulping methods will also be investigated.

2.1.1 Background of the previous research done at Scion

A previous study undertaken at Scion (New Zealand Forest Research Institute Ltd) explored alternative New Zealand-based fibre materials as substitutes for conventional wood-based fibres in moulded fibre packaging (Vries, 2024). The project used three waste fibre sources: grape marc, the byproduct from wine production; bark fibre, derived from log processing; and coleslaw, consisting of 85% of cabbage, 15% of carrot and 5% chopped onion (selected to represent market garden waste), blended with conventional wood pulps with the aim of improving the moulded fibre properties. To methodically evaluate the impact of these blends, 0%, 10% and 50% by weight of the fibre sources were blended with BCTMP to create handsheets following T205 standard sp-02 (Vries, 2024). Barrier properties arising from beeswax and PHO (poly-hydroxy-octanate) coatings were also assessed compared to uncoated samples.

The results, as shown in **Figure 2**, indicated a slight increase in the density of coleslaw handsheets and a significant decrease for handsheets containing grape marc and bark from 10% to 50%. Gurley test results, which tested the air resistance, showed a similar trend with the density, which was due to the bonding quality and fibrous structure between waste fibres and BCTMP. Mechanical indexes of the coleslaw blend handsheets had a slight reduction from 100% BCTMP sheets but were still stronger than the other two materials, as shown in **Figure 3**.

a.

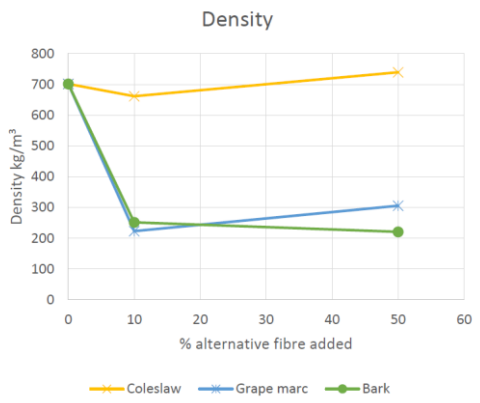

b.

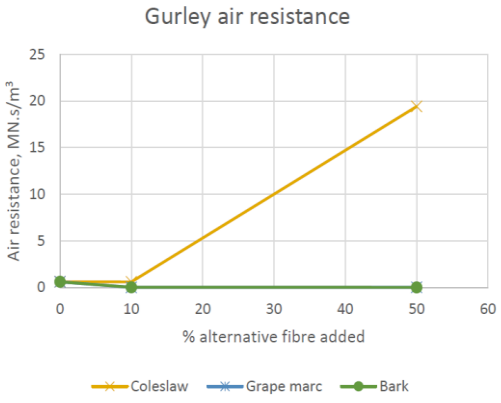

Figure 2. (a). Density trend of the handsheets made by BCTMP with coleslaw, grape marc and bark. (b). Air resistance trend of those handsheets. Referred to Vries (2024).

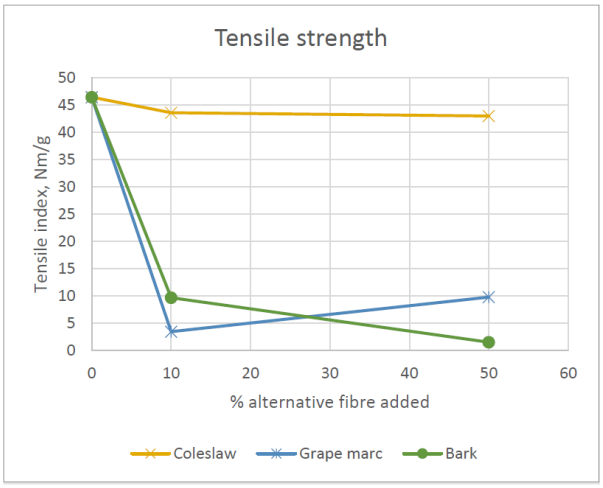

Figure 3. Tensile strength trend of the handsheets made by BCTMP with coleslaw, grape marc and bark, corrected for density. Referred to Vries (2024)

As presented in **Figure 4**, barrier testing indicated that handsheets with 10% coleslaw exhibited the best water resistance for the uncoated samples, and those with 50% coleslaw demonstrated superior grease resistance, which aligns with the increase in density. Application of either coating significantly bolstered barrier performance, with beeswax achieving nearly zero water absorption (g/m^2) and PHO providing remarkable grease resistance particularly for the coleslaw handsheets, notably extending grease show-through time to longer than five hours. Overall, those evaluations indicated that a mixture of coleslaw and BCTMP could yield the most favourable outcomes, but more blend ratios were recommended to see a comprehensive change in the properties.

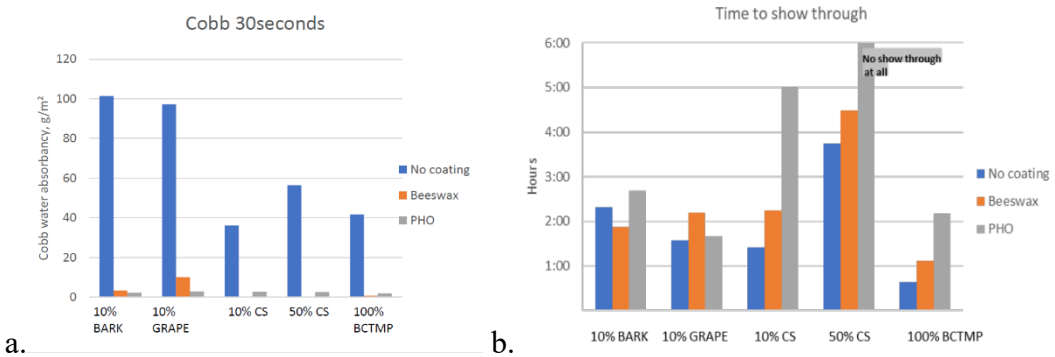

a. b.

Figure 4. Comparison of (a). Water resistance and (b). grease resistance of handsheets made by BCTMP with coleslaw, grape marc and bark, referred to Vries (2024). Note: CS – Coleslaw, PHO – Polyhydroxy Octanoate, BCTMP - Bleached Chemi-Thermo Mechanical Pulp.

2.1.2 Problem definition

The escalating demand for sustainable packaging solutions highlights a critical gap in the utilisation of food processing fibre residues for moulded fibre packaging for takeaway containers within New Zealand. This literature review seeks to discover one or more New Zealand food processing fibre residues, in additional to the previously studied coleslaw, that could be compatibly blended with conventional wood pulp (BCTMP in this study) to produce a handsheet with enhanced mechanical and barrier properties at a standard compared to the those made of wood fibres only, where it can be effectively utilised for at least four hours. This is required to manipulate the mechanical and barrier properties in the further experimental stage.

2.1.3 Objectives of the literature review

- Understand the fibre composition and structure of various food processing waste streams and how these are linked to the water/oil resistance and mechanical strength.
- Understand the pulping/papermaking processes.
- Understand the moulded fibre production processes.
- Explore the available industrial waste fibres within NZ that could be converted to moulded fibre products.
- Review the enhancer additives that could be added to improve the mechanical and barrier properties of moulded fibre products.

2.2 Fibre

The broad category of fibres can be divided into natural and synthetic fibres. Natural fibres are commonly categorised by their origins, like plant, animal or mineral, which differ by their compositions as cellulose-based, protein-based and asbestos mineral-based fibres, respectively (Pickering et al., 2016). Synthetic fibres are often plastic for reinforcement, categorised into polypropylene, polyester, polyethylene, glass and nylon fibres (Hejazi et al., 2012). This project focused on natural plant fibres derived from the food processing residue streams within New Zealand.

2.2.1 Fibre constituents

Plant fibres represent complex organic matrices comprising three main components: cellulose, hemicellulose, and lignin, as well as a small percentage of other extractable compounds like wax, pectin, lipid, protein and ash (Jones et al., 2017).

2.2.1.1 Cellulose

Cellulose is a natural organic compound and a type of polysaccharide made up of linear sequences containing hundreds to thousands of β(1-4) linked D-glucose molecules (See **Figure 5**) (Jones et al., 2017).

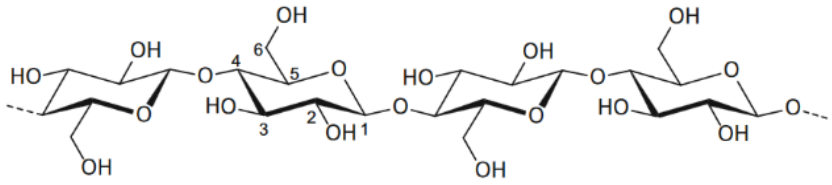

Figure 5. Representation of single cellulose molecule, refer to (Heinze, 2016).

Hydrogen bonding and crystallinity

Hydrogen bonding is important for forming the microfibril from cellulose chains (See **Figure 6** (a)). Those hydrogen bonds are formed by the hydroxyl groups (OH^-) in the glucose monomer units that makes cellulose hydrophilic, which influence the moisture absorption of fibres. However, the intra- and intermolecular hydrogen bonds of cellulose connect those single molecules in series and parallelly and limits the accessibility for solvent molecules, and hence its solubility. It also enables crystallinity, (Chen et al., 2015; Heinze, 2016). Cellulose chains are connected in parallel to form the microfibrils and those microfibrils aggregate and intertwine to form macroscopic fibres as shown in **Figure 6** (b), and result in higher crystallinity which leads to more ordered molecular chains and enhanced tensile strength, stiffness and hardness of the fibre (Marrot et al., 2013).

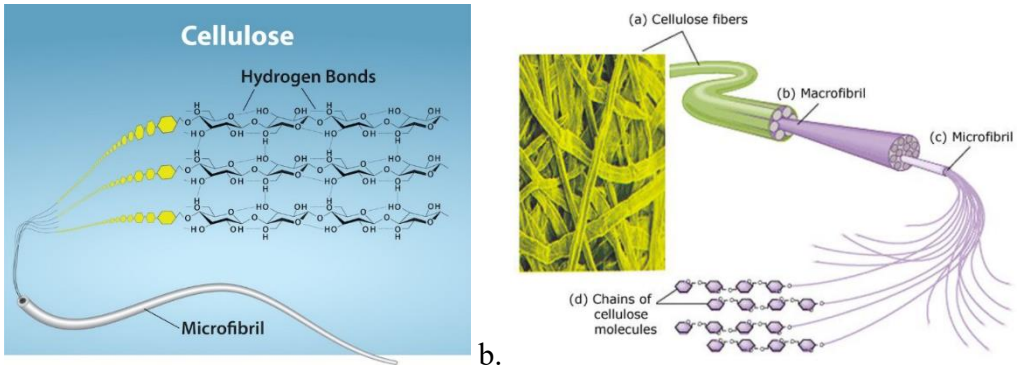

a. b.

Figure 6. (a) The inter and intra hydrogen bonds connect the cellulose molecules together to form the microfibril from Chemistry (2024), (b) Formation of fibre from molecular chains to cellulose fibres from Kuokkanen et al. (2018).

Microfibrils

The plant secondary cell wall is made of three layers (S1 to S3), as illustrated in **Figure 7**, with the highly crystalline cellulose fibrils formed on the S2 sublayer. The crystallinity enhances the stiffness, strength and thermal stability of fibres, but reduce their flexibility (Marrot et al., 2013).

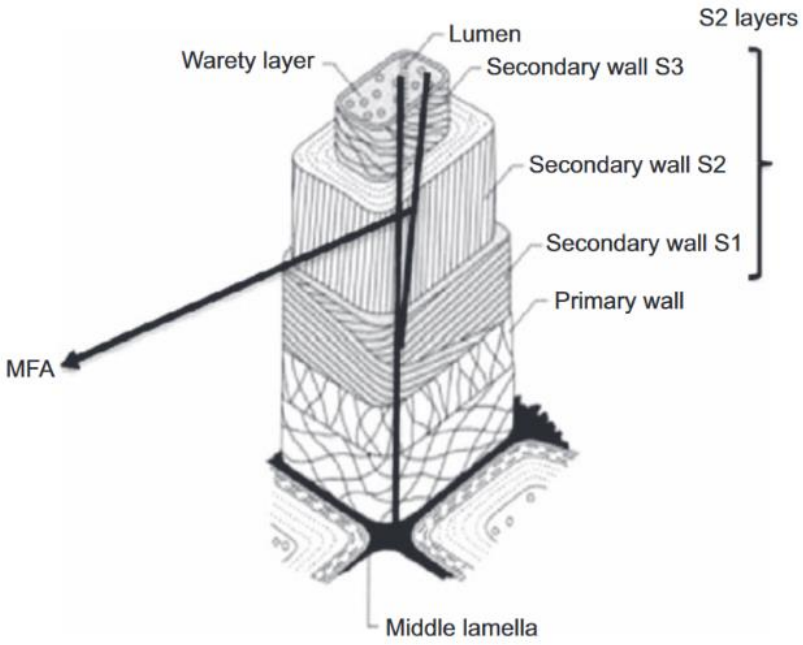

Figure 7. Schematic diagram of cell wall layers and MFA, from Petroudy (2017).

Those fibril groups together to create microfibrils and the orientation of microfibrils, which is known as the microfibril angle (MFA), determines the tensile strength of the

fibre (Heinze, 2016). MFA has negative correlation with the stiffness and tensile strength of fibres, with larger MFA could decrease the stiffness but improve the flexibility of the wood fibres (Petroudy, 2017). Hence, MFA and crystallinity in a nature plant fibre could be one criterion to evaluate its mechanical strength and moisture absorption.

2.2.1.2 Hemicellulose

Hemicelluloses is an amorphous and heterogeneously branched polymer composed of: xylans, mannans, xyloglucans and mixed-linkage β-glucans (See **Figure 8**), where xylan exists in the plant secondary cell wall; xyloglucan is a diverse polysaccharide in the primary cell wall; mannans is involved in the maintenance of cell wall storage and structure; mixed-linkage β-glucans is specifically in cell walls of grasses (Qaseem et al., 2021). Hemicellulose together with lignin constitutes the matrix for the cellulose microfibrils, as illustrated in **Figure 9**) (Sadrmanesh & Chen, 2019).

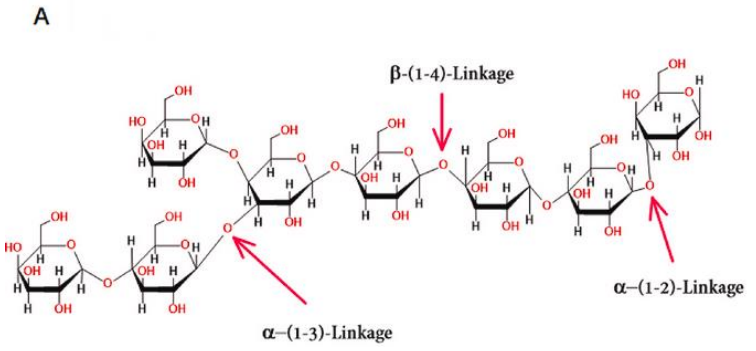

a.

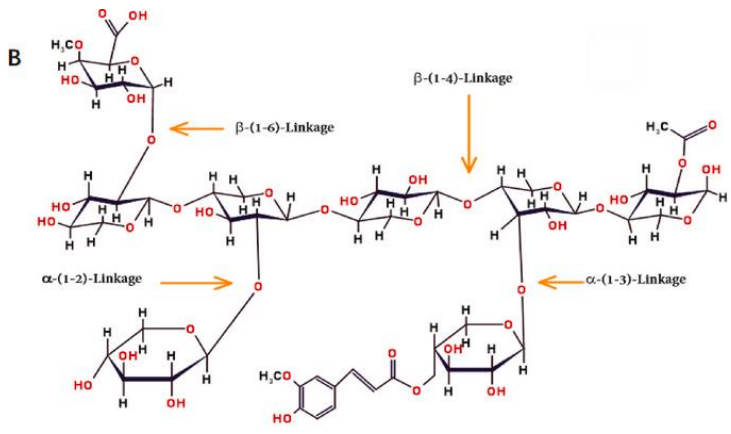

b.

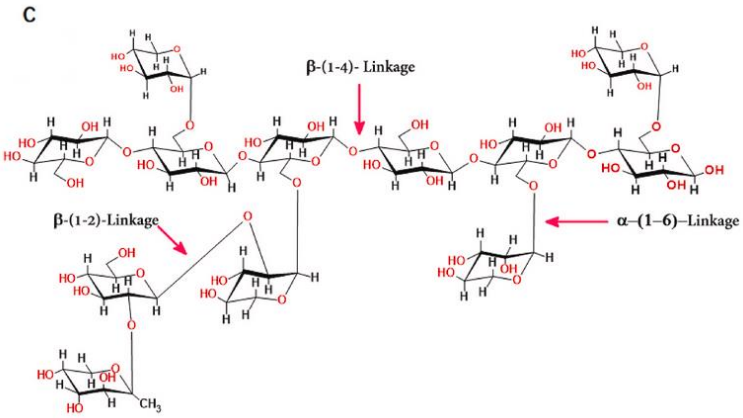

c.

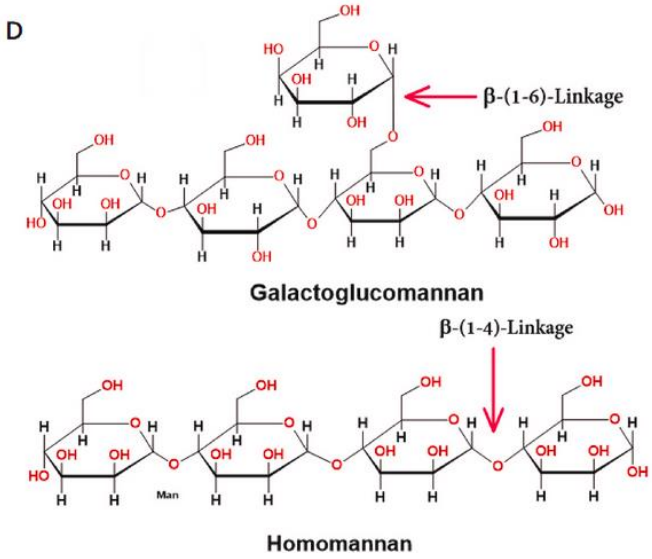

d.

Figure 8. Structure of four classes of hemicellulose: (a). mixed linkage glucans, (b). xylan, (c). xyloglucan, (d). mannans from Qaseem et al. (2021).

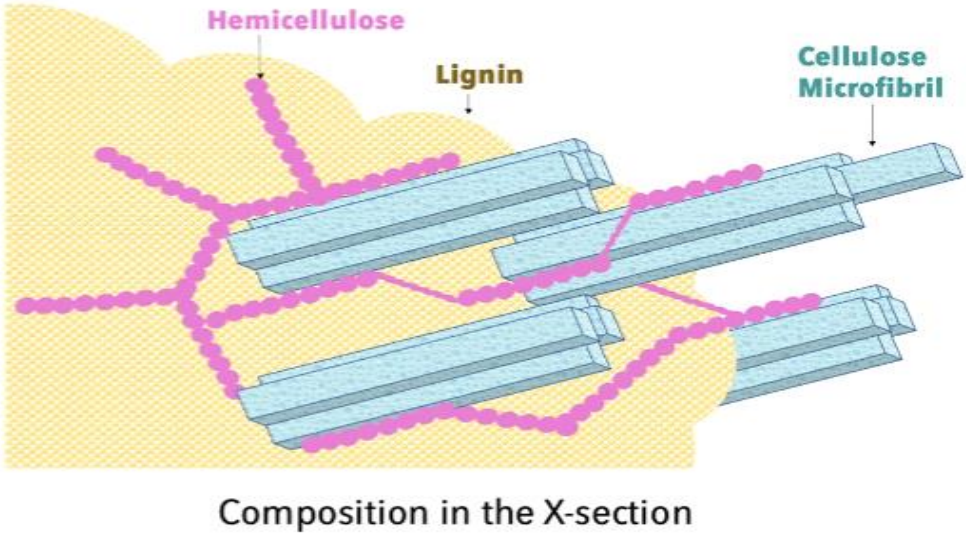

Figure 9. Matrix of microfibril, from Shuvo (2020).

Hemicellulose exhibits a low degree of polymerisation (DP) between 50 and 200, which makes it amorphous and readily hydrolysable, as noted by Yang et al. (2019), indicating its hydrophilic and low mechanical strength characteristic. Its amorphous structure does not provide stiffness or strength to fibre, as Kabir et al. (2021)'s research on impact of hemicellulose on the mechanical strength suggests that partially removal of hemicellulose can improve strength properties such as compressive and flexural strength. Additionally, hemicellulose is also recognised for its low oxygen permeability and high aroma permeability (Qaseem et al., 2021).

2.2.1.3 Lignin

Lignin is a complex and amorphous polymer composed of phenyl-propane units, distinct for its three-dimensional structure that makes it resistant to hydrolysis (Jones et al., 2017), and its predominantly hydrophobic nature. According to Yang et al. (2019), the hydrophobic lignin could act as a coupling agent filling in the gaps that exist in the cellulose-hemicellulose network to improve the water and oil barrier properties of paperboards. In addition, the presence of lignin provides rigidity to the fibres, thereby improving the stiffness of the cellulose-hemicellulose network (Jones et al., 2017; Yang et al., 2019).

2.2.1.4 Other components

Pectin

Pectin is a compound found in bast fibres and fruits that contributes to their flexibility (Komuraiah et al., 2014). Structurally, pectin is composed of galacturonic acid units, which are highly polar due to the presence of carboxyl groups (-COOH), and multiple hydroxyl groups (-OH) along the backbone of the polymer, making pectin a soluble fibre with high water-holding capacity, as shown in **Figure 10**. Therefore, high pectin content could lead to high solubility and hydrophilicity, with lowering water barrier properties. Nevertheless, its hydrophilic and gelatinous nature makes it an effective repellent of non-polar substances like oil, resulting in a large contact angle of oil droplets on the paper surface.

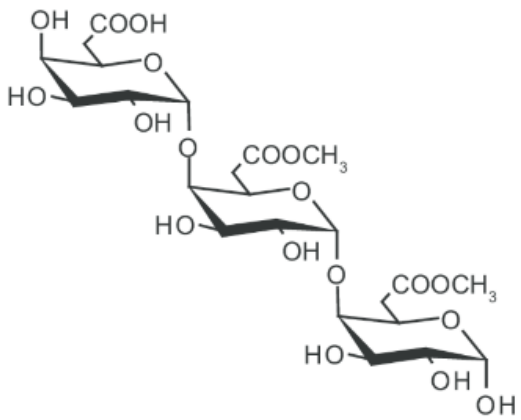

Figure 10. Structure of pectin, showing the carboxyl groups (-COOH) and multiple hydroxyl groups (-OH).

Wax

Waxes are esters of long-chain fatty alcohols made up of extensive non-polar hydrocarbon chains that do not allow water molecules to adhere (Jahangiri et al., 2024). Its hydrophobicity was demonstrated by Wang et al. (2021), who achieved the superhydrophobic surface of filter paper with coatings incorporating with waxes. Wax particles also feature low surface energy and high surface roughness, which means a waxy fibre creates conditions unfavourable for water molecules to attach or spread across.

Protein

Protein is another critical component in some fibre that significantly influence the characteristics. Cheng et al. (2017) used cottonseed protein as an additive on paper to improve the mechanical properties, showing that adding 11% cottonseed increased the paper's dry and wet strength by 33% and 16%, respectively, and caused slight improvement to the tensile modulus and maximum tensile strength. They found that the interaction between the cationic amino acid and carboxylate groups could promote the fibre bonding to enhance those properties (Cheng et al., 2016; Cheng et al., 2017).

Additionally, protein-rich fibres can improve the smoothness of the paper, which has demonstrated by Han and Krochta (2001), because proteins can modify the fibre's surface characteristics. In the term of water and oil resistance, protein's hydrophilic nature could provide enhanced oil-resistance but inferior water barrier, evidenced by Han and Krochta (2001) who showed a whey-protein-isolate coating resulted in excellent oil resistance from the decreased absorption rate.

Ash

Ash makes up a small portion of fibre composition, which comprises of various inorganic compounds. As mentioned in Gouw et al. (2017), a high ash percentage in fibres can degrade the mechanical properties of products made of them. This degradation may occur because the impurities disrupt the inter-fibre bonding and create large voids that increase the porosity and reduce the density, which can adversely affect mechanical and barrier properties.

2.3 Natural Plant Fibre Categories

2.3.1 Hard and Soft Wood fibres

Wood-based fibres for paper making originate from the lignin-rich trunks and branches of trees, which contain more lignin than fibres derived from non-wood sources (Jones et al., 2017). They are typically classified into hardwood and softwood fibre categories based on the sources, sizes and physiochemical properties.

Hardwood fibres are sourced from angiosperm trees with shorter fibre length between 0.9 to 1.5 mm. In contrast, softwood fibres come from coniferous gymnosperm trees, and have typically longer fibre length of between 3 and 3.6 mm (Jones et al., 2017). Due to their shorter length, hardwood fibres tend to have lower flocculation tendency (Levlin, 1980), resulting a more uniform distribution and smoother paper. On the other hand, the longer softwood fibres tend to entangle well in the pulp to provide stronger tearing strength, higher bulk, and more air permeable paper due to the larger voids.

Hardwood fibres also have a relatively thicker cell wall, for example, Kiaei and Samariha (2011) measured the cell wall thickness of five important hardwood fibres ranged between 4 - 7 μm, which contributes to higher stiffness and collapse resistance in paper compared to most softwood fibres with 2 - 5 μm (Levlin, 1980). According to Jajcinovic et al. (2016), hardwood fibres can be used as a constitute of printing and writing paper blends to achieve enhanced smoothness, bulk and opacity, while softwood fibres are still the mainstream materials for paper manufacturing.

2.3.2 Non wood fibres

Non-wood plant materials commonly have longer fibres, which can be further divided into seed hair, bast fibres, leaf fibres and grass/crane fibres (Jones et al., 2017; Petroudy, 2017).

2.3.2.1 Bast fibres

Bast fibres are defined as those obtained from the outer cell layer (phloem) of the stems of various plant., including hemp, flax, kenaf, jute, and ramie (Jones et al., 2017; Sadrmanesh & Chen, 2019). According to Sadrmanesh and Chen (2019), the stem is divided into three main parts: the protective bark, fibre bundles and the inner core, and single fibres are grouped into bundles held together by pectin-rich middle lamella (See **Figure 11** (a), (b)) Each fibre comprises a primary wall and a much thicker secondary wall with three layers as forementioned, as shown in **Figure 11** (c). Their lignin content is as low as 4 – 6% for flax and hemp (Jones et al., 2017; Sadrmanesh & Chen, 2019).

The crystallinity of bast fibre is 80 – 90%, which is higher than that of wood fibres at 50 – 70%, indicating a stiffer fibre.

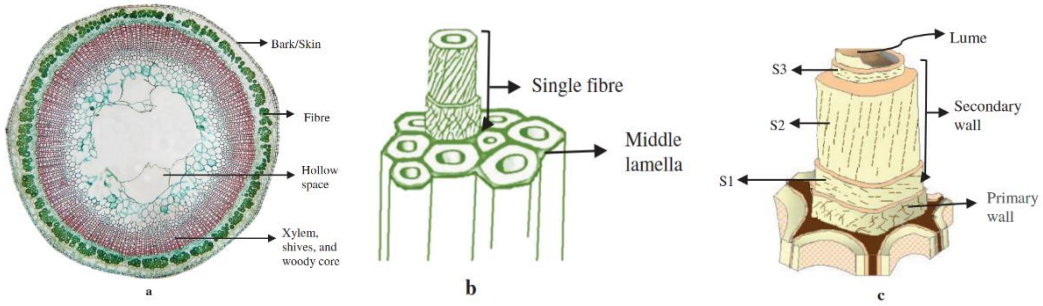

Figure 11. Structure of (a) bast plant stem, (b) fibre bundle, (c) single fibre.

2.3.2.2 Leaf fibres

Leaf fibre is derived from the leaves of various plants by scraping away the nonfibrous material, and the fibre produced is often coarser than other fibres (Jones et al., 2017). Leaf fibres are generally stiffer and coarser than other natural plant fibres because of its high cellulose content between 70 – 80% and relatively high lignin content ranged 8 – 14% (Sfiligoj Smole et al., 2013). Their properties of the fibres vary over the location on the leaf. The lower grade fibre can be processed by the paper industry, while the rest is used for making ropes, baler and some handicraft goods (Sfiligoj Smole et al., 2013).

2.3.2.3 Cane and Grass fibres

Cane and grass fibres are typically extracted from the vascular bundles of various grass stalks. The typical examples of cane fibres include bagasse and bamboo, while examples of grass fibres come from forage crops. Cane fibres are rich in lignin, which gives them superior mechanical properties. Lokantara et al. (2020) tested the properties of a large range of grass types, revealed that grass fibres contain 43.2 – 80% of cellulose, 10 – 33.7% hemicellulose, and lignin content ranged between 3.44 and 21.63%. Among them, Belulang grass exhibited the lowest Young's modulus and elongation, at 0.97 GPa and 0.98%, respectively. In contrast, broom grass and corn husks displayed the highest

Young's modulus and elongation at 18.28 GPa and 21.08%, respectively. Sisal has the beast tensile strength at 640 MPa.

2.3.2.4 Seed hair fibres

Seed fibres are the most common non-wood fibre, with cotton is a typical example. They have higher cellulose content (85% - 91%) that contributes to strength and durability, and are normally applied on textile fields (Jones et al., 2017; Petroudy, 2017). Fruit fibres are from the outer coverings or husks of fruits, with coconut coir as a well-known example. These fibres are generally coarser and more robust than seed fibres, providing greater durability and resistance to rot. However, the high pectin content in some tropical or citrus fruit fibres can negatively impact the water barrier, thus limiting their use on paper industry application. Some fruit fibres contain a certain percentage of waxy or lipid substances, which can improve their barrier properties.

2.4 Pulping and Moulding

2.4.1 Pulping process

Pulping is the process, where fibrous raw materials are manufactured into pulp, that serves as the base material for making paper products. Various pulping methods involve the use of chemical, mechanical and biological methods to rupture bonds of fibrous materials and separate the cellulose fibres from hemicellulose and lignin (Mboowa, 2024).

2.4.1.1 Chemical pulping

Chemical pulping is used for the production of fibre for high-quality papers and packaging. Chemicals are added to degrade and remove lignin and hemicellulose through reactions at a high temperature (130 – 170°C) (Sixta et al., 2006), leaving intact cellulose fibres to ensure the flexibility and strength of paper products. The downside of the chemical pulping process is the 40 – 50% lower yields than mechanical pulping

(Mboowa, 2024). Kraft and sulphite pulping processes comprised around 95% of the world's chemical pulp (Sixta et al., 2006).

Kraft pulping

The Kraft process is economically viable due to the ability in recovery of cooking chemicals (Laftah & Wan Abdul Rahman, 2016), while fully burning the waste (lignin, hemicellulose, etc.) to producing supplementary energy through recovery boiler (Mboowa, 2024). Kraft pulping involves heating the fibrous materials in a sodium hydroxide (NaOH) - sodium sulphide (Na_2S) solution, at 155 – 180°C for 1 – 2 hours under 800 kPa steam pressure to effectively breaks down lignin into hydroxyl (OH^-) and hydrosulphide (SH^-) ions (phenolic compounds) and partially degrades carbohydrates like hemicelluloses, and also removing other extractables (Gierer, 1980; Mboowa, 2024). The Kraft pulp are stronger than sulphite pulp, and its paper products have superior tearing strength due to the removal of lignin, which inhibits inter-fibre bonding (Laftah & Wan Abdul Rahman, 2016; Mboowa, 2024).

Sulphite pulping

Sulphite pulping is a process that cooks wood chips at high temperatures using a cooking liquor composed of sulphurous acid and its salts, such as ammonium bisulphite (Mboowa, 2024). This method is particularly suitable for wood species with low extractive content, as it produces pulp with higher extractive levels compared to Kraft pulps (Mboowa, 2024; Sitholé et al., 2010). Sulphite pulping produces brighter pulp that is easier to bleach and achieves high yields, although resulting in weaker mechanical properties compared to Kraft pulps (Bajpai, 2015). It can be used across the entire pH spectrum, which categorised into acid sulphite, bisulphite, and alkaline sulphite pulping processes (Bajpai, 2015; Mboowa, 2024).

Acidic sulphite pulping uses liquor at a pH of 1.5 – 2.0, with cooking temperatures of 125 – 145°C over 7 hours, while bisulphite pulping uses liquor at a pH of 3 – 5, with temperatures of 160–180°C for 3 hours (Biermann, 1996). Alkaline sulphite pulping utilises mixture of sodium hydroxide and sodium sulphite at temperatures of 160 –

180°C and requires longer cooking times than bisulphite pulping for 3 – 5 hours (Mboowa, 2024). Sulphite pulping is known for producing brighter pulp that is easier to bleach and achieves high yields, although it results in weaker mechanical properties compared to Kraft pulps (Bajpai, 2015).

2.4.1.2 Semi-chemical pulping

Semi-chemical (SC) pulping is a two-stage pulping process that involves both chemical and mechanical pulping processes, using the chemicals to soften and remove some portions of hemicellulose and lignin, before being exposed to mechanical refining. The yield of SC pulping is around 75%, with excellent stiffness. There are three types of SC pulping methods:

Neutral Sulphite Semi-Chemical (NSSC)

The Neutral Sulphite Semi-Chemical (NSSC) process is a three-stage method where fibres are impregnated with a sodium sulphite cooking liquor, cooked at 160 – 190 °C, and then defibrated using disk refining. Sodium sulphite is buffered with sodium carbonate, sodium hydroxide, sodium bicarbonate, or sodium bisulphite to make the cooking liquor with controlled pH, aiding in lignin removal and fibre separation (Mboowa, 2024). This process yields pulp with some residual lignin, but still makes the paper higher strength than mechanically pulped paper, as chemical pulping stage removes a portion of the lignin (Mboowa, 2024).

Ahmadi et al. (2010) investigated the application of NSSC pulping for rapeseed residues, that it was NSSC pulped using a cooking liquor made from a 3:1 sodium sulphite-sodium carbonate solution, and a pulping temperature of 175°C. The amount of active alkali (NaOH) and the duration of the pulping process was varied. The outcomes indicated that the yield increased with a lower percentage of alkali and longer pulping times, due to an increase in residual lignin, which negatively affected the paper's tear, tensile, and burst indexes, and breaking length, as displayed in **Table 1**.

Table 1. Comparison of rapeseed NSSC pulps' yield, kappa number, mechanical properties and brightness. Referred to Ahmadi et al. (2010). The Kappa number reflects the amount of lignin in pulp, with larger values meaning more lignin content.

Trail code	Active alkali (%)	Pulping time	Total yield (%)	Kappa No.	Caliper (μm)	Tear index ($mN.m^2g^{-1}$)	Tensile index ($N.mg^{-1}$)	Breaking length (km)	Burst index ($kPa.m^2g^{-1}$)	Brightness (%)	Opacity (%)
A_1	8	20	72	66	205	6^{a}	35.6^{a*}	3.63	1.7^{a}	41.2^{a}	97.2^{ab}
A_2	10		71.5	65	200	6.2^{ab}	38.2^{b}	3.89	1.75^{a}	39.1^{a}	98.2^{c}
A_3	12		69	64.5	195	6.4^{bc}	39.2^{b}	3.99	1.87^{ab}	40.2^{a}	97.6^{bc}
A_4	14		68.5	63.5	185	6.6^{cd}	42^{c}	4.28	2.03^{b}	42.3^{a}	96.6^{a}
A_5	16		67	56.5	180	6.9^{d}	44^{d}	4.48	2.04^{b}	43^{a}	97^{ab}
B	12	40	63.5	50	140	7.4	57.8	5.89	2.46	22.6	99.2
C		60	58.7	45	130	7.5	66.5	6.78	2.57	21	99.9

Rudi et al. (2016) and Rudi and Resalati (2015)(n.d.) also conducted experiments to demonstrate the feasibility of NSSC to process waste sunflower stalk fibres using the cooking liquor composed of a 4:1 ratio of sodium sulphite to sodium carbonate and 175 ℃ pulping temperature, while employing a 200 micron mesh as screening standard. They varied the resolution for refining from 2000 – 6000 rpm (Rudi et al., 2016) and 150 – 500 PFI(Papirindustriens Forskningsinstitut) – revolution (Rudi & Resalati, 2015), discovered that the stalk fibres were sensitive to refining speed, resulting in lower freeness. They observed that handsheets made with a greater percentage of low freeness, indicating fine particle, pulps exhibited increased tensile index and stiffness, see **Table 2**, because the low freeness is associated with small particles and dense structure, which results better mechanical properties.

Table 2. Mechanical properties of handsheets. A means the wood pulp, B means the sunflower stalk pulp with low freeness, from Rudi and Resalati (2015). B pulp had smaller particles resulting in denser specimens and better mechanical properties.

Type of pulp	Tensile index (N.m/g)	Breaking length (Km)	Stiffness (kN/m)	CMT (N)	RCT (kN/m)	Tear index ($mN.m^2/g$)	Burst index ($kPa.m^2/g$)
A	35.11±0.61	3.57±0.04	483±17	186±5.5	1.38±0.09	5.01±0.07	2.13±0.02
B	41.29±2.95	4.20±0.30	685±61	263±10.4	1.94±0.01	6.06±0.05	2.01±0.02
90%A+10%B	35.14±0.49	3.77±0.04	511±12	194±10.1	1.46±0.05	5.80±0.11	2.10±0.06
80%A+20%B	37.02±1.20	3.77±0.02	563±14	196±6.1	1.86±0.07	5.52±0.10	1.98±0.08
70%A+30%B	37.41±4.19	3.81±0.04	567±30	211±8.3	1.82±0.07	5.08±0.08	1.98±0.08

High-yield chemical pulping

High-yield chemical pulping aims to increase pulp yield through modified sulphite and Kraft processes by incorporating a refining step, cooking at lower temperature of 120

– 130°C with low acidic liquors, and refining on a low energy disk refiner (Mboowa, 2024). This retains more lignin that makes the pulps with lower brightness, and also results in a lower strength pulp and a weaker paper (Liu et al., 2016).

Cold soda pulping

The cold soda pulping process treats fibres with a room temperature sodium hydroxide solution before refining, with a fast impregnation time of 15 – 120 minutes to cause fibre swelling and avoid loss of polyose (Mboowa, 2024). This method ensures high pulp yields due to minimal lignin degradation, which results in lower brightness (compared to chemical pulping) and it can be easily bleached for use in higher-grade papers (Pratley, 1965).

While semi-chemical pulping has a great potential to enhance the properties of pulp and handsheets by lignin removal/softening with chemical pre-treatment, its higher cost compared to mechanical pulping due to chemical involved could be the constraint for fibre moulded containers. This is more suitable for high-value product packaging, such as electronics. However, when applied to food packaging, it presents a constraint that would significantly increase the overall cost of food products, making it neither acceptable nor feasible.

2.4.1.3 Mechanical pulp

Mechanical pulping is a process that produces fibres from wood by using mechanical energy to breakdown the lignocellulosic matrix. Mechanical pulping comprises of grinding and refining that retains lignin and cellulose, which results in inferior properties of paper products (Mboowa, 2024). Mechanical pulping generally results in high yield but low strength pulp due to the lignin remaining on the fibres, which weakens inter-fibre bonding in paper (Zhang et al., 2022). There are five main types of mechanical pulping techniques: groundwood pulping, refiner mechanical pulping, thermomechanical pulping (TMP), chemi-thermo-mechanical pulping (CTMP), and bleached chemi-thermo-mechanical pulping (BCTMP) (Laftah & Wan Abdul Rahman, 2016).

Groundwood pulping and Refiner mechanical pulping (RMP)

Groundwood pulping is the oldest pulping technique, which uses a fast-rotating grindstone to tear the woods into fibres. The resulting slurry is then screened to remove large particles and thickened by water removal, 95% of the lignin is retained. This method is inexpensive and results in the lower quality of paper products, so it is usually used in newsprint and low-cost packaging (Laftah & Wan Abdul Rahman, 2016).

RMP is a similar technique to groundwood pulping, also usually without pre-heating (Höglund, 2009). The technique involves shredding and grinding of wood chips between rotating metal discs using a refiner at atmospheric pressure to defibrillate and loosen the fibre structure to increase the flexibility (Mboowa, 2024). While it requires more energy, the paper produced by RMP pulp is stronger. (Laftah & Wan Abdul Rahman, 2016; Mboowa, 2024).

Thermo-mechanical pulping (TMP), Chemi-TMP (CTMP) and Bleached-CTMP (BCTMP)

TMP is more complicated than RMP as it involves preheating under high temperature of 115 – 155°C and steaming pressurised system at 20 – 40 psi (Höglund, 2009; Mboowa, 2024). The TMP process is multi-staged with elevated and ambient temperature and pressure steps (Mboowa, 2024), where the steaming soften the chips for easing fibre separation (Das & Houtman, 2004). For high quality TMP, latency treatment is often utilised for removing the latency, a phenomenon of curling fibres, to achieve even fibre dispersion and enhance formation quality. TMP produces stronger paper than RMP, but the energy consumption is much more, which makes it more suitable for superior packaging materials (Das & Houtman, 2004; Mboowa, 2024).

CTMP is based on the TMP process but involves the impregnation of wood chips with a combination of steam and lignin-softening chemicals, such as carbonates, hydroxides, sulphite, and peroxides (Mboowa, 2024). Höglund (2009) pointed out the chemicals used on softwood and hardwood are different, as shown in **Figure 12**, which could be

considered as distinguish for their compositions. The CTMP technique increases the strength properties of pulps compared to TMP and long fibre fraction of the pulps by the mild pretreatment, also with less energy consumption (Laftah & Wan Abdul Rahman, 2016; Mboowa, 2024).

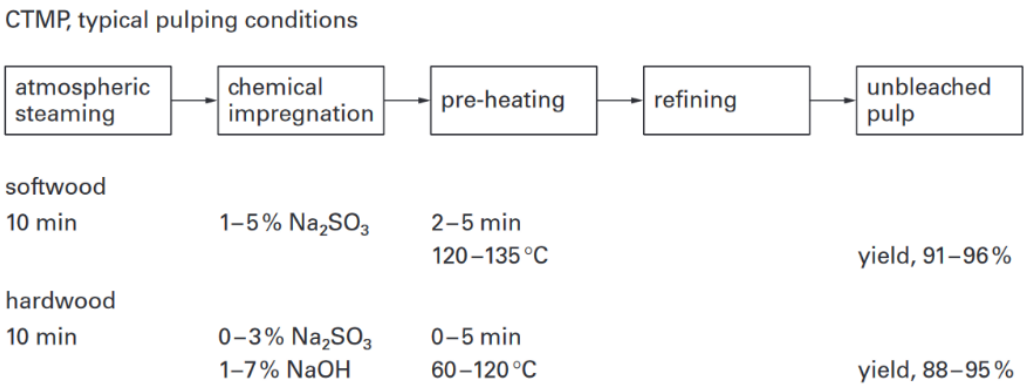

Figure 12. Steps of CTMP production as well as the chemicals involved from Höglund (2009).

Literally, BCTMP is produced by adding a bleaching procedure after refining and screening process, According to Palonki (2021), adding the bleaching procedure is to enhance the brightness and stiffness of the paper products, which is influenced by the removal of residue lignin, discarded cell wall, and bonds between fibres.

2.4.1.4 Pulp blending

Pulp blending is a process of combining different types of pulp to optimise the cost, performance, and production efficiency of paper products. This approach typically mixes a small proportion of high-strength pulp, such as softwood Kraft pulp, with more affordable pulp sources, such as recycled pulp or agricultural residues. Nandkumar (2009) applied this method to study the effects of blending long-fibered and short-fibered pulps, using Ipomoea carnea and bamboo fibres. The study found that blending these pulps results in superior physical strength properties compared to their separate use. Similarly, Behera et al. (2015) blended sisal pulp with waste paper pulp in handmade papermaking and observed that adding sisal pulp enhanced the mechanical properties of the paper compared to using waste paper pulp alone, which highlight the benefits of pulp blending in recycled pulp applications. There are many other studies

on blending different types of agricultural and recycled pulps that further support its high acceptance as an effective pulping method.

2.4.2 Handsheet manufacturing

Handsheet manufacturing is a laboratory process used to produce paper test specimens to evaluate the qualities of pulp to enables manufacturers to test pulp qualities and processing conditions before full-scale production. A handsheet is a small sample sheet of paper made by hand for testing purposes. The standard for making handsheet is typically the TAPPI standard (Technical Association of the Pulp and Paper Industry) T205. It provides the standard process of dispersing a pulp sample in water to form a slurry, which is then drained through a screen mesh to form a sheet in a handsheet maker. The handsheet is then pressed and dried to remove excess water under specified conditions at 23°C and 50% relative humidity. To replicate potential thermoforming conditions and determine optimal settings to prevent undesirable manufacturing issues, the handsheets should undergo thermal treatment, specifically through hot pressing with preset temperature, force and duration, after standard pressing. The T205 standard also illustrates the specific parameters of the equipment utilised for making standard sheets. Consistency of the slurry indicates the percentage of dry pulp/fibres in the slurry, impacts the fibre distribution and overall grammage of the sheets, thereby influencing the physical properties of the paper. The pulp freeness measures the rate that water drains from a pulp slurry, it is critical to estimate the dewatering time, which reflects the production efficiency.

$$\text{Consistency} = \frac{\mathrm{M}_{\text{dry pulp}}}{\mathrm{M}_{\text{slurry}}} * 100\%$$

2.4.2.1 Hot-press

To simulate the properties of a handsheet matrix during the thermal moulding process, hot-pressing is an effective technique that is typically performed after standard pressing and prior to conditioning. The handsheets are compressed under a controlled high temperature, pressure, and set period to determine the optimal thermal treatment

conditions for the matrix and ensure its feasibility for thermal moulding. There is a phenomenon known as hornification occurs after hot-pressing, mentioned by Lo et al. (2024), which refers to the structural and chemical changes in cellulose fibres resulting from cycles of wetting and drying. These changes can impact the fibres' properties, such as flexibility, barrier characteristics, and other functional attributes.

2.4.3 Moulded fibre packaging

Moulded fibre is an eco-friendly packaging option which can be crafted from natural fibres or recycled paper. There are three types of moulded fibres products: thick wall, transfer moulded and thermoformed that are distinguished by their manufacturing techniques and product characteristics. The thermoformed moulded process is the most advanced approach, where the formed product is pressed in a heated mould for a specific drying period to produce thin-walled (2 to 4 mm) product with accurate dimensions that closely resemble thermoformed plastic without the need for oven curing (Didone et al., 2017; Didone & Tosello, 2019).

The manufacturing process for moulded fibre packaging involves vacuum forming and drying steps. In the vacuum forming stage, pulp is sucked onto a mould to form the desired shape, where a significant amount of water is extracted, leaving the solid content between 40% and 55%. The subsequent drying step uses heat to eliminate the remaining water content down to about 4% to 8%, which is critical for replicating the product geometry (Didone et al., 2017). The drying process is categorised into two types: plain moulding and precision (or thermoformed) moulding. The plain process involves using an oven to dry the products, while thermoform moulding applies heat via the surfaces of a matching mould, as displayed in **Figure 13**. (Didone et al., 2017).

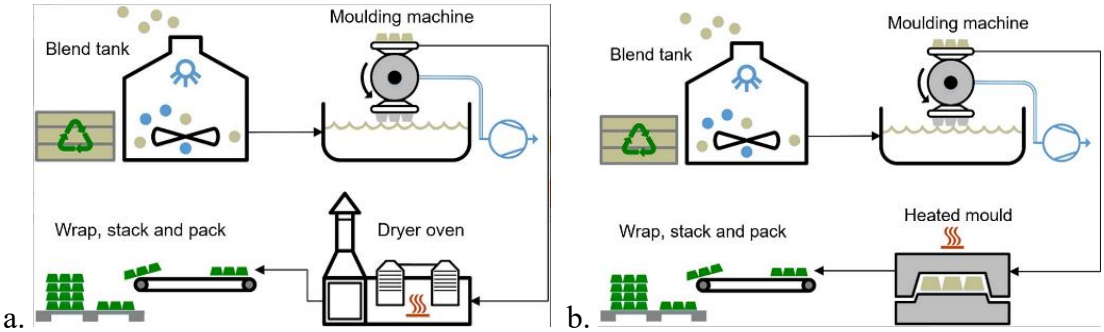

Figure 13. Schematic of (a) plain moulding drying (involve a dryer oven). (b) thermoform moulding drying (involve matching mould), from Didone et al. (2017).

Didone and Tosello (2019) also illustrated an advanced drying technique combining both mechanical pressure (1.5 MPa to 8 MPa) and intensive heat (100 to 400℃), for extremely short drying time of 20 to 50 ms. This technique generates high-pressure steam at the surface of the paper web to assist in displacing and removing water trapped between fibres, resulting in a paper product with enhanced qualities.

2.5 Factors affecting mechanical and barrier properties of paper products.

The functionality of paper and packaging significantly depends on its mechanical and barrier properties, which are determined by the fibre composition and the structural network of the fibres. As forementioned, the fibre crystallinity plays a decisive role on the mechanical and water/oil resistance of paper, the crystalline regions formed by hydrogen bonds are areas of high molecular order with restricted hydroxyl groups for water bonding to enhance the moisture resistance of the paper (Farmahini-Farahani et al., 2015). In addition, the crystalline regions within the polymer matrix are more orderly and tightly packed, which provide greater resistance to stress and strain, but it will also reduce the flexibility.

2.5.1 Porosity

The porosity of fibre network directly impacts its permeability to water, gas, and oil. A denser structure usually gives a lower porosity material, with fewer and smaller interconnected pores, thereby reducing the channels for moisture and oil to penetrate the material. Lo et al. (2024) also found that almost all mechanical properties of

handsheets, including tensile strength, bursting and tearing strength were also positively correlated to the density. The porosity is influenced by various factors, such as the size of the fibre, the use of additives, composition, as well as the processing methods. It was proposed by da Luz et al. (2017), Gouw et al. (2017) that larger fibre size potentially leads to less fibre-to-fibre interactions as the fibres are less tightly packed, which increases the pore size between fibres. Tanpichai et al. (2019) also suggested that the application of fillers with smaller particle sizes could help fill the voids within fibrous structure, who applied the nano-fibrillated cellulose (NFC) to the bamboo cellulose paper to fill the gaps (**Figure 14**), and mechanical and barrier properties were improved.

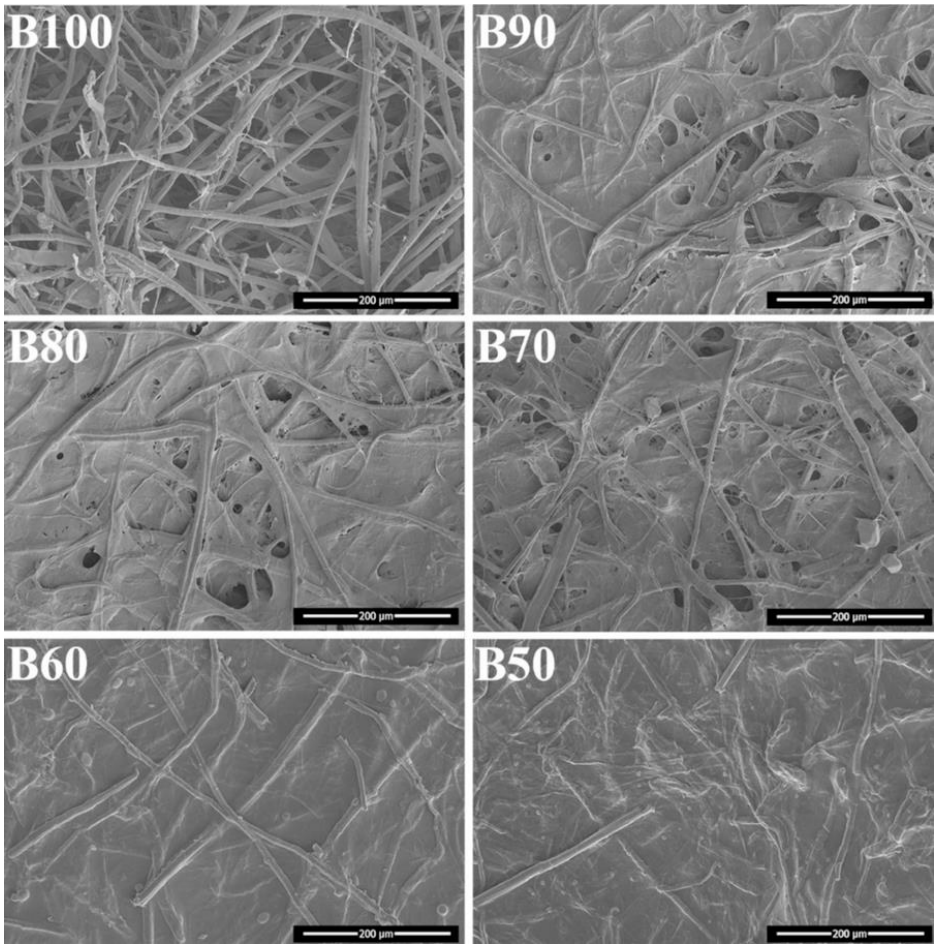

Figure 14. The Surface morphologies of the paper made of NFC and extracted bamboo fibres: B100 indicated sample made of 100% bamboo fibres, B90 indicated sample made of 90% bamboo fibres + 10% NFC, B80: 80% bamboo fibres + 20% NFC, B70: 70% bamboo fibres + 30% NFC, B60: 60% bamboo fibres + 40% NFC, B50: 50% bamboo fibres + 50% NFC, from Tanpichai et al. (2019).

In the term of density, a higher percentage of fine material leads to a denser fibre matrix structure, presenting obstacle to water vapour or oil molecules passing through the fibre

network (Kang & Min, 2010). The short fibres are more tightly packed and result in more interfacial adhesion, and increased bonding area that helps resist stress. The composition can also impact the porosity by influencing the quality of inter-fibre bonding, such as the forementioned impact of additives, for example ash (Gouw et al., 2017). Additives (coupling agents, fillers, etc) can also help fill the voids that exist in the fibrous network and enhance the bonding, In some cases, retention aids (alkaline and cationic agents) are added to help retain those small particles (Semple et al., 2022). Sizing agent is also utilised as it reacts with the hydroxyl groups on the fibre to form easter bonds to prevent the water bonding, which would be reviewed in the following sections.

2.5.2 Pulping and handsheet making process

In the pulping process, mechanical pulping results in paper with lower mechanical strength than chemical pulping due to the lignin content and shorter fibre length. However, the short fibres have better packing to result in less pores to improve the barriers. Mechanical treatment such as refining can be used to increase the fibrillation of fibres to create more surface area and bonding sites, leading to a denser packing of fibres to improve the mechanical and barrier properties. However, the low freeness of the pulp after mechanical treatment can be a challenge (Rudi & Resalati, 2015; Rudi et al., 2016) as it may lengthen the draining time during paper formation. In addition, the removal of hemicellulose in pulping process can decrease the proportion of the amorphous regions in the fibre to create barriers. The pH of the slurry is also a critical factor that impacts the retention of fine particles, which in turn directly affects the bonding quality and the effectiveness of the additives (Abd Rahman & Azahari, 2012).

Changing the handsheet forming process also affects the porosity, for example, a higher pressure in the sheet forming process tends to compress the fibres more tightly as described by Lo et al. (2024), who used hot-pressing to simulate thermoforming of the paper sheet. In their study, a phenomenon called hornification, which means collapse and reformation of hydrogen bonds within the fibre structure, was found after hot-pressing. The hornification enhanced the water barrier by increasing the rigidity and reducing the swelling capacity.

2.5.3 Surface roughness

Surface roughness is also a factor that influences the water/oil repellency, as a rougher surface creates a Cassie-Baxter state that increase the contact angle by reducing the contact area, the surface energy and adhesion. Hsieh et al. (2005) demonstrated that the consistency affects the surface roughness, with higher consistency causing fibre clumping resulting in a rougher surface, and a rougher surface displayed an excellent water and oil repellency with an extreme large contact angle (>100°).

2.6 New Zealand Food Processing Waste Fibre Sources

Food processing waste fibre streams within New Zealand offer a significant opportunity for conversion to sustainable packaging materials. The country's strong food sector facilities generate a substantial amount of waste fibres such as grape marc, fruit/vegetable pomaces/skins, and oilseed meal residues. WasteMINZ (2018) reported that these food industries generate approximately 40,800 tonnes of waste annually, with 28% (11,424 tonnes) sent to landfill. Fibres occupy 60% of the total organic waste from food industries, with 26% of them going to landfill.

Unfortunately, the information on food wastes is limited. There are only limited information from various sources: 10,000 – 15,000 tonnes of apple pomace, 20,000 tonnes of carrot pomace (Archer et al., 2019; Granucci et al., 2023). Some data of the post manufacturing food fibre wastes without specific values for each type of categories was published by the Bioresource Processing Alliance (BPA) and other sources, as shown in **Table 3**. The availability of the food processing waste fibre sources is also presented.

Table 3. The availability of some waste fibres within New Zealand. PM: Post-manufacturing.

Category	Amount (kg/a)	Region	Supply month	Source
Apple pomace	470,000	Hasting	Apr to Dec	BPA 2023 Statistics
Apple skin and core	400,000	Hasting	Apr to Dec	BPA 2023 Statistics
Other pomaces	4,200,000	Unknown	Unknown	BPA 2023 Statistics
Lucerne crop	Unknown (not provided due to Intellectual Property)	Manawatu	July to September	Plant and Food Research Institute
Grape marc	765,000 (2022)	Unknown	Unknown	BPA 2022 Statistics
Grain	750,000	Unknown	Unknown	BPA 2022 Statistics
Skins	600,000	Unknown	Unknown	BPA 2022 Statistics
Other	1,902,000	Unknown	Unknown	BPA 2022 Statistics
Packaged food	2,600,000	Unknown	Unknown	BPA 2022 Statistics
Yeast	446,000	Unknown	Unknown	BPA 2022 Statistics
Corn grain	205,000	All New Zealand	February to April	Index mundi (2024)
Corn grain (for starch production)	50,000 – 60,000 tonnes	All New Zealand	Whole year	New Zealand Starch (2020)

For this project, the whole wasted fruits, such as unsold/unharvest/stock fruits will not be considered. Among the New Zealand local food processing waste fibres mentioned above, grape marc, cabbage, carrot have been researched by Scion previously (Lo et al., 2024; Vries, 2024). Thus, the fruit pomaces/skins such as apple pomace and citrus peels present a new opportunity. They are available from juicing companies nationwide, featuring 470 tonnes of apple pomace sourced from Hastings and 600 tonnes of skins, including citrus peels collected nationwide. Additionally, New Zealand's citrus production was reported to over 30,000 tonnes, including 10,000 tonnes of oranges in

2020 (Citrus New Zealand, 2020), indicating the significant potential availability of orange peels. Although they are seasonal fruits, the waste streams are collected from food factories, who will have a reserve for continuous production and a constant supply of residues. Furthermore, a thermoforming process utilising seasonally available fibres would be worthwhile if sufficient quantities are accessible to produce a practical volume of products.

New Zealand produced 205,000 tonnes of corn in 2023 (Index mundi, 2024), which keeps increasing annually, and New Zealand Starch reported 50 – 60,000 tonnes of corn grains were processed annually in 2020 (New Zealand Starch, 2020), which could bring through large amounts of related fibrous byproduct such as corn husk, corn germ, corn bran (Zhang et al., 2021).

2.7 Feasibility analysis of common NZ food processing wastes as potential moulded fibres

2.7.1 Apple pomace

Apple pomace (AP) is the byproduct generated during apple juice production with approximately 25 – 30% of each tonne of fresh apples processed for juice becomes pomace waste (Santhosh et al., 2021). AP is a heterogeneous mixture consisting of peel, core, seed, calyx, stem and flesh, comprised of around 2.2 – 3.3% seed, 0.4 – 0.9% stem, 70.0 – 75.7% apple flesh. AP contains an average fibre content of 36.8% and insoluble carbohydrates of 54.4%, which includes cellulose, hemicellulose, as well as lignin (Sharma et al., 2017). The exact composition depends on the several factors including preharvest condition and varieties. The normal pH of apple pomace ranges from 3.2 – 3.4, which will acidify the pulp slurry when combining with wood pulp. As mentioned in Section 2.5.2, the acidic pulp slurry could reduce the retention of small particles.

Research conducted by Gouw et al. (2017) and Lang et al. (2022) explored the potential of AP blended with recycled newspaper pulp (NP) and cardboard pulp (CP) to improve the overall functional properties of the resulting paper. Gouw et al. (2017) utilised the

AP containing 18.87% pectin, 70.48% of cellulose (65.83% of α-cellulose, 5.95% β-cellulose, and 28.23% γ-cellulose), 8.72% of acid-insoluble lignin, and 1.93% of ash, where the presence of β-cellulose and γ-cellulose function as hemicellulose, and the lignin providing the thermal resistance. The high pectin, cellulose and hemicellulose indicate the AP is hydrophilic (Zdunek et al., 2014), because of their hydroxyl group as previously introduced in section 2.2.1 for fibre constitutes. The high cellulose content indicates that AP could provide sufficient fibrous compounds to support the mechanical performance. In terms of microstructure, **Figure 15** presents the microscopic images of AP slurry (unpulped), which showed AP's large and thick fibres, which had potential to increase the tensile properties of the paperboard but also the absorbance of water due to increased porosity as well (Gouw et al., 2017).

Figure 15. The images of AP slurry, (a) naked eye, (b) stereomicroscope of AP fibre at 4x magnification, (c) SEM of AP fibre with magnification of 200x, from Gouw et al. (2017).

They tested many different blend ratios of AP with NP. The paper made with a 1:1 ratio of AP and NP and 0.15% nano-cellulose fibre had the lowest water absorption of 278.3%, compared to 341.14% of pure NP sheets. The higher the proportion of added AP, the greater the water absorption of the sheet. The water absorption of AP sheets remained higher than that of other fruit pomaces. The author attributed this to the higher hemicellulose and pectin content in AP, which led to a more porous structure and its relatively larger fibre size (compared to the other two fruit pomaces) decreased fibre entanglement and adhesion interactions with other cellulosic compounds (α-, β-cellulose, etc), despite it partially filled the pores of NP fibres (Gouw et al., 2017). It also had a rougher surface and weaker inter-fibre bonding than other two fruit pomaces (blueberry and cranberry).

Its flexural strength and strain measured 4.26 MPa and 4.64%, respectively, which had minimal improvement over the 3.48 MPa and 4.31% of NP. This suggests that the AP

fibre lacks flexibility, potentially impacting the stretch and tearing properties of the handsheet. However, the addition of nano-cellulose fibre significantly increased the flexure strength (Gouw et al., 2017). Overall, the author suggested that AP could be substituted for NP, but the blend ratio should be optimised to avoid excessive water absorption.

Lang et al. (2022) studied the potential of blending AP with cardboard fibre (CBF), and they added chitosan, rhubarb pomace (RBP) and glycerol as additives. They tested 20 samples, found that the optimal blend ratio of AP and CBF was 2:1 with 3% solid in the pulp, incorporating 26.86% RBP (w/w, dry basis), 15.73% chitosan (w/w, dry basis), and 0.039% glycerol (w/v, wet basis). This blend had improved water resistance and flexural strength, but reduced elasticity as shown in **Table 4**, which further proved the limited flexibility of the AP fibres.

Table 4. Comparison of properties of AP blends, from Lang et al. (2022).

Coating treatment	Type of board	Water retention value of pulp	Water absorption (WA, %)	Water solubility (WS, %)	Flexural strength (MPa)	Modulus of elasticity (MPa)
Uncoated	Control	1.62 ± 0.12	275.73 ± 9.99	0.96 ± 0.27	10.33 ± 1.93	393.3 ± 89.3
	OPB	1.80 ± 0.05	166.54 ± 6.40	1.02 ± 0.41	13.66 ± 1.23	157.0 ± 127.0

Note: OPB indicates uncoated optimised pomace board.

Based on the findings from Gouw et al. (2017) and Lang et al. (2022), apple pomace could help improve the mechanical properties, but has limited flexibility, which means the handsheets made with AP would be rigid with less stretching. In addition, it falls short in terms of water barrier due to the large fibre sizes, and pectin/hemicellulose contents. When blended with BCTMP, the large fibres may not fit into the gaps but stack together instead to increase porosity. A possible strategy to address this weakness is to apply an additional mechanical treatment to reduce its particle size, and an additional pectin and hemicellulose removal process could be employed. Both studies show that using additives could help improve barrier and mechanical properties. Other substrates like a seed fibre could be considered as a filler to fill the fibre gaps.

2.7.2 Orange peel

As the byproduct of one of the world's most popular juices, orange peels are readily availability. Up to 50% of the original fruits become by-product from juicing, with majority being outer skin and seeds (Granucci et al., 2023). Garcia-Amezquita et al. (2019) analysed the composition of orange peels as presented in **Table *5***.

Table 5. Composition of orange peels per 100 g dry basis.

	Fibre	Protein	Fat	Ash	Soluble pectin	Soluble fibre sugars	Carbohydrates
g	48.7	4.9	1.5	4.2	5.6	0.9	40.6
Error (±)	0.6	0.1	0.1	0.1	0.2	0.1	0.3

Note: The fibre including 42.7 ± 0.5 g insoluble and 6.4 ± 0.3 g soluble fibre.

Buxoo and Jeetah (2020) investigated the feasibility of making paper cups from pineapple peels (PIP), orange peels (OP) and hemp leaves (HL), by combining them in different ratios. The study outlined the composition of those three substances. **Table 6** revealed that OP have the lowest levels of cellulose (10.33%) and lignin (2.65%), leading to the weakest tensile strength of the fibre material. Notably, the proportion of hemicellulose to cellulose in OP was higher than PIP, with a more amorphous structure to weaken the fibre strength and water resistance.

Table 6. Composition of PIP, OP and HL from Buxoo and Jeetah (2020).

(%)	Pineapple peels	Orange peels	Mauritian hemp leaves
Total dry solids	15.28 ± 1.14	25.43 ± 0.21	13.99 ± 0.63
Moisture	84.72 ± 1.14	74.57 ± 0.21	86.01 ± 0.63
Ash	7.03 ± 0.66	3.76 ± 0.54	5.73 ± 1.03
Lignin	9.21 ± 1.12	2.65 ± 0.70	10.99 ± 1.77
Cellulose	36.41 ± 1.40	10.33 ± 1.12	69.50 ± 1.63
Hemicellulose	26.19 ± 1.48	13.18 ± 1.96	18.71 ± 2.42

Note: The components such as ash, lignin, cellulose, and hemicellulose are part of the total dry solids content, which also includes some moisture. Therefore, the percentages can be considered separately, with total dry solids plus moisture together making up 100%, while the remaining components are calculated as individual percentages.

In their experiment, increasing the OP content in paper resulted in a smoother surface but was more susceptible to cracking (Buxoo & Jeetah, 2020), which was attributed to the short and weak nature of orange peel fibres, which tended to break during the drying

process. In the crack analysis, specimen with certain percentages of OP and PIP failed and were excluded from the tests for other properties. The study found that paper cups with 60% PIP exhibited the best mechanical performance, particularly in tensile strength, as illustrated in **Table 7**. This superior performance was likely due to stronger interfacial bonding and the stronger tensile strength given by the higher cellulose and lignin content of PIP fibres. Conversely, OP cups displayed poorer results in tensile strength, Young's modulus, and force at break but performed better in terms of elongation. These results highlight the inherent weaknesses and low toughness of OP fibre compared to those from PIP, concluding its limited suitability in applications in food packaging. Note, all blends involved hemp leaves, so the bonding/chemical reactions between HL fibres and OP fibres could be a potential interference, so the results could just be the reference to support the potential performance of OP.

Table 7. Mechanical properties of specimen from Buxoo and Jeetah (2020).

	Control	Ratio of hemp:pineapple peels composite cup			Ratio of hemp:orange peels
		20:80	40:60	60:40	40:60
Grammage, *g* (g/m^2)	228.68	269.36	304.69	479.34	378.79
Elongation at break (mm)	5.23	0.60	0.61	1.31	2.67
Elongation at peak (mm)	5.16	0.53	0.57	1.06	0.89
Force at break (N)	145.50	9.81	22.99	0.64	0.11
Force at peak (N)	149.30	11.48	25.14	1.20	1.20
Time to failure (s)	63.02	7.26	7.35	15.83	32.16
Strain at break (%)	3.49	0.40	0.41	0.88	1.78
Stress at break (N/mm^2)	15.73	0.36	0.85	0.02	0.01
Young's modulus (N/mm^2)	1092.35	148.53	284.24	3.87	28.26
Width of strip (m)	0.025	0.025	0.025	0.025	0.025
Tensile index, *I* (Nm/g)	26.12	1.70	3.30	0.01	0.13

Another study examined the potential of using OP as a biopolymer material (Yaradoddi et al., 2022), which might provide some relevant insights on handsheet performance. The researchers found that the film made from OP mixed with glycerol has a great water retention (903 ± 57 permeation) and oil resistance (16.2 ± 3 permeation) compared to normal glycerol coatings, suggesting that while OP could potentially provide good oil barrier, but the water resistance might be the challenge. Additionally, the study noted the good degradability of OP-based films that can be degraded within 4 weeks, which might be a challenge for commercialisation if utilising OP as the blend material.

In summary, both studies pointed out the high-water absorption/permeability of OP-based packaging materials, suggesting that water resistance would be a challenge, which might be improved through the use of sizing agents.

2.7.3 Potato peels

Potato peel (PP) is a byproduct from potato chip and frozen potato product manufacturing. The weight of PP recovered from each potato varies based on the peeling process used, with an average of 27 % w/w (Galhano dos Santos et al., 2016). According to Liang and McDonald (2014), PP waste consists of about 25% of starch, 30% of non-starch polysaccharide, including cellulose and hemicellulose, acid insoluble and acid soluble lignin (20%), protein (18%), lipids (1%), and ash (6%).

Lo et al. (2024) investigated the potential of blending 20% PP with BCTMP pine pulp (BPP) to make handsheets using with an additional hot-pressing stage. Results showed that the handsheets without hot-pressing had larger pores on the surface, as shown in **Figure 16**. Regarding mechanical properties, PP handsheets demonstrated better tensile strength, stiffness, elongation, and tearing strength than controls without PP, and PP handsheets subjected to hot-pressing had the best overall performance. The enhanced properties of PP handsheets were attributed to the high cellulose and lignin content, while hot-pressing further improved the bonding strength and density to enhance the mechanical properties.

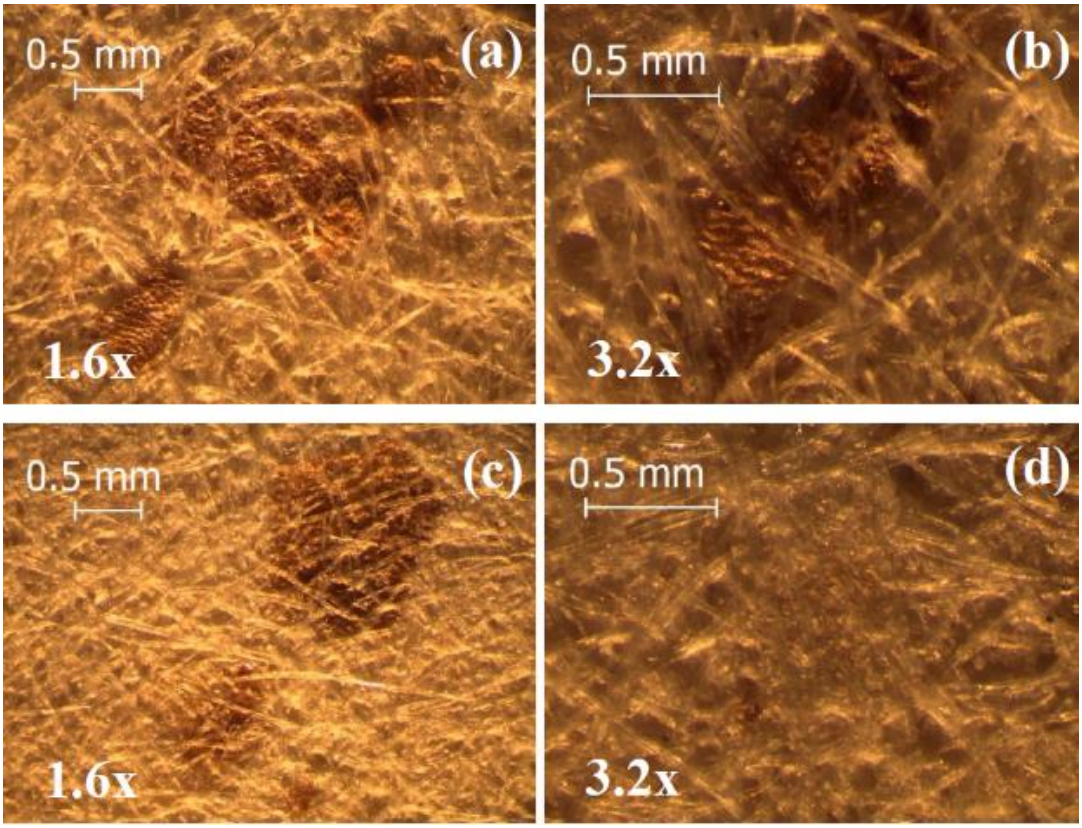

Figure 16. The micrographs of handsheets: (a) 1.6x PP. (b) 3.2x PP, (c) 1.6x PP with hot-pressing, (d) 3.2x PP with Hp, from Lo et al. (2024).

In the term of barrier properties, the PP containing handsheets showed superior water resistance compared to BPP handsheets, but lower oil barrier, showing a breakthrough time of 96 minutes compared to 204 minutes for BPP, with hot-pressing significantly shortening the oil barrier time (see **Table 8**). This suggests that hot-pressing might negatively impact the oil resistance, disagreeing with the expectation that a denser structure repels oil, which might be due to the high temperature destroying some compounds that contributes to oil barrier, or caused some micro-cracks on the surface.

Table 8. Comparison of grease breakthrough time of handsheets, refer to Lo et al. (2024).

	BPP	BPP -Hp	PP	PP -Hp
Breakthrough time (min)	204	36	96	26

There are limited studies on utilising PP in moulded fibre production but some researchers had explored using PP to create biopolymer films to improve water barrier properties, and outcomes from the PP-based film properties could offer some inspiration. Kang and Min (2010) developed a PP-based biopolymer film, and the

findings showed that its moisture barrier was better than those of calcium caseinate, wheat gluten, and whey protein isolate films, but still not desirable due to the inherent hydrophilicity of polysaccharides in PP and its larger pore. However, the water vapour permeability (WVP) and water solubility results demonstrated that the film with 5%w/w PP has better WVP and less solubility than those with 3%w/w PP with the same amounts of additives, suggesting that PP's relatively high lignin content might enhance water barrier properties. In addition, a summary report on plant processing byproduct used in films and coatings (Santhosh et al., 2021) proposed that the addition of PP enhanced the tensile strength from 2.5 – 9.0 MPa, due to its high cellulosic contents, and reduced WVP by 61% of the PP-based films.

Therefore, the potato peel has great potential to provide superior mechanical and barrier properties to the handsheets, but the conditions of pressing should be controlled to achieve better water and oil resistance.

2.7.4 Corn byproducts

Corn is a highly starchy cereal crop. Various byproducts from corn starch processing, are corn bran (12.0%), corn germ (7.5%) and steep liquor (Zhang et al., 2021), in which the corn bran and corn germ are rich in fibre, exhibiting large potential to be utilised. Zhang et al. (2021) also detailed the component of corn bran and corn germ, as shown in **Table 9**.

Table 9. Components of corn bran and corn germ from Zhang et al. (2021).

	Moisture	Protein	Fat	Fibre	Cellulose, Hemicellulose	Lignin	Ash
Bran	8 - 10	10 – 13	2 – 3	12.3	20% 30 – 50%	2.2	2 – 5
Germ	10 -12	12 - 21	18 - 41	10.4	Not available	2.4	3 – 5

The high hemicellulose content in corn bran indicates more amorphous region, which was also highlighted in Yadav et al. (2016). Thus, the hemicellulose removal treatment needs to be applied on corn bran if being used as a blend material. No literature on using corn bran as reinforcement materials for food packaging or paper products has been found, but the hemicellulose extraction method for corn bran was reported by Yue et al.

(2022), which suggested using 10% KOH at 25 °C for 16 hours at a solid/liquid ratio of 1:20 g/mL, resulting 92.2% of removal ultimately. In contrast, corn germ's high fat content could potentially offer excellent water/oil barrier, Therefore, there is potential to combining corn bran and germ as an alternative mixed fibre, with the corn germ is more likely to be an enhancer additive.

Corn husk, the covering ear of the corn plants, is also a waste from corn products production that has great potential to be utilised as an alternative fibre material. Corn husk fibre's (CHF) basic constitution are 38.2% cellulose, 44.5% hemicellulose, 6.6% lignin, 2.8% ash, and 1.9% protein, with a medium fibre length between hardwoods and softwoods (Ahmad Rassdi, 2013). Its relatively high hemicellulose content, may affect the barrier and strength of handsheets made of corn husk. Ahmad Rassdi (2013) studied the possibility of utilising corn husk fibre and recycled paper (RP) for food packaging materials, and made three specimens, 70% CHF + 30% starch, 70% CHF + 20% starch + 10% RP (70/30 sheet), 60% CHF + 20% starch + 20% RP (60/40 sheet). The outcomes suggested that the increase in RP-starch mixture proportion increased the smoothness of the surface, and the strength of paper, from 0.84 MPa at 30% to 1.30 MPa at 40% (**Figure 17** and **Figure 18**). In the term of water absorption, the 70/30 sheet had the highest moisture absorption at 11.97% due to poor adhesion between fibre particles and binders (RP-starch mixture), generating voids. By contrast, that of 60/40 paper was 9.74%, which was a bit lower that 70/30, which means the corn husk fibre was potentially making the fibre network denser and providing more crystalline structure. The addition of binder increased the performance by around 20%, however, two matches were not enough to determine the enhancement, so more blends with higher portion of binder would bring more comprehensive sight.

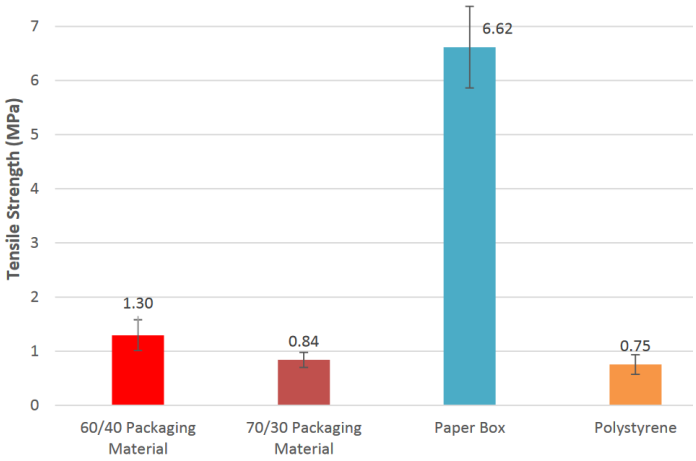

Figure 17. The tensile strength of specimen made of 60% CHF + 20% starch + 20% RP, and 70% CHF + 20% starch + 10% RP (70/30 sheet), paper box, and polystyrene from Ahmad Rassdi (2013).

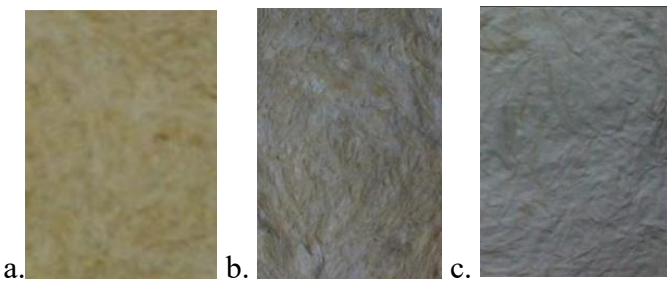

Figure 18. Surface appearance of those three specimens. (a) 70% CH + 30% starch. (b) 70% CH + 20% starch + 10% recycled paper. (c) 60% CH + 20% starch + 20% recycled paper from Ahmad Rassdi (2013).

2.7.5 Oil extraction processing byproducts

2.7.5.1 Canola meal

Canola meal (CM) is a byproduct of canola oil extraction, containing the 17% - 36% of extractable protein. Mustafa et al. (1996) identified two types of CMs: a high fibre CM and a low fibre CM, which differ in protein contents. Bell and Keith (1991) tested the component of CM, finding an average neutral detergent fibre (NDF) of 23.54%, 19.09% acid detergent fibre (ADF), 13.13% crude fibre, 41.85% crude protein and 3.92% other components, where NDF is the sum of cellulose, hemicellulose and lignin, while ADF is the sum of cellulose and lignin. The components are associated with the processing method and plant source.

While no studies specifically address the use of canola meal in moulded fibres products, the protein of the canola has been utilised for the production of biopolymer materials. Li et al. (2019) studied the mechanical properties of CM blended with cellulose fibre (CLF), and the outcomes revealed that the CM content with higher protein percentage led to an increase in elongation, with these effects were not affected by particle sizes. In addition, increase the CLF loading to 30% exhibited higher tensile and interfacial interactions, indicating CM still lacks sufficient functional performance to be the major fibre material. Thus, CM with smaller fibre sizes could be utilised as a protein derivative and increase the capillary force, as well as reduce the void fraction without significant impact on mechanical properties.

2.7.5.2 Olive pomace

Olive pomace (OLP) is the solid lignocellulosic byproduct from olive oil production, composed of the residual skin, pulp and crushed stone fragments (Lammi et al., 2018). According to Khwaldia et al. (2022), the OLP constitutes 35 – 40% of the total weight of olives processed, with the stone accounting for 10% of weight, comprising 20.9% cellulose, 26% hemicellulose, 35.6% lignin, 26.6% xylose, 1.4% galactose, and 1.3% arabinose. Its low cellulose content suggests the OLP may have limited mechanical properties. Research on using OLP in food packaging mainly explores its antioxidant properties from pectin in biopolymers, or as a bio-composite filler added to plastics, but its feasibility on moulded fibre or paper products remains unknown.

de Moraes Crizel et al. (2018) added OLP flour and OLP microparticles to chitosan-based film, observing that these additions increased the WVP by around 30%, which is not desirable for takeaway containers, as it indicates more absorption of water (See **Table 10**) The increased percentage of microparticles and flour also influenced the tensile strength, elongation and Young's modulus of the films, as shown in **Table 11**.

Table 10. Water Vapor Permeability (WVP), Moisture Content (MC) and Water Solubility (WS) of the control film and films with OLP flour and microparticles, from de Moraes Crizel et al. (2018).

Film	WVP ($g.mm/m^2$ h kPa)[a]	MC (%)[a]	WS (%)[a]
Flour			
10%	1.32 ± 0.03^{bc}	18.87 ± 1.06^{a}	31.93 ± 4.22^{b}
20%	1.52 ± 0.05^{b}	17.76 ± 0.07^{a}	31.40 ± 4.35^{b}
30%	2.23 ± 0.14^{a}	16.47 ± 0.87^{ab}	44.55 ± 1.28^{a}
Microparticles			
10%	0.96 ± 0.04^{d}	18.97 ± 0.19^{a}	31.31 ± 3.59^{b}
20%	1.06 ± 0.06^{d}	17.38 ± 0.58^{ab}	28.64 ± 2.55^{b}
30%	1.09 ± 0.02^{cd}	15.04 ± 0.28^{b}	26.16 ± 2.13^{b}
Control	0.85 ± 0.00^{d}	18.28 ± 0.92^{a}	32.61 ± 0.73^{b}

Table 11. Thickness, tensile strength, elongation, Young's modulus of the control film and films with OLP flour and microparticles, from de Moraes Crizel et al. (2018).

Film	Thickness (mm)[a]	TS (MPa)[a]	%E (%)[a]	YM (MPa)[a]
Flour				
10%	0.218 ± 0.01^{b}	7.58 ± 0.23^{c}	17.57 ± 0.28^{d}	40.42 ± 0.29^{b}
20%	0.237 ± 0.01^{b}	5.49 ± 0.21^{cd}	$15.39 \pm 0.44d^{e}$	25.79 ± 2.55^{c}
30%	0.305 ± 0.00^{a}	2.89 ± 0.06^{d}	13.31 ± 0.77^{e}	12.39 ± 0.39^{d}
Microparticles				
10%	0.140 ± 0.01^{c}	22.40 ± 0.22^{a}	33.01 ± 0.66^{a}	35.90 ± 2.48^{b}
20%	0.140 ± 0.01^{c}	14.55 ± 0.43^{b}	23.58 ± 0.73^{b}	23.43 ± 1.63^{c}
30%	0.145 ± 0.01^{c}	6.51 ± 0.02^{cd}	20.93 ± 0.69^{c}	16.28 ± 0.83^{d}
Control	0.123 ± 0.00^{c}	16.76 ± 3.51^{b}	23.05 ± 1.36^{bc}	69.11 ± 2.10^{a}

It could be summarised that OLP's highly hydrophilic nature makes it require a certain percentage of coupling or sizing agent to improve the interfacial adhesion with cellulose fibres and minimise the voids.

2.7.6 Lucerne press-cake

The lucerne press cake is the residual fibre stream from the lucerne protein extraction process. It offers a great source of fibre, and a typical lucerne waste fibre contains 56% of cellulose, 17% of hemicellulose, 25% of lignin (Bahreini et al., 2022). Unfortunately, there is no prior study on using lucerne crop on pulp or packaging materials, but it also means this could be a novel material to be researched. By analysing the components, its high cellulose and lignin contents indicate it could potentially contribute to the strong

mechanical properties of packaging materials. Additionally, its moderate hemicellulose content means a moderate level of water absorbability. However, the presence of pigment may affect the colour and aroma of the final moulded fibre tray, that affect the taste of foods, which could be a concern for certain applications. The lucerne crop is available for most of the year apart from June to September, and the residue can be supplied during that period.

2.7.7 Hemp seed husk

Hemp seed husk is outer shell of the hemp seed, which is a byproduct from hemp seed processing stage of hemp oil production (El-Sohaimy et al., 2022). There is no study found specified its composition, but the hemp seed contains 46% cellulose, 22% hemicellulose and 31% of lignin, with rest are oil and ash. (El-Sohaimy et al., 2022), which could provide some insights. Its fibre content of nearly half makes it suitable for moulded fibre applications, but its elevated hemicellulose levels can increase hydrophilicity. There is currently no research found using hemp seed husk for paper or moulded fibre application, but many studies researched the hemp hurd fibre, such as Stevulova et al. (2015) and Lo et al. (2024), who demonstrated the great potential of hemp hurd as an alternative moulded fibre material. Since the hemp seed husk is originally from hemp seed, it may contain some oil compounds and high cellulose content, it could potentially serve as an effective filler material to fill voids between fibrous network and enhance barrier properties.

2.7.8 Comparison

After reviewing the potential of enhancement in mechanical and barrier properties and final properties of the food processing waste materials mentioned above, one or two fibrous materials will be selected using a scoring method as primary material for blending, which is illustrated in the **Table 12**. Some fibrous materials not listed in the table are intended for use as fillers, which is also screened by scoring (see **Table 13**).

Table 12. The screening of the food processing waste material could be potentially utilised for moulded fibre.

Criteria	Apple Pomace	Orange Peel	Potato Peel	Corn husk	Olive pomace	Lucerne press-cake
Availability	1	1	1	1	0.5	0.5
Mechanical improvement	1	0.5	1	1	0.5	0.5
Barrier improvement	0.5	0.5	0.5	0.5	0.5	0.5
Potential as major fibre	1	0.5	1	1	0.5	1
Overall	3.5	2.5	3.5	3.5	2	2.5

Note: There are four criteria to assess the feasibility of the fibre material, availability, potential enhancement in mechanical and barrier properties, as well as whether the fibre could be utilised as a major fibre material for blending. The full score for each criterion is one mark, which means this material has relatively satisfying characteristics, while 0.5 score indicates relatively less satisfying, and zero score indicates the material does not seem to provide the functionality.

Among these materials, apple pomace, orange peels and potato peels have the highest scores, and the analysis is showed below:

The apple pomace is readily available from juicing industries. It contains long fibres with notable potential for improving mechanical properties, and its suitability as a primary fibrous material for producing paper and packaging has been demonstrated in numerous studies. However, its long fibres may reduce fibre packing, leading to increased porosity that negatively affects water/oil barrier performance. To address this limitation, the application of sizing agents or fillers is essential to minimise pore formation. Alternatively, mechanical treatment to reduce the particle size of apple pomace can help increase overall density and enhance mechanical properties based on the findings from Lo et al. (2024), which could be another solution to these limitations.

Potato peels are also highly available from chips industries in NZ with demonstrated potential in enhancing mechanical and barrier properties, although the oil barrier was significantly reduced after hot-pressing, which provides a topic for potential research. However, this material has already been studied by Scion, so it will not be chosen.

Corn husk shows strong potential for enhancing mechanical properties based on the findings from other studies. Similar to apple pomace, the longer fibre length of corn husk can lead to voids that increase water absorption and oil penetration, which requires additives or special mechanical treatment to resolve it. In addition, researchers have noted that a binder matrix is needed to effectively hold the fibres together, suggesting the potential for ineffective fibre bonding when using corn husk.

Table 13. The screening of the food processing waste material could be potentially utilised as additives/fillers.

Criteria	Hemp seed husk	Canola meal	Corn bran	Corn germ
Availability	1	0.5	0.5	0.5
Mechanical improvement	0.5	0.5	0.5	0.5
Barrier improvement	0.5	0.5	0	1
Potential as filler/additive	1	1	1	1
Overall	3	2.5	2	3

Other fibres such as olive pomace, corn brans and germs, as well as hemp seed husks also shows some potential for improving mechanical strength or barrier properties. However, either their limited availability or lack of supporting literature on their use as primary blending fibrous materials, but the additives, suggests they are better suited as fillers. Among these materials, hemp seed husk stands out due to its high availability and potential ability to enhance the barrier performance of handsheets.

2.8 Additives for barrier enhancement

Various additives can be added into pulp to enhance the properties of the resulting handsheets. The additives are necessary to increase mechanical and/or barrier performance (Semple et al., 2022). As aforementioned, porosity and hydrophilicity have the main impacts on barrier properties of handsheets and these properties can be improved by adding multiple functional additives such as coupling agents, sizing agents and small particle fillers.

2.8.1 Sizing agents

2.8.1.1 Alkyl ketene dimer

Alkyl ketene dimer (AKD) is a synthetic sizing agent used in paper making to increase hydrophobicity of cellulosic products (Kumar et al., 2016). The mechanism explained by Liu et al. (2020) shows that AKD reacts with the cellulose's hydroxyl groups through esterification to form β-carbonyl ester, orient the hydrophobic groups away from the cellulose surface to enhance the liquid-repellent properties, as shown in **Figure 19**. Semple et al. (2022) pointed out that higher concentrations of AKD could improve the thermal insulation properties of sheets when being exposed to hot liquid/steam. Glenn et al. (2021) also proposed that the liquid-repellent properties from the low-energy surface created by AKD has some effects on preventing the water droplets from spreading or penetrating into pores between fibres.

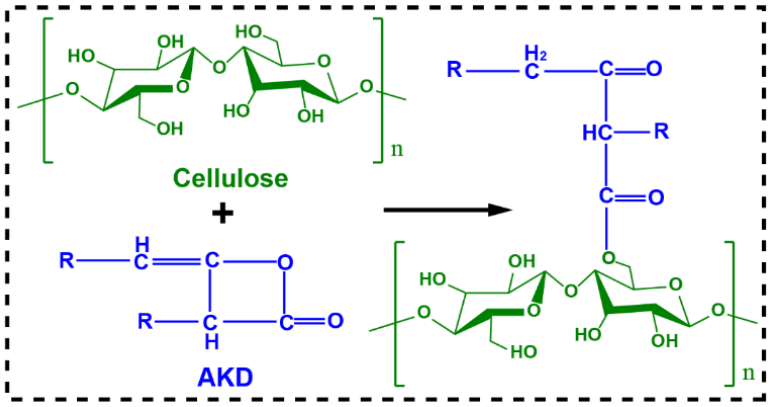

Figure 19. Reaction of AKD with cellulose. Refer to Liu et al. (2020).

However, the sizing agent might not bind properly to the fibre surface during pulp mixing and lead to low retention. Incorporating fixing agents, which are positively charged additives such as cationic agents, helps adhesion of AKD to fibres and boost its effectiveness. Semple et al. (2022) suggested using cationic polyacrylamide as the fixing agent to help bind the AKD to the pulp fibres to minimise loss during the dewatering process, and they found that AKD mixing rate at 1% with 1% of a not specified fixing agent was the most effective at increasing the contact angle from 12° to nearly 90° on recycled newsprint handsheets, and that for bleached Kraft pulp

handsheets were larger than 100°. It is also worth noting that the Food and Drug Administration (FDA) limits the addition of AKD in food packaging to a maximum of 0.4% (FDA, 2024), so the retention needs to be noticed because of the tiny amount added.

2.8.1.2 Alkenyl succinic anhydride

Alkenyl succinic anhydride (ASA) is another sizing agent used to impart surface water resistance and hydrophobicity (Rui et al., 2024). Similarly, it works by reacting with cellulose fibres to decrease the surface tension, and creating hydrophobic groups, making water droplets bead up on the surface of the paper (Glenn et al., 2021). The advantages of ASA compared with AKD is its faster reacting speed, but it hydrolyses quickly in water into succinic acid and loses its effectiveness as a sizing agent, whereas, AKD is more durable and stable than ASA (Glenn et al., 2021).

2.8.2 Coupling agents

Coupling agents are used to enhance the interactions between fibre-filler, or fibre-fibre networks, by improving the adhesion characteristics to reduce the porosity, which can significantly affect the mechanical and barrier properties of the final paper product. Since the target of this project is to make the moulded fibre materials which are biodegradable at end-of-life, any coupling agent selected must be degradable to meet with this objective.

2.8.2.1 Starch

Starch is a natural polymer that can be utilised as a coupling agent to enhance the barrier properties by improving the fibre adhesion. It can increase the pH and viscosity of the pulp mixture to form a cohesive matrix within the sheet as well as ensuring the retention of small particles due to its positive charge density. Both Semple et al. (2022) and Amode and Jeetah (2021) demonstrated starches can be utilised to replace PFAS to bring grease resistance, and cationic tapioca starch could significantly enhance the strength and resistance to water absorption of hemp-waste paper moulded fibre

handsheets, Additionally, the corn husk handsheet study by Ahmad Rassdi (2013) used the matrix of recycled paper and cationic starch to enhance the tensile strength and moisture barrier, which further confirm the efficacy of starch.

2.8.2.2 Protein derivative

The functions of protein in fibre has already been introduced. Cheng et al. (2017) research showed how cottonseed protein used as an additive on the paper attributes to mechanical properties of the paper. They found the interaction between the cationic arginine in the protein, effective up to a pH of 12, and the negatively charged carboxylate groups promoted the fibre bonding (Cheng et al., 2016; Cheng et al., 2017), and other animo acids in the protein could potentially provide specific functional benefits to the paper properties (Cheng et al., 2017), although no details of those benefits are given. Existing research on using protein as an additive in paper mainly discuss the modifications in mechanical properties rather than barrier properties. Nevertheless, Han and Krochta (2001)'s study on applying protein derivatives for coating, to address oil resistance of paper products, gave some insights mainly around the quantity of protein used.

2.8.2.3 Nanocellulose (NC)

Nanocellulose (NC) is a nanoscale form of cellulose increasingly utilised as an additive in paper processing due to its great biodegradability and enhancement in barrier and mechanical properties. NC is defined as a fibrous material shorter than 100 nm in at least one dimension, with some general types like the nanocrystalline cellulose, cellulose nano-whiskers, and cellulose nanofibrils (A. Li et al., 2021). According to Boufi et al. (2016), NC acts as an adhesion promotor by filling the voids to reduce the porosity, thereby producing a denser structure that improve the overall properties. However, its fine particles can reduce the drainage, thereby, extend the production time. However, the commercialisation of NC presents challenges due to high production cost (A. Li et al., 2021). Therefore, choosing the proper NC is critical to optimise its functionality and production costs.

2.8.3 Enhancer filler

Adding fillers can physically enhance handsheets by filling the gaps of the fibre network. This can not only prevent the penetration of moisture and oil but also increase the density to improve their overall strength. Certain fillers, such as hemp seed husk, corn germ, and canola meal, provide high fat and protein contents as mentioned above, which offer extra functions to the sheets. This approach also provides opportunities to make full use of more waste fibres that might not be suitable as major blend materials, which is applicable for various packaging applications where moisture resistance and enhanced strength are critical.

2.9 Conclusion

Moulded fibre materials play an important role in reducing non-degradable packaging, by offering a sustainable alternative that can be composted or recycled. Alternative fibre materials can be used as substitutes for conventional wood-based fibres in moulded fibre packaging, and their mechanical and barrier properties of moulded fibre products vary depending on fibrous components, pulping methods, and manufacturing processes. Based on the current review, apple pomace and corn husk show potential for enhancing these properties, although they have some limitations. Hemp seed husk is selected to serve as a filler that potentially enhance the performance by filling gaps within fibrous network. Particle sizes of these materials need to be controlled to minimise voids, so that performance would be enhanced through densification. With the consideration of commercialisation, only mechanical pulping would be utilised to keep production costs low. The literature provides solutions regarding pulping methods that may have limited application in this study as the particles of apple pomace and corn husk involved in this study are predicted to be large. Therefore, this study will also explore treatments such as refining, grinding following with particle sieving to control and investigate the proper particle sizes, to enhance barrier properties while maintaining the material's inherent mechanical strength.

Chapter 3 Preliminary Formulation Screening

3.1 Introduction

The focus with fibre-based packaging materials is improving their low water and oil resistance, which compromises mechanical properties and limits their usability. From the literature review, apple pomace and corn husk were selected as potential fibres to improve mechanical performance of traditional wood based moulded fibre materials, due to their great mechanical properties and high availability. Hemp seed husk was incorporated as a functional additive to further consolidate the barrier properties of the handsheets by filling the voids. The study was carried out in two stages. In the first stage, standard handsheets made following the TAPPI T205 standard were produced and tested at Massey University to identify the optimal formulations by evaluating their tensile force, and resistance to water/grease using the $Cobb_{60}$ and oil penetration tests. After identifying one to two promising formulations, they will then be manufactured and comprehensively tested at Scion to determine the best performing formulation, which will be used for moulded fibre tray prototype production and assessment.

Research shows that paper made form mechanical pulp tends to exhibit inferior mechanical properties compared to chemically pulped paper (Mboowa, 2024; Zhang et al., 2022). However, with the consideration of the commercial viability of this study, the simple and cheaper mechanical processing techniques will be employed to process the alternative fibre stream (apple and corn). Therefore, decreasing porosity to increase handsheet density and fibre bonding will be the primary focus to improve both mechanical strength and barrier properties, with the help of the functions from original compositions of fibre materials.

3.2 Apple pomace slurry preparation

3.2.1 Disintegration

Apple pomace (AP) was sourced from Profruit in Hastings, New Zealand, and stored at -18°C. It was suggested by Gouw et al. (2017) to use 200 g of AP in 1 L of distilled water for disintegration. The rotating speed of the disintegrator (JEFFCO C200) was set at 3000 rpm. The resulting slurry was then screened using standard sieves with mesh sizes of 212 μm and 1 mm.

3.2.2 Wet sieving

Based on research by Vries (2024) and da Luz et al. (2017), the use of large sized fibres (> 500μm) can result in unbound particles due to the reduced adhesive interaction between cellulosic compounds. Therefore, large seeds and skin residues were screened out by wet sieving the slurry following disintegration. To retain the essential fibre components and remove larger particles from apple skin that could float on the surface of the pulp slurry, which affect the overall grammage and draining speed, 212 μm and 1 mm sieves were used to separate the larger particles. The AP slurry was first poured onto the 1 mm sieve, which was then sieved by pouring 1L of distilled water gradually for several times to sieve out the larger particles such as seeds and skin residues, a container was placed underneath the sieve to capture the mixture of apple pomace with particle size smaller than 1 mm. When sieving out the smaller particles, a spatula was utilised to swap and press the apple pomace slurry, to speed up the dewatering and capture as many fine particles as possible. The mixture (with particles < 1mm) in the container was then poured onto the 212 μm sieve, and another spatula was used to agitate the mesh to accelerate water drainage and thicken the slurry (**Figure 20**), and in this process, adding some water could help speed up the drainage, but it was not necessary as only the solid slurry on the mesh would be retained. The solid content level was not specified because the consistency was accurately measured for each batch of slurry.

Figure 20. Screened apple pomace slurry with fine particles.

The purpose of sieving was to eliminate the suspended fibre residues (larger skin fragments), as shown in **Figure 21**, to avoid clusters of fibre residues, which accumulate on one side of the handsheet if they were not removed (See **Figure 22**).

Figure 21. Large fibres and fragments left on the wall of the cylinder when making handsheet.

Figure 22. The suspending fibres left on the surface of the handsheet specimens that might influence the appearance.

3.2.3 Consistency measurement

The consistency was measured by placing small amounts of the AP slurry into three pre-weighed aluminium drying dishes and then drying in an oven at 105 °C overnight. The total dry weights were recorded the next day to determine the average consistency of the slurry sample using the following equation:

$$Consistency = 1 - \frac{W_{dt} - W_{dish}}{W_{wt} - W_{dish}}$$

where dt and wt mean dry total and wet total, respectively.

3.2.4 Hemp seed husk powder preparation

Hemp seed husks sourced locally from Hemp Connect Ltd were ground using a lab-scale blender operating at its maximum power setting to create a fine powder, which was then sieved to achieve a particle size below 106 μm, based on research finding by Alghamdi (2021). This research highlighted that a filler particle size ranging from 50 to 90 μm could enhance tensile modulus by 95% and strength by 7%. However, due to limited production capabilities for this specific particle size range of hemp seed husk powder and considering the particle size of apple pomace fibres, it was decided to adjust the hemp seed husk particle size to about half that of apple pomace to effectively fill the voids, which was around 106 μm.

3.3 Blend of BCTMP and apple pomace fibres

The blend of BCTMP and AP fibres and hemp seed husk powder were prepared following the TAPPI standard TAPPI 205 sp-02, which requires a standard total amount of 24 g dry material. The designed ratios of BCTMP to biomass are shown in **Table 14**.

Table 14. Formulation of the handsheet specimens.

Formulation	BCTMP	Apple pomace	Hemp seed husk powder
1	100%	0%	0%
2	90%	0%	10%
3	80%	20%	0%
4	70%	20%	10%
5	65%	35%	0%
6	50%	35%	15%
7	50%	50%	0%
8	30%	50%	20%
9	20%	80%	0%
10	0%	80%	20%

3.4 Standard handsheet forming

3.4.1 Handsheet formation

The standard handsheet sample produced is based on the TAPPI T205 standard in 159 mm diameter. However, the handsheets made for preliminary screening were in 150 mm diameter due to the fixed size of the forming wire on the handsheet machine utilised (**Figure 23)**, however, the process still followed the standard procedure. The drainage outlet of the handsheet machine was connected to the vacuum in case of excessive drainage period due to low freeness of pulp. To create a handsheet with a basis weight of 225 g/m² from apple pomace, 1333 mL of a 0.3 wt.% stock pulp slurry was poured into the handsheet maker, mixed with 8 L of water, and agitated six times. After a 5-second settling period, the water was drained to form the handsheet on the 125-mesh forming wire.

Figure 23. Handsheet machine utilised for preliminary screening stage. The draining pipe was connected to the vacuum, and an airgun was connected to the compressed air for removing couched handsheets.

The formed sheet was then covered with a piece of standard blotting paper (Ahlstrom-Munksjö, Grade 240, 20.32 cm x 20.32 cm), with the smoother side in contact with the formed sheet. A rubber flat and circular couch plate matching the wire size was placed on top, and a 13 kg roller was rolled over it five times, backward and forward, to complete the couching process. The handsheet was removed using compressed air from an airgun (**Figure 23**), and then placed on a new sheet of blotting paper with a polished steel plate on top. The forming and couching processes were repeated until a stack of ten handsheets was formed. The stack was pressed using an Instron universal testing machine with circular platen parts (**Figure 24**) at 50 psi (approximately 6100 kg based on the sheet's surface area) for 5 minutes to strengthen the fibre network and consolidate the sheet formation. The stack was then re-pressed with fresh blotting paper for an additional two minutes with the same pressure. Finally, the pressed handsheets were placed in drying rings (3D printed to fit the size) (**Figure 25**) and left in a temperature- and humidity-controlled room (TCR) at 23°C and 50% relative humidity to equilibrate.

Figure 24. The circular platen part of Instron tensile tester utilised for pressing process.

Figure 25. Drying ring that 3D printed to fit the size of handsheets.

3.4.2 Specimen conditioning

In accordance with the T402 sp-08 standard, "Standard Conditioning and Testing Atmospheres for Paper, Board, Pulp HandSheets, and Related Products," all handsheets were conditioned prior to testing at 23.0 ± 1.0°C and 50 ± 2.0% relative humidity. They were kept in the drying rings overnight, followed by an additional 24 hours of conditioning outside the drying rings.

3.5 Mechanical and barrier testing

During the preliminary formulation screening stage, only tensile force, water/oil resistance, along with the grammage and thickness were measured to identify which formulations could offer the best overall performance.

3.5.1 Grammage and thickness

Grammage was measured by weighing each handsheet using a laboratory analytical balance (Sartorius, BCE224I-1S) with a precision of 0.0001 g, and the results of the eight sheets were averaged. The area of each specimen was approximately 0.0177 m^2 for the 150-mm handsheets. Grammage was calculated by dividing the weight of the handsheet by its area with the unit of g/m^2.

The thickness of the handsheets was measured using a digital caliper, following the TAPPI T411 om-97 standard method “measuring the thickness (Caliper) of paper, paperboard, and combined board.” Each conditioned handsheet was measured from ten different locations, and the thickness data was recorded in millimetres to two decimal places and the mean value was calculated.

3.5.2 Tensile strength

Tensile strength is a particularly important property for packaging materials, as it measures their ability to withstand mechanical stresses from stretching and loading from heavy goods. The tensile test for paper and packaging involves gradually pulling the specimen from both ends until it breaks to assess the material's resistance to such forces.

The tensile test for the preliminary screening was conducted following the TAPPI T494 om-01 method, "Tensile Properties of Paper and Paperboard," using an Instron machine with wedge-action grip parts (**Figure 26**). Due to the size of the handsheets, test strips were cut to a width of 15 mm and a length of 120 mm with two stripes cut from each handsheet. Each strip was clamped with 10 mm held on each side, leaving a 100 mm gap between the grips. The grips were then separated at a rate of 25 mm/min until the strip broke. The results of the maximum force at break were recorded to determine the tensile property. The position of the cracks on the strip was observed, as if the crack occurred at the gripped area, within 10 mm from each side, the result was identified as a failure. The tensile force data was normalised with the grammage for an objective comparison.

Figure 26. The mechanical wedge action tensile grip parts of Instron tensile tester that utilised for tensile test. From Instron's official site.

3.5.3 Cobb test

The Cobb test is designed to evaluate the water absorbency of packaging materials over a specified period. The $Cobb_{60}$ test (with "60" referring to 60 seconds) was conducted using a manually constructed Cobb tester (**Figure 27**), following the method outlined in the TAPPI T441 om-09 standard, "Water Absorptiveness of Sized (Non-Bibulous) Paper, Paperboard, and Corrugated Fiberboard (Cobb Test)."

Figure 27. Cobb tester constructed following the illustration in TAPPI stand.

Each specimen was weighed and positioned on the plastic base beneath a cylinder with an area of 100 cm^2. The specimen was then securely clamped underneath the cylinder by tightening four screws symmetrically along the edge of the base. Approximately 100 mL of water was poured into the cylinder, allowing the specimen to absorb the water for 45 seconds. After removing the water, an additional 15 seconds were given for further absorption. The wet sheet was then placed on blotting paper, and excess water was removed by rolling a 13 kg metal roller over it once, back and forth. The sample was weighed again, and the Cobb value was calculated in g/m^2 using the following equation:

$$Cobb\ value = \frac{m_2 - m_1}{A}$$

m_2 = the weight of specimen with water absorbed
m_1 = the initial weight of the specimen
A = the area of the $Cobb_{60}$ tester (typically 100 cm^2)

3.5.4 Oil barrier testing

For the oil barrier test, each handsheet specimen was cut into two rectangular pieces (10.5 cm by 12 cm) from the central part of the sample and firmly adhered to a blotter to ensure immediate detection of oil penetration, as illustrated in **Figure 28**. Then, 0.8 mL of rice bran oil was pipetted onto the sample, and timing began. The penetration was observed every 10 minutes during the first hour, and every 30 minutes after the first hour until five and half hours.

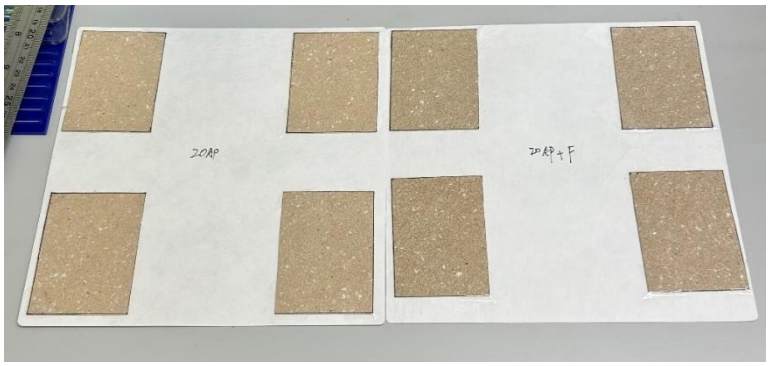

Figure 28. Template for oil penetration test in preliminary trial.

3.6 Results and Discussion

3.6.1 Apple pomace handsheet formation

The standard apple pomace and BCTMP handsheets are illustrated in **Figure 29**. Apple pomace was utilised as the primary biomass material, while hemp seed husk powder was added as a functional additive to fill voids within the fibre network to enhance barrier properties. All handsheets are labelled using abbreviations that represent the percentage of apple pomace (AP) and hemp seed husk powder, which serves as a functional additive (F). For example, a handsheet containing 35% apple pomace and 15% hemp seed husk powder is abbreviated as 35AP+15F.

Figure 29. The standard apple pomace handsheets made for preliminary screening. The formulation from left to right are 100% BCTMP, 90% BCTMP + 10% F, 20% AP, 20% AP + 10% F, 35% AP, 35% AP + 15% F, 50% AP, 50% AP + 20% F.

The handsheets appeared darker as the proportion of apple pomace and hemp seed husk powder increased, which contributed to the darkening of the surface, and the increase in apple pomace content seemed to intensify surface curling. This effect could be due to moisture imbalances during air-drying caused by the rapid moisture removal from apple pomace fibres in the TCR, causing the shrinking of fibre in response to moisture changes, leading to stress imbalances (Caulfield, 1987).

In addition, the apple pomace handsheets did not form properly when the BCTMP content dropped below 30%, resulting in a pasty mixture on the forming wire that was difficult to remove, as illustrated by **Figure 30**. Since handsheets made of 50% AP and 20% F were successfully formed, it indicates that a minimum of 30% BCTMP pulp is required for proper apple pomace sheet formation. Also, when the apple pomace content increased to 35%, differences in the appearance of the handsheet sides were observed

as the non-wire side had a higher concentration of seeds on the surface. This may be because of differences in settling rates caused by the various densities of seeds, skins, and other slurry components. Seeds and skin fibres are generally less dense than other fibres with slower settling rates, so they accumulated on the upper side of the sheets. A similar observation was reported by Rajala (2012), who described a phenomenon called two-sidedness. This occurs when high filler or small particle content combined with uneven water drainage in the wire section of a paper machine, that creates structural differences between the two sides of the paper, resulting in variations in brightness, smoothness, colour, and gloss.

Figure 30. Pasty handsheet made of 80% apple pomace and 20% BCTMP blend. The fibre materials stuck to the forming wire that was unable to be removed.

3.6.2 Grammage, thickness and density

Summarised values of weight, thickness, density and grammage, including the standard deviation (SD) for the standard handsheets are presented in **Table 15**. The area of the handsheets was consistent (0.0177 m^2) and density was calculated using the following equation:

$$\text{density} = \frac{\text{Weight (g)}/1000}{\text{Area (m}^2) * (\frac{\text{Thickness (mm)}}{1000})}$$

Table 15. Physical properties of apple pomace handsheets, including weight, thickness, density and grammage.

Parameter	BCTMP	10F	20AP	20AP + 10F	35AP	35AP + 15F	50AP	50AP + 20F
Area (m^2)	Consistently as 0.01767							
Weight (g)	3.959	3.932	3.898	3.845	3.967	3.754	3.855	3.683
SD	0.104	0.099	0.027	0.028	0.027	0.023	0.026	0.027
Thickness (mm)	0.741	0.701	0.655	0.642	0.562	0.515	0.514	0.456
SD	0.022	0.025	0.017	0.019	0.031	0.025	0.013	0.033
Density (kg/m3)	302.38	317.41	336.76	338.93	399.50	412.51	424.12	457.15
SD	7.96	7.96	2.35	2.47	2.75	2.54	2.88	3.42
Grammage (gsm)	224.06	222.51	220.58	217.60	224.52	212.44	218.16	208.46
SD	5.896	5.581	1.539	1.584	1.547	1.305	1.483	1.558

Note: the values in front of AP and F indicate the percentage values.

The density of the standard handsheets increased with a higher proportion of AP and F, while the thickness decreased. This can be attributed to the short fibre lengths of AP and F via the increased packing density of these short fibres. Similar findings were demonstrated by Giertz (1958) who examined that shorter fibres produced from beating showed enhanced inter-fibre bonding, thereby increased density. However, the tearing strength was reduced due to the excessive beating, which required a balance of strong bonding and individual fibre flexibility (Giertz, 1958). In addition, the reduction in thickness with added biomass was likely due to the fineness of these fibres that allowed fibres to fit more closely together, filling gaps and reducing the overall stacking effect, as supported by Joseleau et al. (2012). In contrast, handsheets with a higher proportion of longer BCTMP fibres tended to have a looser and more porous structure with greater stacking, leading to thicker specimens.

In this study, the AP fibres likely served as fillers within the BCTMP fibrous network to improve the inter-fibre bonding and increase the density of the handsheets, and the F particles appeared to have filled some remaining tiny voids for further densification. However, the density of specimens with F showed an increase compared to those without F, and the grammage decreased with the addition of F. This may be attributed to the strong suction from the vacuum setup used to expedite drainage, which likely caused the smaller particles to become trapped on the forming wire then passed through it. The low pH also negatively impacted filler retention and cohesion that led to particle loss during drainage (Semple et al., 2022).

The pH of apple pomace, ranging from 3.5 to 4.5, significantly lowered the overall pH of the pulp slurry, which altered the surface charge of F and other fibres. This likely resulted in the fibres becoming positively charged, causing repulsion and reducing cohesion between them (Petersson, 2011), thereby influenced the fibre bonding. As discussed in Section 2.7.1.1, small particles like AKD require the use of fixing or cationic agents to enhance their attachment to cellulose (Semple et al., 2022), suggesting the approach could be applied to F to maintain the retention. Furthermore, research by Abd Rahman and Azahari (2012) suggested that increasing the pH of the slurry beyond 8.0 helped improve filler retention. Therefore, incorporating calcium salts to raise the pH could be a viable strategy to enhance the effectiveness of the fillers (Gill, 1995). However, the commercial viability and compliance with food safety standards are important considerations, so it would be preferable to achieve the desired properties without additional chemicals.

3.6.3 Tensile force

The **Figure 31** summarises the tensile force of handsheets made of different ratios of BCTMP and AP. Among the standard handsheets without F, increasing the apple pomace fibre content improved indexes of force at break, with the 50AP having the maximum mean force at break of 0.462 $N \cdot m^2/g$, which was 60% higher than 20AP at 0.29 $N \cdot m^2/g$, 20% stronger than 35AP at 0.386 $N \cdot m^2/g$, and nearly four times higher than BCTMP handsheets at 0.093 $N \cdot m^2/g$. These results indicated that the addition of apple pomace improved the tensile strength, which was consistent with the results from

Gouw et al. (2017) and Lang et al. (2022), who reported improved mechanical properties when blending AP with traditional paper pulp. However, unlike those studies that utilised the AP's long fibre size to boost mechanical performance, the current study relied on their short sizes after disintegration to enhance inter-fibre bonding and increase handsheet density, thereby enhancing the tensile force (Alince et al., 2001; Giertz, 1958).

It is also notable that when comparing the tensile force indexes of handsheets with those having the addition of hemp seed husk powder, decreases in indexes of force at break was observed (some of them was significant while some were not), despite the increase in density. Studies such as I'Anson et al. (2008) and Lo et al. (2024) have suggested that higher density can improve tensile properties by enabling closer fibre packing and increasing bonding sites. However, tensile force is not only determined by density, the quality of fibre bonding also plays a critical role. While the short particles from F filled voids and increased density, they had disrupted bonding or effective stress absorption due to the low retention rate under acidic environment. Furthermore, multiple factors, such as higher lignin content of mechanical pulp, short fibre sizes, raised a range of issues in fibre bonding, as well as lower surface quality (Mboowa, 2024).

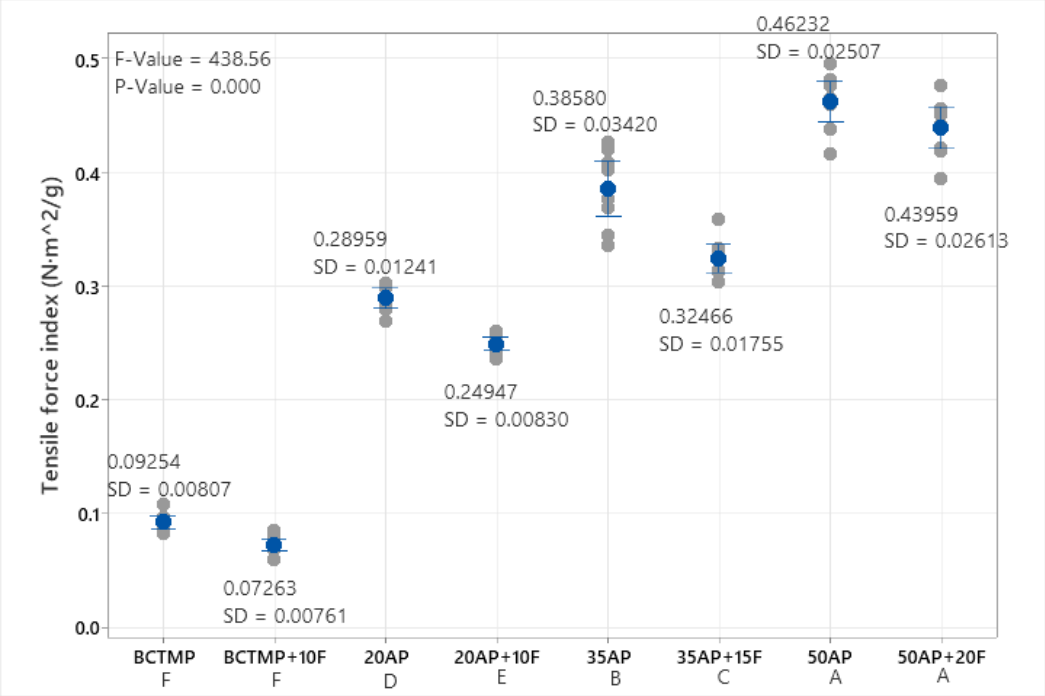

Figure 31. Tensile force indexes of all handsheet formulations with/without F.

3.6.4 Water and oil barrier properties

The mean Cobb values (in the unit of g/m²) of the handsheets, along with a corresponding comparison graph, are provided in **Table 16** and **Figure 32**. Lower Cobb values represent improved water resistance, indicating the material's capacity to resist water absorption (Li et al., 2020). The Cobb values decreased as the apple pomace and hemp seed husk powder increased.

The mean Cobb value for the BCTMP handsheets was 877.16 g/m², which considerably dropped with the addition of AP to 632.54 g/m² for the 20AP and 353.36 g/m² for the 50AP. **T**he water resistance was further improved with the addition of hemp seed husk powder, with the value of 50AP + 20F, 35AP + 15F, 20AP + 10F, and 10F further dropped to 319.05, 428.42, 546.52, and 731.79 g/m^2, respectively (**Figure 32**). The improvement in water resistance is likely due to the increased density as smaller particles filling the gaps between fibres (**Figure 33**), preventing water molecules from penetrating, and similar observation has been reported by da Luz et al. (2017) and Rajala (2012).

Table 16. Mean Cobb values of all handsheet formulations.

	BCTMP	10F	20AP	20AP + 10F	35AP	35AP + 15F	50AP	50AP + 20F
Cobb Value (g/m²)	877.16	731.79	632.54	546.52	515.00	428.42	353.36	319.05
SD	14.58	3.30	8.41	13.64	22.42	12.93	27.29	14.89

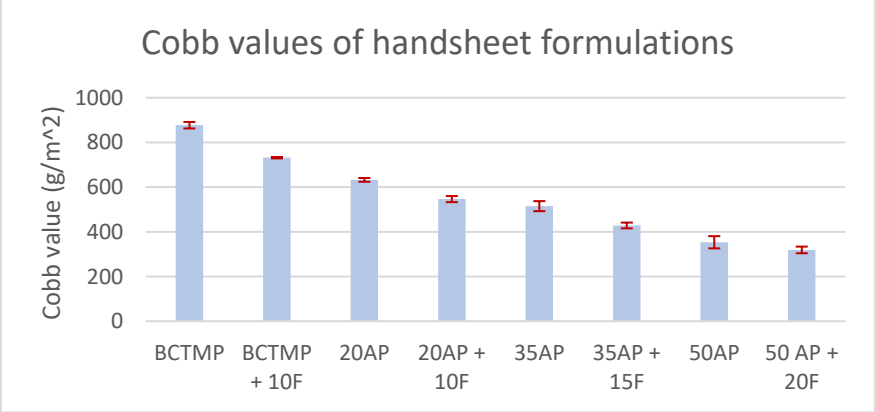

Figure 32. Trend of Cobb values of handsheets the proportion of apple pomace and hemp seed husk powder.

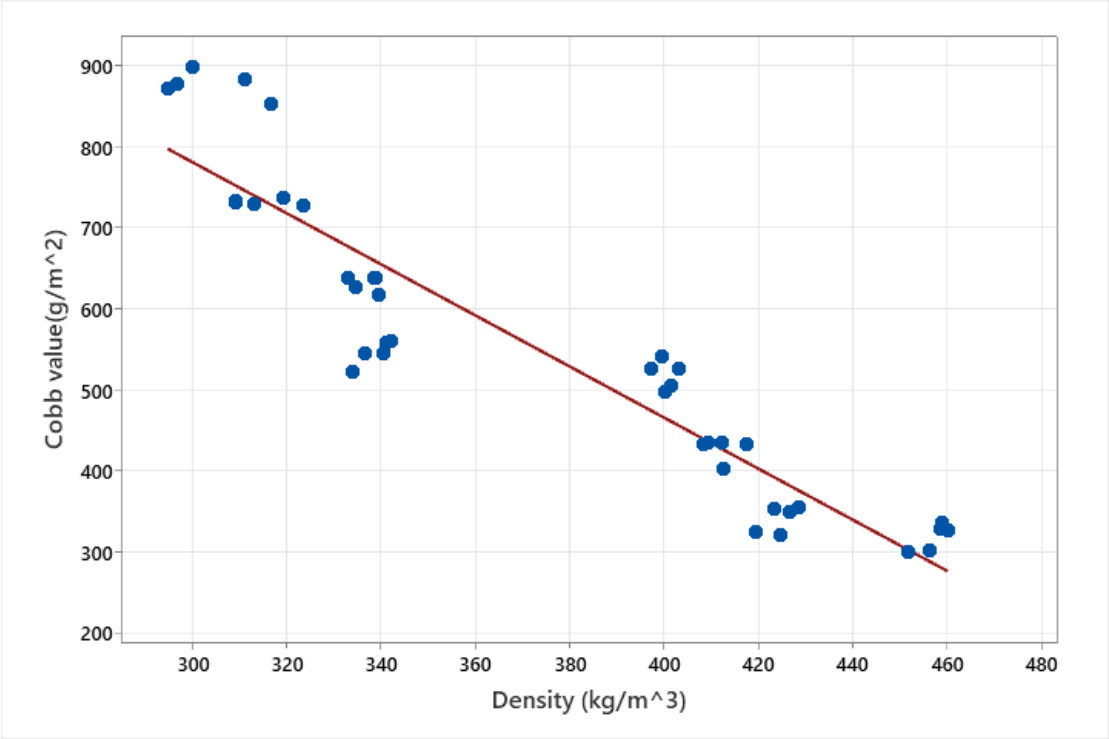

Figure 33. Graph of Cobb value versus density that showing the trend of Cobb values corresponding to the change in density, which have a negative correlation. It indicates that higher density leads to better water resistance of the specimen.

It is also noticeable that 50AP and 50AP + 20F showed minimal water absorption during the testing period with almost no water penetration, as illustrated in **Figure 34**. Since Lo et al. (2024) had found that hot pressing can further enhance waterproofing properties due to densification and hornification (a phenomenon of irreversible changes that occur in cellulosic fibre after hot-pressing, as introduced in literature review). Incorporating this process into formal production trial could potentially achieve further improvements in water resistance.

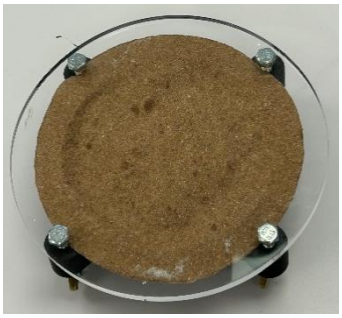

Figure 34. Nearly no water penetration on the back side of the 50AP + 20F after $Cobb_{60}$ test.

3.6.5 Oil barrier property

Table 17 present the oil penetration time (show-through time) for each specimen, showing that oil resistance improved with increasing AP/F content. As discussed in the previous section, shorter fibres from these biomasses effectively filled the voids, indicating increase density, that prevents oil molecules from passing through (**Figure 35**). A significant increase in show-through time was observed from the 35AP onward, raised from 46 minutes for 20AP + 10F to 3 hours for 35 AP, while the 50AP and 50AP + 20F exhibited no oil penetration within 5 hours, with unabsorbed oil remaining on the surface. These results indicate that these two specimens are well-suited for short-term applications such as takeaway containers, as without requiring additional barrier coatings is one of the objectives of the study.

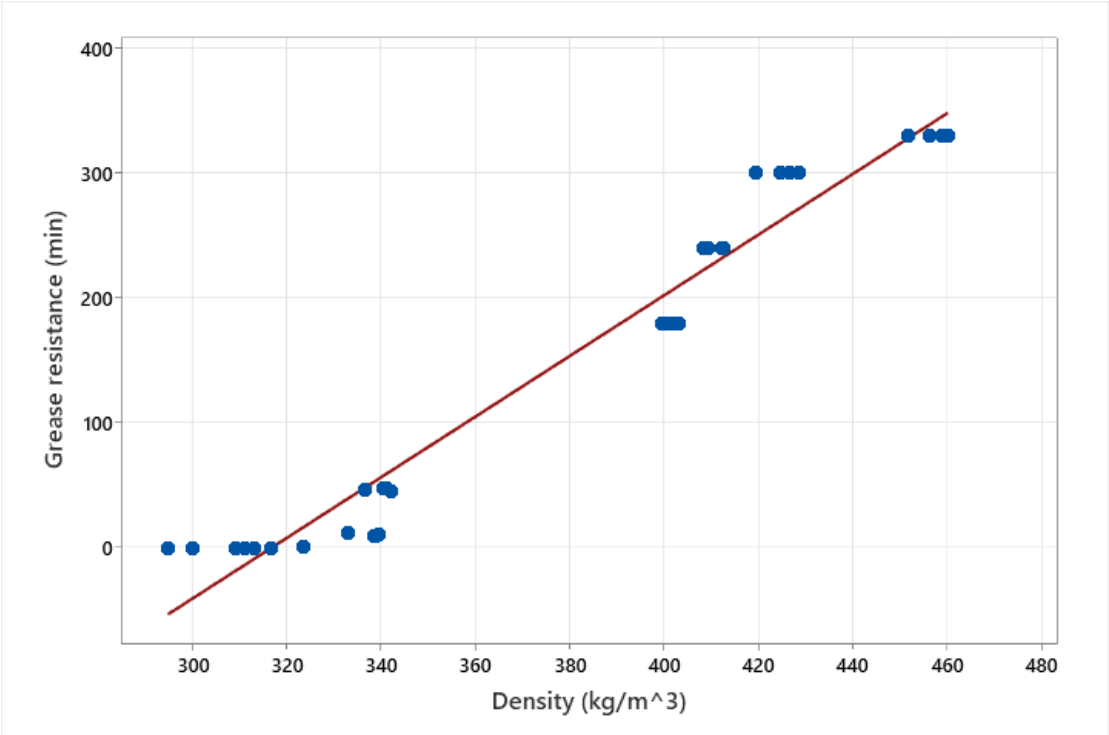

Figure 35. Graph of grease resistance (Penetration time) versus density that showing the trend of grease resistance corresponding to the change in density, which have a positive correlation. It indicates that higher density leads to longer time for oil to penetrate the specimen.

Table 17. The oil penetration time of the handsheets with apple pomace.

Specimen	BCTMP	10F	20AP	20AP + 10F	35AP	35AP + 15F	50AP	50AP + 20F
Penetration time (min)	0.3336 (20 sec)	0.3417 (22 sec)	10	45	180	240	>300	>300
	immediate penetration							

3.7 Conclusion from preliminary tests

Based on the preliminary experiments, hemp seed husk powder will not be used in further experiments, as the low pH of the slurry might hinder the retention of small particles. The use of chemicals in the slurry to improve retention also does not meet with the requirements of commercialisation, as it could raise both the cost and complexity of the process. Among the formulations without hemp seed husk powder, the 50AP formulation demonstrated the best tensile property, along with excellent water and oil resistance, which was the most promising option for potential manufacturing at scale. However, since vacuum suction was used for sheets with high apple pomace percentages to reduce drainage time, the 25AP formulation would also be produced as a contingency to ensures an alternative was available if vacuum suction was not accessible or if the drainage time for 50AP was excessively long. Their hot-pressed specimens will also be made and tested to assess whether they had improved performance, as moulded fibre production can involve thermoforming, which has a similar process to the hot-pressing.

Chapter 4 Manufacturing of the screened apple pomace handsheet formulation at Scion.

4.1 Standard handsheet making

Standard 159-mm-diameter handsheets were made following the TAPPI standard T205 sp-02 at Scion, the procedure is outline in the following sections.

4.1.1 Latency removal and pulp blending

- BCTMP pulp latency removal

Latency in mechanical pulping means delay of the fibre swelling and flexibility due to the residual rigidity with presence of lignin. The process of latency removal is to address the residual rigidity, which separate and straighten fibres to improve the mechanical quality of pulp and reduce energy inefficiency (Gao, 2014). The BCTMP dry pulp underwent a latency removal process. A dry BCTMP pulp sample (100 g) was mixed with 32 L of water. The mixture was then placed in the heating tank of the latency removal system, as shown in **Figure 36**. The latency was removed by disintegrating the pulp at 85 °C for 10 minutes, with all settings pre-programmed into the system. After the process, the pale-yellow-coloured slurry was collected and diluted to a 0.3 wt.% consistency using 1.33 L of cold water, while agitating at the same time, then left to cool to room temperature. The BCTMP pulp slurry was stored in a refrigerator at 4 °C when not in use, and the slurry was stirred for at least 30 seconds before weighing for making the handsheet to prevent uneven fibre distribution due to rapid precipitation of the fibre.

Figure 36. Latency removal system.

- Apple pomace-BCTMP pulp blend

The apple pomace slurry was prepared in advance and frozen, so it was thawed prior to use, and consistency was measured. Mixtures of apple pomace and BCTMP were then prepared in a stock beater at ratios of 1:1 (50% AP) and 1:3 (25% AP) as dry basis, based on their respective consistencies. The mixtures were stirred for 15 minutes at room temperature, as shown in the **Figure 37**. After mixing, the resulting light-coloured slurry (25% AP) and dark-coloured slurry (50% AP) were adjusted to a consistency of 0.3 wt.%, covered with lids, and stored at room temperature. The pulp slurry was thoroughly stirred before use to ensure uniformity.

Figure 37. Lab-scale stock agitator.

4.1.2 Handsheet formation

To form a 225 g/m² apple pomace handsheet, 750 mL of both AP and BCTMP pulp slurries based on 0.3%wt consistency were poured into the handsheet maker (MESSMER, model no. 38 M156200, as illustrated in the **Figure 38**), and mixed with 8 litres of water for 10 seconds. After mixing, the water was drained, forming a handsheet on the 200-mesh forming wire. The drainage time for the 50% apple pomace handsheets was approximately 5 minutes. The formed handsheet was then covered with a standard blotting paper (Whatman® gel blotting paper, Grade GB005), ensuring its smoother side attached to the handsheet. A flat, circular metal couch plate was placed on top, applying 8 psi pressure for 3 seconds during the couching process. The handsheet was flipped and removed from the wires, then placed into a press (as shown in the **Figure 39**) with a piece of blotting paper underneath and a polished steel plate on top. This process was repeated until a stack of ten handsheets was assembled. The entire stack was pressed at 50 psi for 5 minutes to strengthen the fibre network and consolidate the formation. It was then pressed again with fresh blotting paper for 2 minutes. Finally, the pressed handsheets were transferred to drying rings and kept in a

temperature- and humidity- controlled environment (23°C, 50% RH) overnight to be dried.

Figure 38. Handsheet maker - MESSMER, model no. 38 M156200, utilised for making standard sheets at Scion.

Figure 39. Standard press utilised for pressing the form sheets.

4.1.3 Hot press

After the pressing of standard handsheets, hot-pressed handsheets were produced using a laboratory-scale automated hydraulic Siempelkamp press (**Figure 40**). The sheets were placed on a hot plate and hot-pressed for 30 seconds at a temperature of 230 °C, with a pressing force of 7.8 kN per sheet, replicating the hot-moulding conditions used on the pilot scale moulded fibre thermo-former (KIEFEL Technologies® KFT Lab Natureformer KFT 90.1), in order to ensure the sheets met the practical requirements for moulded fibre tray production. After pressing, the handsheets were placed in a

temperature- and humidity- controlled environment (23 °C, 50% RH) to condition overnight prior to testing.

Figure 40. laboratory-scale automated hydraulic Siempelkamp press utilised for hot pressing.

4.2 Mechanical and barrier properties testing

4.2.1 Specimen conditioning

All handsheets were conditioned before testing under the same conditions at a temperature of 23.0 ± 1.0 °C and a relative humidity of 50 ± 2.0% RH. The sheets were initially conditioned in drying rings overnight, followed by an additional 24 hours of conditioning outside the drying rings.

4.2.2 Grammage

To determine the grammage, all handsheets were weighed using a laboratory micro-balance with a precision of 0.0001 g. Each specimen had an area of approximately 0.02 m². The grammage, expressed in g/m², was calculated by dividing the weight of each handsheet by its area. The average grammage of the sheets was calculated from these measurements.

4.2.3 Thickness

The thickness of the handsheets was measured by a digital micrometre (Lorentzen & Wettre, L&W) as shown in the **Figure 41**). The measurements followed the TAPPI T411 om-97 standard, "Thickness (Caliper) of paper, paperboard, and combined board." Each conditioned handsheet was placed on the anvil with a porous template, and the micrometre measured the thickness at ten non-overlapping points on eight sheets, respectively. The thickness of each handsheet was calculated as the average of the ten measured values on the sheet.

Figure 41. Lorentzen & Wettre (L&W) digital micrometre for measuring thickness.

4.2.4 Microscopic imaging

Microscopic images of the handsheets were captured using Optical Coherence Tomography (OCT) (OQ LabScope 2.0 SX) and the fringe projection (Primos Lite, Canfield Image System) technique used to measure the surface roughness and provide magnified views of the handsheet surfaces to see the porosity and fibre bonding.

OCT (see **Figure 42**) is a technique that employs low-coherence light to measure light reflection within a sample, creating 2D and 3D images. In this study, it was utilised to assess the porosity of handsheets. For porosity measurement and imaging, “Lumedica” software was employed with a 10x magnification lens. The process began by clamping the handsheet sample onto the platform beneath the lens. The microscope light was turned on, and the distance between the sample and the lens was adjusted until the 2D reflection image was clearly displayed on the top of the screen. Then the light was turned off, and the focus was refined to capture the surface image of the handsheets. Both B-scan (a 2D depth image showing the light scattering structure of the surface)

and surface images were saved for further analysis. Five different positions were measured for each specimen.

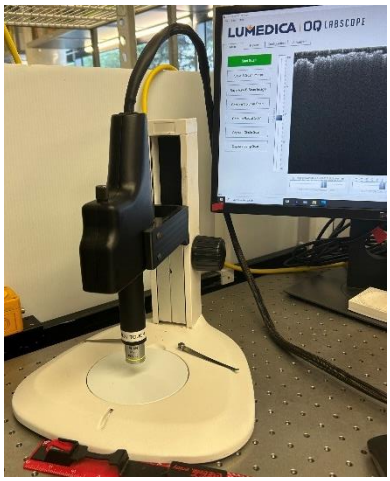

Figure 42. Picture of OCT (Optical Coherence Tomography), manufactured by Lumedica.

Fringe-projection (See **Figure 43**) is an optical technique for measuring the surface topography and 3D shape of an object by projecting structured light patterns on its surface. In this study, it was applied to measure the roughness of the handsheets. To conduct the roughness measurement, the sample was securely clamped onto the platform after starting the equipment. Using the "Primos" software to capture a live image, and the focus was adjusted until the cross on the screen was clearly visible. Once properly focused, a topographic image was taken (see **Figure 44**). The wrinkle analysis done through the software provided data on Ra (Arithmetic Average Roughness), Ry (Maximum Height of the Profile), and Rz (Ten-Point Average Roughness), which represented height measurements from different dimensions to comprehensively describe the surface roughness. Among them, Ra and Rz are the key parameters to determine the roughness and amount of peaks/valleys on the surface. Five different positions were measured for each specimen.

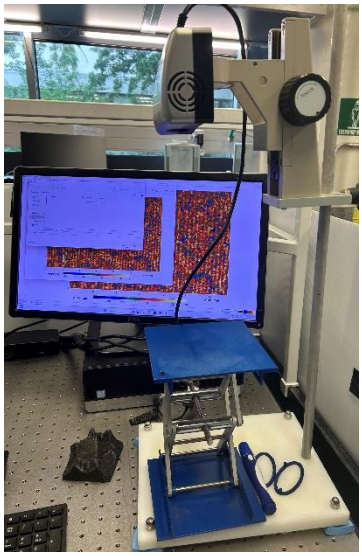

Figure 43. Fringe projection equipment, manufactured by LMI Technologies Gmbh.

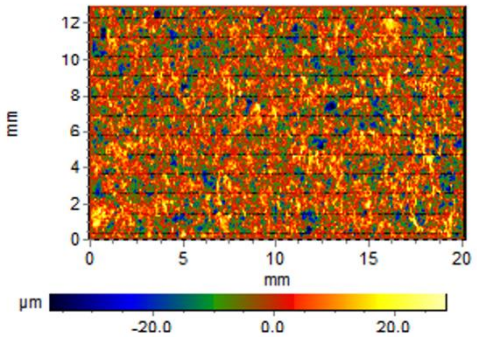

Figure 44. Example of topographic image of the handsheet surface taken by fringe projection.

4.2.5 Tensile test

The tensile test followed the TAPPI T494 om-01 method, “Tensile properties of paper and paperboard,” using an L&W Tensile Tester (**Figure 45**). The equipment measured five properties including tensile force at break, elongation percentage, tensile stiffness, tensile energy absorption (TEA), and tensile strength.

Eight pre-conditioned handsheets were cut into strips with a width of 15 mm and an initial length of 159 mm, which were then trimmed to a final length of 150 mm. Each strip was carefully positioned between the tester’s jaws, with equal lengths on both sides for even clamping. The "handsheets" testing program was selected, with the clamps set 100 mm apart and a separation rate of 25 ± 5 mm/min. During testing, the machine pulled the strip until it broke, and the software automatically analysed the results.

Figure 45. L&W Tensile Tester utilised for determining tensile related properties including tensile force at break, elongation percentage, tensile stiffness, tensile energy absorption (TEA), and tensile strength.

4.2.6 Burst Strength testing

Burst strength also serves as an indicator of a packaging material's ability to protect contents from impacts, stacking pressures, and other mechanical stresses. It is measured by subjecting the specimen to increasing hydraulic pressure until it bursts. The bursting strength testing was conducted using the L&W Bursting Strength Tester, as shown in **Figure 46**, based on the TAPPI T403 om-97 standard, "Bursting strength of paper." This method ensures precise and reliable evaluation of the material's resistance to bursting forces. To measure the burst, eight pre-conditioned handsheets were cut into semi-circular shapes with dimension of 124 mm diameter. Each test specimen was clamped and covered by a rubber diaphragm. A consistent pressure within the testing period of 30 ± 5 kPa was subjected and expanded by the hydraulic system to the testing sample until the specimen ruptured. The bursting strength data was generated by the machine and expressed in kilopascals.

Figure 46. L&W Bursting Strength Tester utilised for testing burst strength of specimens.

4.2.7 SCT testing

The short-span compression testing (SCT) evaluates the maximum compressive force at which paper and cardboard begin to fracture over a short span of typically 0.7 mm. The tests were performed using the L&W Compression Strength Tester STFI (See **Figure 47**) in compliance with TAPPI T826 om-08, "Short span compressive strength of containerboard." The results were recorded in units of N/m. Again, eight SCT strips with 150 mm × 15 mm were prepared and clamped between the tester's jaws. A clamping force of 2300 ± 500 N was applied, and the compression was conducted at a speed of 3 ± 1 mm/min to determine the maximum compressive load. The machine's software automatically recorded and analysed the test results.

Figure 47. L&W Compression Strength Tester STFI utilised for testing SCT.

4.2.8 Tearing strength testing

Tearing resistance is a measure of the energy lost by the pendulum of a tearing tester as it tears through a paper specimen when released from a specific height. In this study, the Elmendorf tearing test was employed, following the TAPPI T414 om-98 standard, "Internal Tearing Resistance of Paper (Elmendorf-type method)." The L&W Tearing Tester, as shown in **Figure 48**, was used for the tests. The tearing strength results were reported in units of mN/ply.

Eight handsheets were cut into strips measuring 53 mm in length and 63.00 mm in width. A pendulum determining test was conducted to select the appropriate pendulum for the correct force range and the required number of plies of specimens. During the formal test, the pendulum was lifted and positioned at its preset initial point. Each specimen was securely clamped and notched with knife to facilitate tearing. The pendulum was then released to tear the specimen. After tearing, the results were displayed on the monitor, and the pendulum was returned to its original position for the next test. This process was repeated for all specimens.

Figure 48. L&W Tearing Tester utilised for conducting Elmendorf tearing test.

4.2.9 Gurley test

Gurley test is utilised to evaluate the air permeability by measuring the time required for a specified amount of air, typically 25 mL in this study, to pass through a 6.45 cm^2 circular sample area. The testing followed the AS/NZ standard method, “Gurley Air

Permeance of Paper," using an L&W Densometer (see **Figure 49**). Eight replicates were tested for each formulation to ensure accuracy and consistency in the results.

As illustrated in the **Figure 49**, the Gurley test was operated by using a gravity-loaded cylinder to squeeze air inside a cavity using an oil seal to generate an air pressure of 1.22 kPa and was then directed to the specimen. As it passes through the sample, it escapes into the atmosphere via holes in the downstream clamping plate. The time for air permeance was recorded automatically by the device with a precision of 0.1 second.

Figure 49. L&W Densometer utilised for Gurley test.

4.2.10 Cobb test

The Cobb test measures the water absorption capacity of paper and cardboard materials, which quantifies the amount of water absorbed in grams per square meter (g/m^2) over a specific area and period (Li et al., 2020). The $Cobb_{60}$ testing was performed by using the Cobb sizing tester which is shown as **Figure 50**, based on the same TAPPI method as screening trial.

Eight specimen was cut into 20 cm x 20 cm square shapes and weighed, then positioned on the base of the Cobb tester, with a metal cylinder placed on top. The specimen was firmly clamped using a vertical toggle clamp with a slotted arm and a metal bar between them. Typically, 25 mL of water was poured into the cylinder, and the sample was left to absorb the water for 45 seconds. After removing the water, the specimen was allowed

an additional 15 seconds to absorb any remaining moisture, then placed on a piece of blotting paper, with a 13 kg metal roller used to roll back and forth once to remove any excess water. The sample was then re-weighed, and the Cobb value, representing the water absorbency in g/m² was calculated using the following formula:

$$W = \frac{m_2 - m_1}{A}$$

m_2 = the weight of specimen with water absorbed
m_1 = the initial weight of the specimen
A is the area of the Cobb tester (0.00255 m^2 for Scion's equipment)

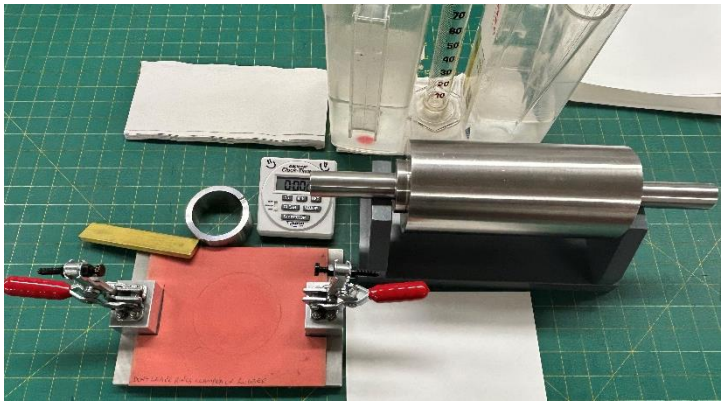

Figure 50. Cobb sizing tester, including a metal roller, timer, clamp, blotting paper, and tow measuring jars.

4.2.11 Grease resistance test

Oil and grease resistance are critical performance metrics for food packaging. In this study, grease resistance was assessed by quantifying the time it took for palm oil mixed with Sudan red (the oil sample used) to permeate the specimen and stain the copy paper underneath, and the amount of oil that broke through the sheet within 24 hours was recorded.

The area of the stain in an elliptical shape can be measured as the level of grease resistance and calculated using the following formula:

$$A = \frac{1}{4} \times \pi \times a \times b$$

a and *b* are the diameters of the major and minor axis of the oil stain.

In this study, the grease resistance test was conducted using grease resistance testing kits (See **Figure 51**), following the SS-ISO 16532-1:2011(E) standard, "Paper and Board - Determination of Grease Resistance - Part 1: Permeability Test," with minor modifications.

Two handsheets were cut into 20 × 20 cm square specimens, with a 3 cm diameter Teflon template placed at their centre. The template was filled with dyed palm oil, and a 54 g weight was placed on top of the grease sample, and time immediately noted. To monitor staining, the copy paper was regularly lifted to inspect the underside, checking every 10 minutes up to a maximum time of six hours, the checking time was flexible that the time was recorded once the stain was found on the copy paper. Once stains were observed, the time taken for the oil to penetrate was recorded, and the oil and weight remained on the specimen for 24 hours. Afterward, the stained areas on the copy paper were measured and calculated.

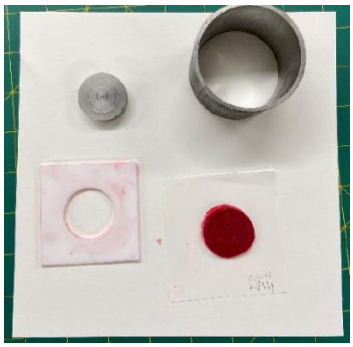

Figure 51. Grease resistance testing kits with Teflon template, grease sample, and weight, referred to Lo et al. (2024).

4.2.12 Contact angle measurement

Besides assessing water absorption, wetting kinetics is also important in determining water resistance, which is affected by the surface roughness and surface energy of the material. The contact angle is a critical measure of a material's hydrophilicity or

hydrophobicity, with the larger the contact angle between the material and a water droplet, the more hydrophobic the surface. The angle of 90° is as a boundary that the angles smaller than 90° denote hydrophilicity and a contact angle greater than 90° signifies a hydrophobic surface (Law, 2015).

The measurement of the contact angle was carried out using a drop shape analyser (B Frame System, model no. FTA 1000B) at room temperature, with its "Sessile Drop" method. This technique involves placing droplets on a solid surface and optically calculating the contact angle to assess the wettability of a localised area. In this study, the sample was cut into a small piece and positioned on an elevating table. Deionised water was slowly pumped until a sufficient volume formed a hanging droplet. The table was then raised to contact the droplet, triggering a loop of image captures stored by the camera. The contact angle was subsequently determined automatically by the software.

4.2.13 Fibre length scanning

The fibre length was scanned on the OpTest Fibre Quality Analyser (FQA), as shown in **Figure 52)**. Five grams of apple pomace slurry was diluted to 2 L with distilled water. A 20 ml portion of this diluted sample was further diluted to 600 mL with water for FQA testing. Three cups of the diluted samples were prepared to serve as triplicates. The FQA software automatically generated data on fines percentage, mean fibre length, curl index, fibre width, and kink index, along with corresponding graphs.

Figure 52. OpTest Fibre Quality Analyser (FQA) for measuring fibre length and width.

4.2.14 Data analysis

To analyse the data, individual interval graphs with two standard errors were plotted using Microsoft Excel and Minitab software. The one-way ANOVA, with a significance level (α) of 0.05, and Tukey HSD analysis was conducted using Minitab to assess the significance of differences in properties between hand sheet samples. The results also provided the mean values and standard deviations. Additionally, to achieve an objective and representative comparison of mechanical properties, the mechanical data was normalised by the grammage into their indexes.

4.3 Result and Discussion

4.3.1 Handsheet formation

The standard and hot-pressed handsheets produced are shown in **Figure 53**. The hot-pressed apple pomace handsheets appear darker compared to the standard pressed ones, likely due to thermal degradation and browning of the apple pomace at 230 °C, as suggested by Heras-Ramírez et al. (2012). Notably, the sheets produced at Scion did not exhibit curling, which support the earlier hypothesis that differences in conditioning methods were a contributing factor that the flowing air caused the moisture gradient, which resulted in the curling, while the static air in this trial prevented the uneven

moisture removal to avoid curling. In this study, the specific airflow rate was not measured because the working mechanism of the TCR was totally different between the preliminary and production trial. In the preliminary trial, the TCR operated by using a fan to regulate temperature, by which the fan started working when the ambient environment was changed. However, the TCR involved in this trial utilised a constant airflow with steady humidity and temperature which resulted in a static ambient air. The difference is most likely related to the faster air velocity of TCR at Massey.

(a).  (b). 

(c). 

Figure 53. (a) The standard- (left) and hot- (right)pressed 50% apple pomace (50AP) handsheets (b) The standard- (left) and hot- (right) pressed 25% apple pomace (25AP) handsheets. (c). The standard- (left) and hot- (right) pressed 100% BCTMP (BCTMP) handsheets.

4.3.2 Thickness and density

The physical properties, including weights, thickness, density and grammage of standard and hot-pressed handsheets are shown in **Table 18**. The density of the handsheets increased with the increased content of apple pomace and the application of hot pressing, while their thickness decreased. These patterns are likely attributed to the shorter fibre length of apple pomace, which allows its small fibres to fill the gaps between BCTMP fibres to reduce the overall stacking effect, aligning with previously discussed in the preliminary screening trial in Section 3.6.2. It is worth noting that the standard deviations of the densities of hot-pressed handsheets are higher than those of

standard sheets. This was likely due to the unparallel hot press, where the positioning of handsheets on different areas of the hot plate resulted in various levels of pressing intensity and densification, which could be referred to the thickness of individual hand sheets displayed in Appendix A.2, and this would affect the mechanical and barrier properties related to density. However, the overall trend of density would not change.

In this study, the mean fibre length was measured at 0.281 mm for apple pomace, compared with that of BCTMP at 1.282 mm, measured by Lo et al. (2024), who use the same BCTMP fibre source. The average fibre length of each formulation/combination was not measured individually, as it could be supposed to be deduced from the ratio of the apple pomace to BCTMP fibres, since the fibre length of these two materials did not appear to change when combined.

Table 18. The mean weight, thickness, density and grammage of standard and hot-pressed apple pomace and BCTMP handsheets. 50AP means 50% apple pomace and -Hp means hot-pressed, while BCTMP means 100% BCTMP.

Formulation	50AP -Hp	50AP	25AP -Hp	25AP	BCTMP -Hp	BCTMP
Area (m^2)	All sheets were 0.02					
Weight (g)	4.839	4.937	4.715	4.886	5.012	5.255
SD	0.028	0.041	0.135	0.174	0.050	0.052
Thickness (μm)	445.85	489.23	523.86	622.75	657.73	1092.85
SD	32.63	5.46	56.79	27.07	54.70	40.21
Density (kg/m^3)	549.32	508.28	458.65	395.44	386.50	242.43
SD	37.09	6.30	51.00	12.61	32.64	7.54
Grammage (g/m^2)	244.40	249.34	238.12	246.76	253.15	265.40
SD	1.43	2.05	6.80	8.78	2.52	2.63

Note: The thickness of each handsheet was measured in 80 replicates, with ten different points on each sheet and repeated on eight handsheets.

Specifically, BCTMP were 123% thicker than 50AP sheets and 75.5% thicker than 25AP sheets. Hot pressing applied additional compressive force that compressed the fibres and producing thinner sheets across all formulations. However, the differences between the thicknesses of hot-pressed sheets were reduced, which was because the handsheets with a higher percentage of BCTMP had more porous structure, which

appeared to have more space available for compression. BCTMP -Hp were 47.5% thicker than 50AP -Hp and 25.6% thicker than 25AP -Hp sheets. Among the samples, the 50AP -Hp demonstrated the highest density at 549.32 kg/m^3, which was 42% and 20% denser than BCTMP -Hp and 25AP -Hp, respectively. The shorter AP fibres serve as effective fillers in blends with BCTMP and other longer fibres to strengthen inter-fibre bonding and densifying the handsheets.

4.3.3 The surface observation of the handsheets

B-scan and surface images generated by OCT at 10x magnification are presented in **Table 19**, only one of the B-scan images of each specimen is displayed in the table, while the rest are provided in Appendix E. The OCT's B-scan utilises a light scattering technique to assess the material's density, with a denser structure allows for more light reflection, and vice versa (Fujimoto et al., 2000). This is illustrated in **Figure 54**, where the top white region represents the surface of the handsheet and the light reflection. It could be observed that some light rays were reflected from the surface, which presents the density of the structure, with more reflection means denser structure (as shown in **Figure 55**), due the tighter molecular structure that results in the higher refractive index (Liu & Daum, 2008). The darker hand sheets with more apple pomace content and application of hot-pressing can also cause more absorption of light, which decreased the light reflection. Furthermore, the dark areas in the white region represents where light scattering does not occur, which indicates the pores or air bubbles. The surface topography could also be seen in the shifts of the uppermost white area, though quantifying this would require fringe projection measurements.

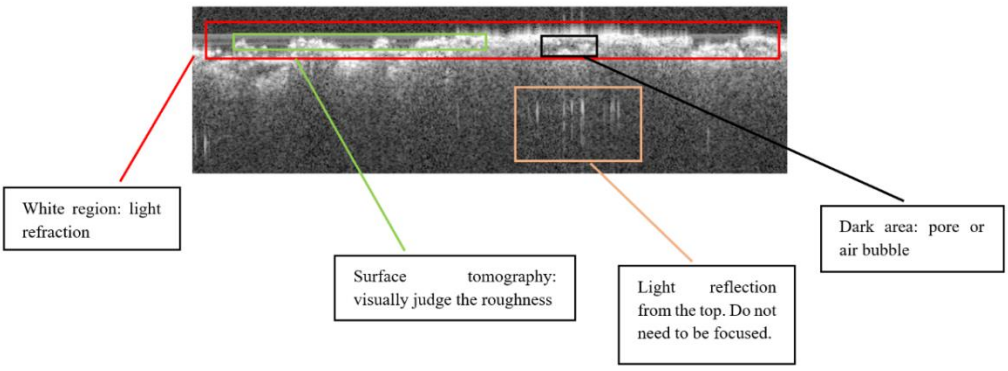

Figure 54. The illustration of the tomographic (B-scan) image interpretation.

Figure 55 shows an example of the comparison between two B-scan images, the one on the left exhibits less light reflection than the one on the right, implying a less dense structure. Additionally, the small dark areas among indicate that no light scattering or reflection occurred, likely due to pores.

a. 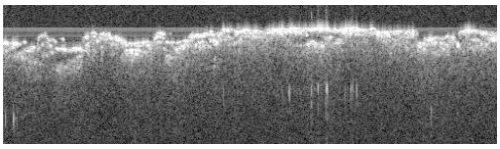 b. 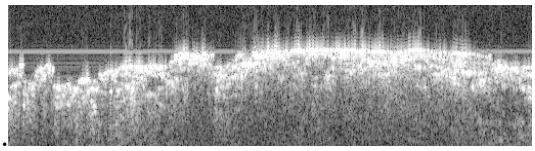

Figure 55. (a). An example B-scan image showing less dense structure. (b). An example B-scan image showing denser structure

Table 19. B-scan and surface images of 25% apple pomace, 50% apple pomace, and 100% BCTMP standard and hot-pressed handsheets taken by the OCT at 10x magnification.

	B-scan image	Surface image
BCTMP	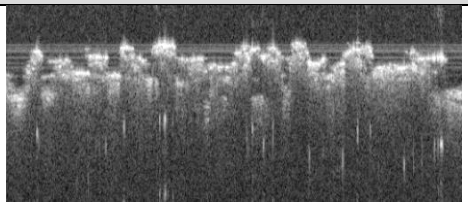	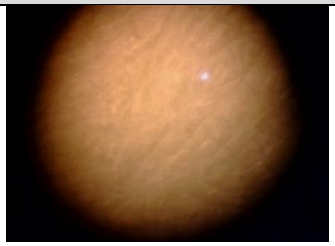
BCTMP - Hp	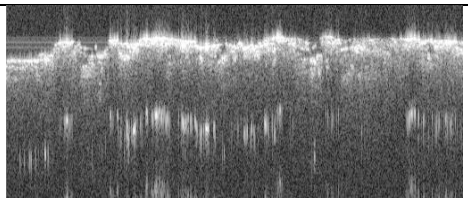	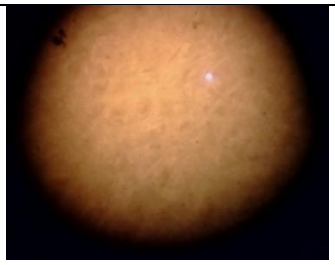
25AP	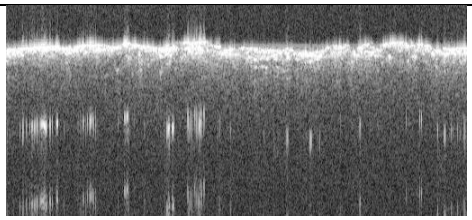	
25AP -Hp	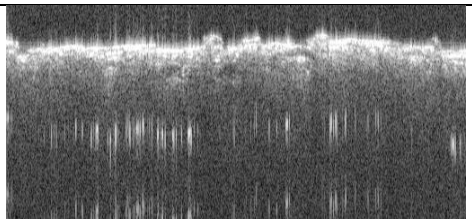	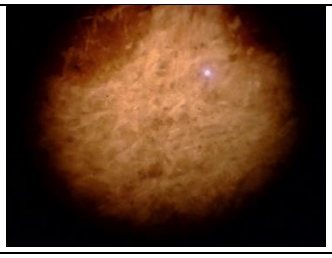

50AP	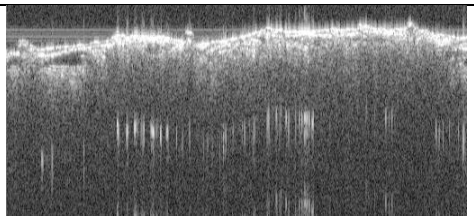	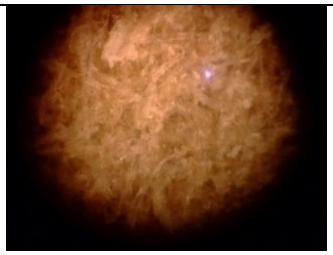
50AP -Hp	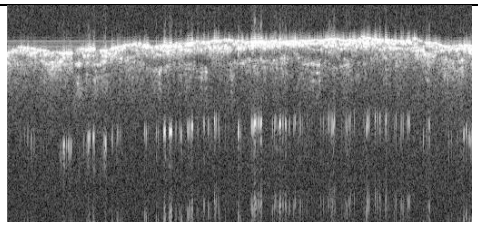	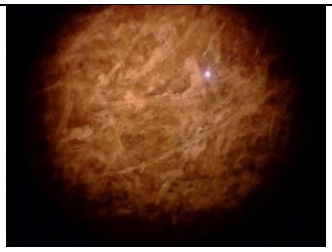

The B-scan images of each specimen showed generally similar porosity, suggesting a uniform distribution of surface porosity and tomography, where the details can be referred to the Appendix E. The B-scan images of 50AP and 50AP -Hp shows more light reflection than other specimens, which reveal their denser structure compared to other samples, aligning with the measurements in **Table 18**. In contrast, BCTMP and BCTMP -Hp showed the least light penetration with an uneven upper surface, representing less dense structure and rougher surface, especially for the BCTMP, numerous dark areas are present among the top region, indicating the large number of pores and uneven surface. This suggests that the increasing apple pomace and application of hot-pressing densify the handsheets, which aligned with the findings from the preliminary screening trial that the addition of fine apple pomace fibres filled the gaps between the wood fibres. Furthermore, the B-scan images displayed that the BCTMP had a rougher surface than 25AP, while 25AP was smoother compared to 50AP, and hot-pressing helped to smoothen the surface. The roughness would be quantified and detailly analysed in the section of roughness and wettability.

When comparing the surface images, blending 25% and 50% apple pomace into wood pulp resulted in visible darkened material, which were apple pomace, that filled the voids between the wood fibres. The hot-pressing process caused additional darkening of the surface, which was due to the browning effect induced by thermal treatment, which occurred as the degradation of polysaccharides and other components happened, as noted by Heras-Ramírez et al. (2012). This aligned with the visual observations of the handsheets. The increased densification after hot pressing could not be observed

from the surface images, as the process compressed the sheets to make the fibres pack more tightly without adding additional material to fill the voids, but this could be evaluated through B-scan images.

4.3.4 Tensile strength

Tensile strength reflects a material's ability to resistance to breaking under some tensile force, whereas the tensile index provides a normalised measure of tensile strength by factoring in grammage, providing a more accurate comparison across different samples. **Figure 56** illustrates the tensile index of apple pomace and BCTMP handsheets. The inclusion of apple pomace enhanced the tensile index, with hot pressing further increasing it.

Among the normal-pressed sheets, the 50AP sheets had the highest mean tensile index of 34.8 N·m/g, which is 522% stronger than that of BCTMP at 6.66 N·m/g and 59.4% higher than that of 25AP at 21.83 N·m/g. These findings support results of the preliminary screening trials although the tensile force measured in this trial was higher. The material loss and curling happened during preliminary trial, and experimental errors, such as overly tight clamps on the sides of the tensile strips by manual operation might lead to the difference.

As discussed earlier, the apple pomace handsheets in this study benefits from the smaller particle size of the pomace, which increased density and subsequently enhanced tensile strength. This improvement likely resulted from the formation of more closely packed fibrous networks and improved bonding between fibres, which pulled firmly on one another and resist breaking more effectively (Stark & Berger, 1997).

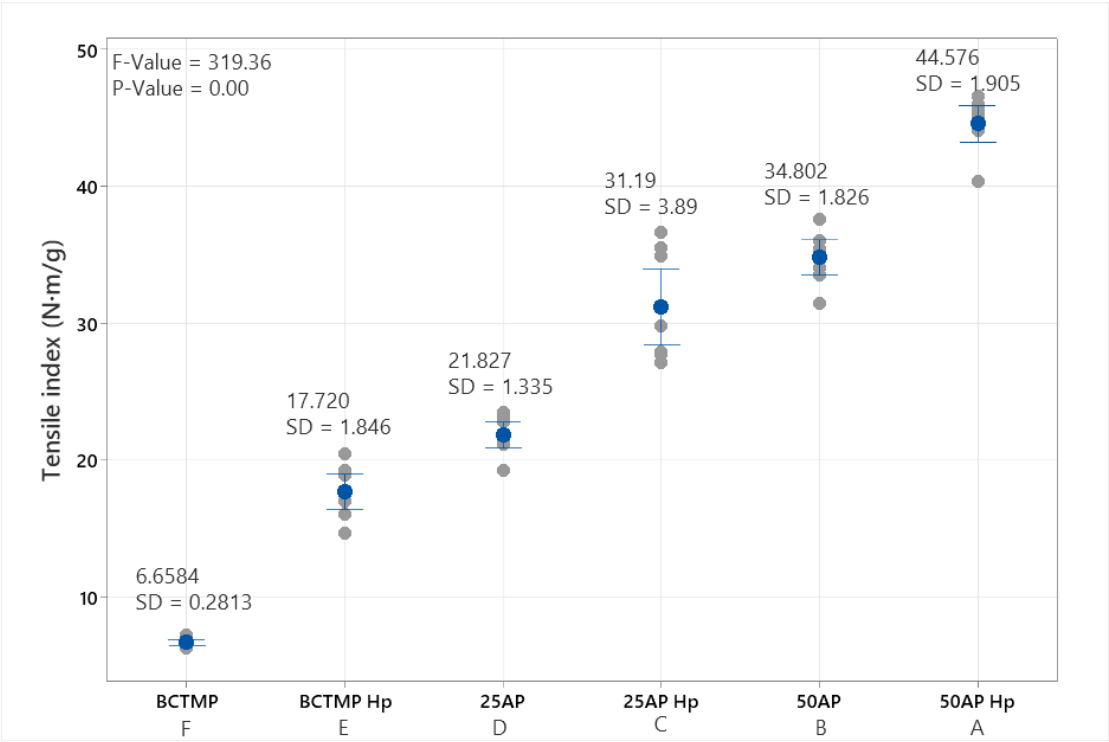

Figure 56. Tensile indexes of 25%, 50% apple pomace and 100% BCTMP standard- and hot-pressed handsheets.

Joelsson et al. (2020) and Lo et al. (2024) have previously suggested that hot pressing enhances the strength of paper products. The findings of this study supports this idea (**Figure 56**), the tensile index of 50AP -Hp, 25AP -Hp, and BCTMP -Hp all increased compared to their normal-pressed counterparts, with 50AP-Hp achieving the highest value of 44.58 N·m/g. which was 2.5 times higher than BCTMP -Hp at 17.72 N·m/g, and 43% higher than 25AP -Hp at 31.19 N·m/g. However, the increase in tensile index due to hot pressing for apple pomace sheets was less pronounced than that for BCTMP sheets. This is likely due to the less proportion of the looser BCTMP structure, which provides less space for densification when adding more apple pomace. The observed trend in the tensile index appears to correlate with density aligns with the initial assumption that mechanical strength could be enhanced by reducing fibre size.

4.3.5 SCT (short-span compressive testing)

Figure 57 illustrates the SCT strength indexes of apple pomace and BCTMP handsheets. SCT strength increased with the increasing apple pomace content and corresponding increases in density. The SCT index of 50AP was the highest at 22.41

N·m/g, showing a 172% increase over BCTMP, which recorded 8.21 N·m/g. The 25AP also showed improvement with SCT index of 16.14 Nm/g. After hot pressing, SCT indexes improved further across all samples, with 33.4 N·m/g, 22.25 N·m/g, and 15.85 N·m/g, for 50AP-Hp, 25AP-Hp, and BCTMP-Hp, respectively. These improvements are attributed to the denser structure of the sheets and possibly stronger fibre bonding associated with higher apple pomace content and the hot-pressing process. Similar findings were reported by Retulainen and Keränen (2017), who noted that increased density positively affects inter-bonding degree that finally enhanced SCT strength in recycled material handsheets. Joelsson et al. (2020) also observed that SCT strength of handsheets made of high-yield pulp improved with increased density after hot pressing. The BCTMP sheets showed the greatest proportional increase after hot-pressing, similar to the trend observed in the tensile indexes. This was likely because their standard sheets had a looser structure compared to the apple pomace hand sheets, which allowed more room for further densification during hot-pressing.

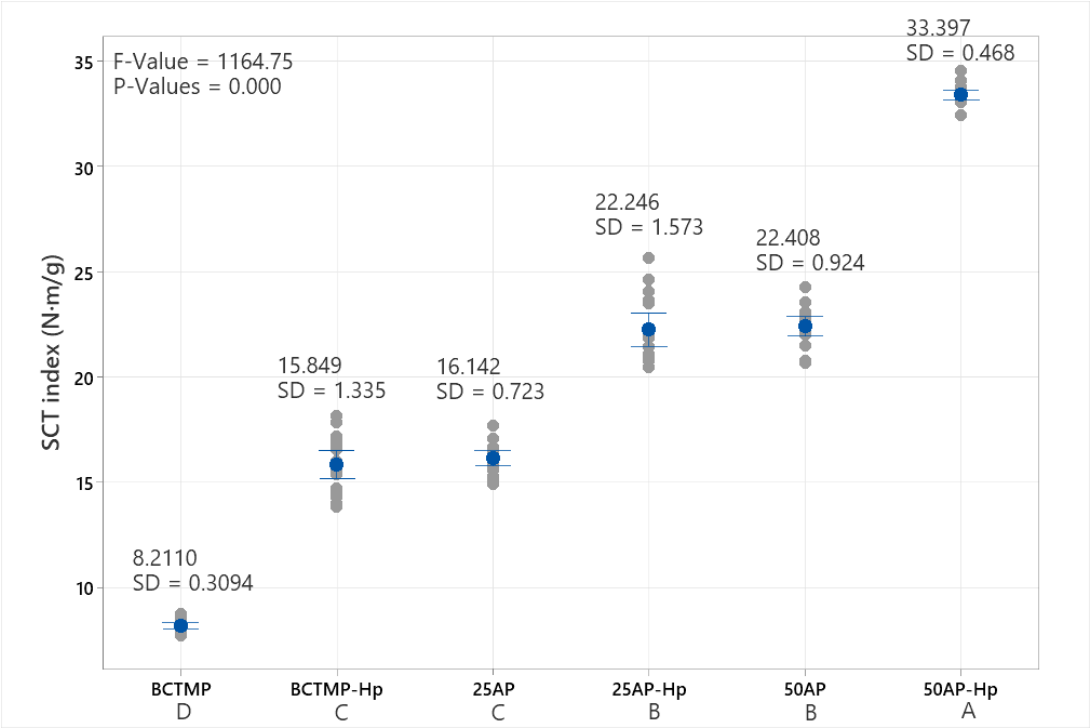

Figure 57. SCT strength of apple pomace and BCTMP standard- and hot-pressed handsheets.

4.3.6 Stiffness, Elongation and Tenile energy absorption (TEA)

Tensile stiffness refers to a material's resistance to stretching and is inversely related to elongation. Factors such as inter-fibre bonding, fibre length and flexibility, and moisture content significantly impact the stiffness of paper (Baley, 2002; Joelsson et al., 2020). **Figure 58** illustrates the tensile stiffness indexes of standard and hot-pressed apple pomace and BCTMP handsheets. Tensile stiffness indexes increased with a higher apple pomace content. Among the normal-pressed specimens, 50AP had a tensile stiffness index of approximately 3.878 N·m/g, which is about three times greater than BCTMP's 1.234 N·m/g, and 40% greater than 25AP's 2.81 N·m/g. This indicates that tensile stiffness increases with density, similar trends have been reported by Motamedian et al. (2019) and Strand et al. (2019). This trend is likely due to the denser structure enhances the rigidity, as tightly bonded particles reduce elasticity and limit excessive elongation.

Hot-pressed handsheets demonstrated greater tensile stiffness compared to their normal-pressed counterparts, as shown in **Figure 58**, likely due to the denser fibrous network formed through tight compression. The tensile stiffness index of 50AP-Hp reached 5.16 N·m/g, which surpassed that of 50AP and exceeded the tensile stiffness indexes of 25AP-Hp and BCTMP-Hp by 34% and 81%, respectively, with values of 3.851 N·m/g and 2.852 N·m/g.

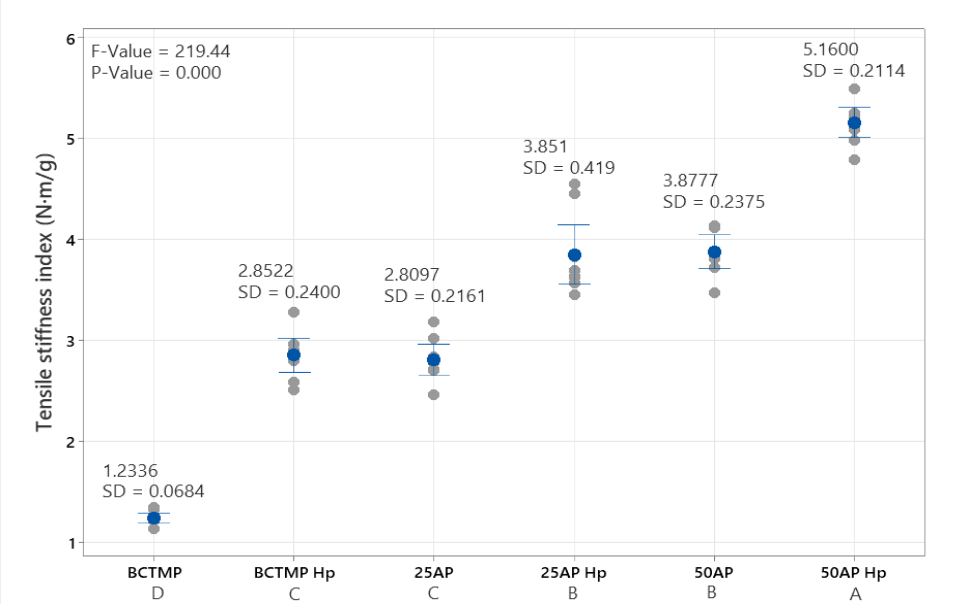

Figure 58. Tensile stiffness indexes of 25%, 50% apple pomace and 100% BCTMP standard- and hot-pressed handsheets.

Tensile energy absorption (TEA) is a measure of the energy a material can absorb before breaking under tensile stress, reflecting its toughness and flexibility, which is also an important attribute for packaging quality. TEA is expressed in J/m² and its index is expressed in J/g. Increasing the apple pomace fibre content in the handsheets improved TEA indexes (**Figure 59**). The TEA index of 50AP was 0.328 J/g, more than 11 times higher than that of BCTMP at 0.036 J/g. This increase is likely due to the density increase that made the fibre bonding tighter, making the sheets to absorb more energy to be pulled apart under the tensile stress.

However, an interesting trend emerged after hot pressing. While the TEA of BCTMP -Hp increased slightly compared to BCTMP, the mean TEA indexes of 25AP -Hp and 50AP -Hp decreased to 0.229 J/g and 0.328 J/g, respectively, with inverse trend of standard pressed sheet that TEA increased with increasing density. The decrease of 25AP -Hp was not significant. A similar inverse trend was observed in elongation results (See **Figure 60**), that the stretch index of 50AP -Hp decreased to 0.0050 %·m^2/g, from 0.0072 %·m^2/g of 50AP, and 25AP -Hp dropped to 0.0051 %·m^2/g from 0.0065 %·m^2/g of 25AP. These reductions became more pronounced with higher apple pomace portion.

This behaviour might be attributed to the composition and structural change after hot-pressing, which influence the structural properties of the handsheets. The literature review suggested that apple pomace has limited flexibility, and when it is subjected to thermal treatment, the degradation of polysaccharides and pectin in the fibres alters the structural integrity of the cell wall, making it more rigid (Schmid et al., 2020). To validate that, some apple pomace slurry samples were oven-dried to obtain dehydrated samples. The resulting dehydrated apple pomace displayed a hard and crispy texture, forming flocculent structures that could not be bent, stretched, or broken, demonstrating extremely high rigidity. Considering the hot-pressing temperature of 230 °C, it is likely that the apple pomace blend underwent dehydration even over the short period of time.

Hot-pressing can also trigger cross-linking reactions, such as lignin demethoxylation, which further reinforces the rigidity of the structure, proposed by Reiniati et al. (2015), who hot-pressed the wood fibre at 220 °C and found the increased crystallinity due to the loss of moduli caused by lignin cross-linking that made the fibre more rigid. The

shorter fibre length of apple pomace could also negatively impact TEA and stretching, as shorter fibres had limited bonding area that led to less capable of transferring stresses smoothly. Additionally, due to the already high density caused by the short fibres, hot-pressing could create an excessively dense structure with exceptionally strong fibre bonding and increased stiffness that might surpass the balance between bonding, stiffness, and flexibility (Giertz, 1958; Vainio & Paulapuro, 2007), which caused the sheets to break before being fully stretched. The hornification, introduced in literature review, could also increases the stiffness by reducing the fibre bonding area (Mo et al., 2024).

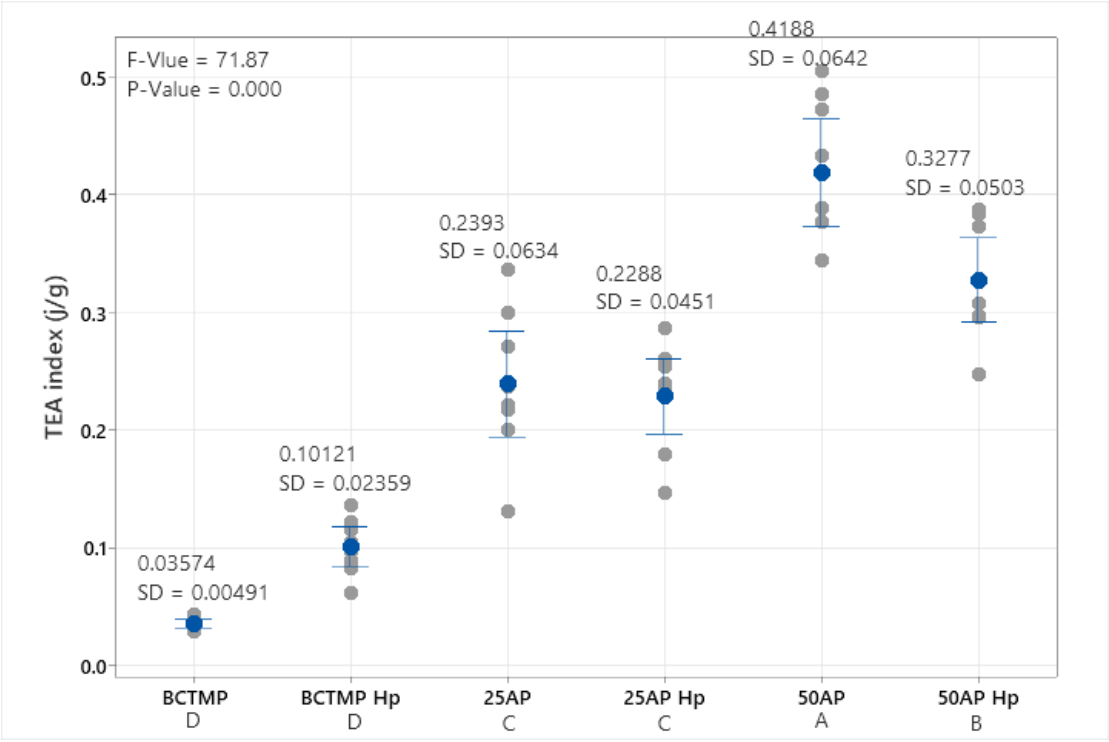

Figure 59. TEA (Tensile energy absorption) indexes of 25%, 50% apple pomace and 100% BCTMP standard- and hot-pressed handsheets.

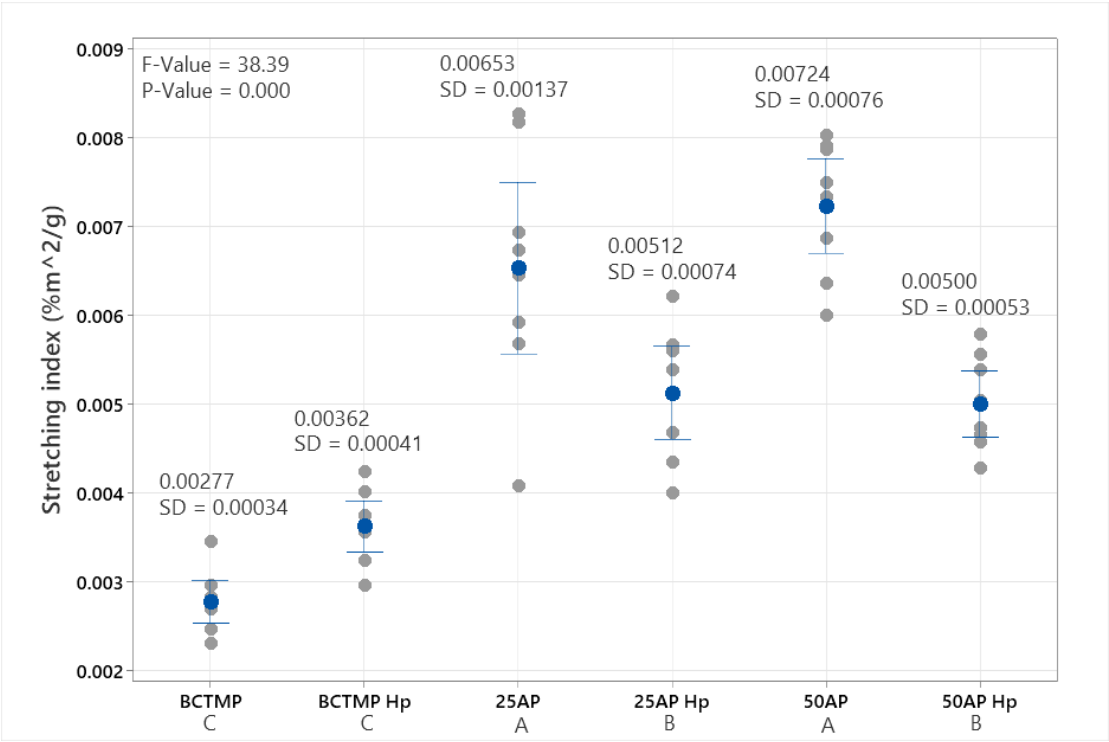

Figure 60. Stretching indexes of 25%, 50% apple pomace and 100% BCTMP standard- and hot-pressed handsheets.

4.3.7 Bursting strength

Figure 61 presents the bursting strength indexes of standard and hot-pressed handsheets. The addition of apple pomace fibres increased the bursting strength indexes along with increasing density. The bursting strength index of 50AP reached 1.545 kN/g, over five times greater than BCTMP at 0.271 kN/g and 42% higher than 25AP at 1.085 kN/g. Similar with the tensile strength and stiffness results, the hot-pressed handsheets exhibited enhanced bursting strength, which is due to the densification effect of hot pressing, resulting tougher and stiffer sheets. The bursting strength indexes of 50AP-Hp, 25AP-Hp, and BCTMP-Hp increased by 8.5% (not significantly), 39%, and 162% compared to their normal-pressed counterparts, reaching 1.676, 1.509, and 0.712 kN/g, respectively. The insignificant increase of 50AP -Hp was likely caused by the limited space for densification that since the 50AP was already highly dense, hot-pressing might have bring it close to its maximum achievable density, and resulted in its peak fibre packing.

In conclusion, bursting strength indexes showed a general positive correlation with both tensile strength and density because of the improved fibre bonding (Anjos et al., 2014; Bayatkashkoli, 2013).

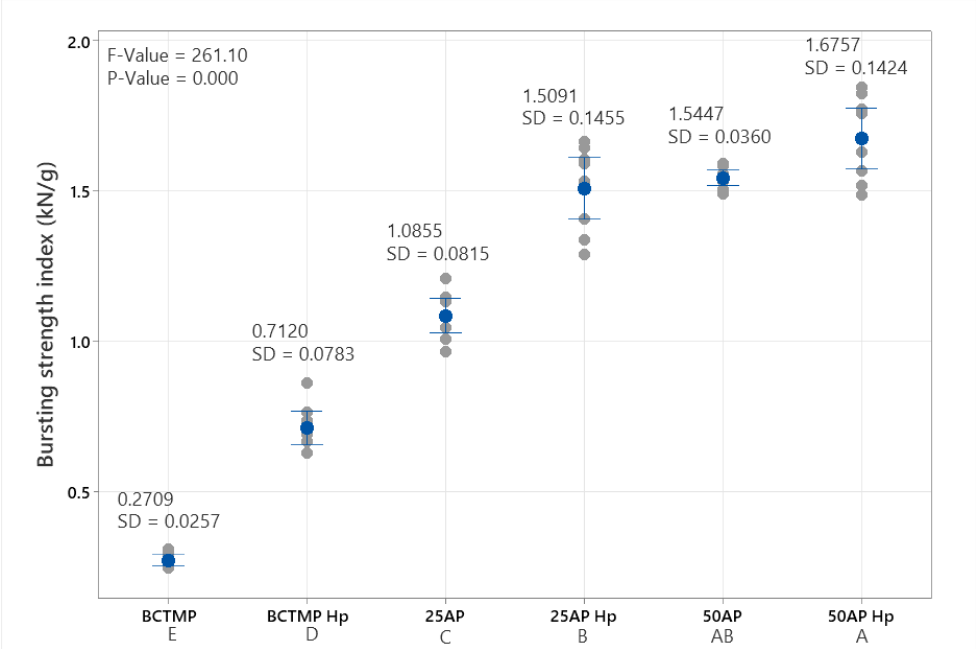

Figure 61. Burst strength of 25%, 50% apple pomace and 100% BCTMP standard- and hot-pressed handsheets.

4.3.8 Tearing strength

Tearing strength depends on several factors, including fibre length, inter-fibre bonding, and flexibility, indicate a material's resistance to the propagation of a tear once a cut or puncture is introduced. As shown in **Figure 62**, the tearing strength indexes of handsheets followed a trend similar to TEA and stretching indexes with a decrease for apple pomace sheets after hot pressing.

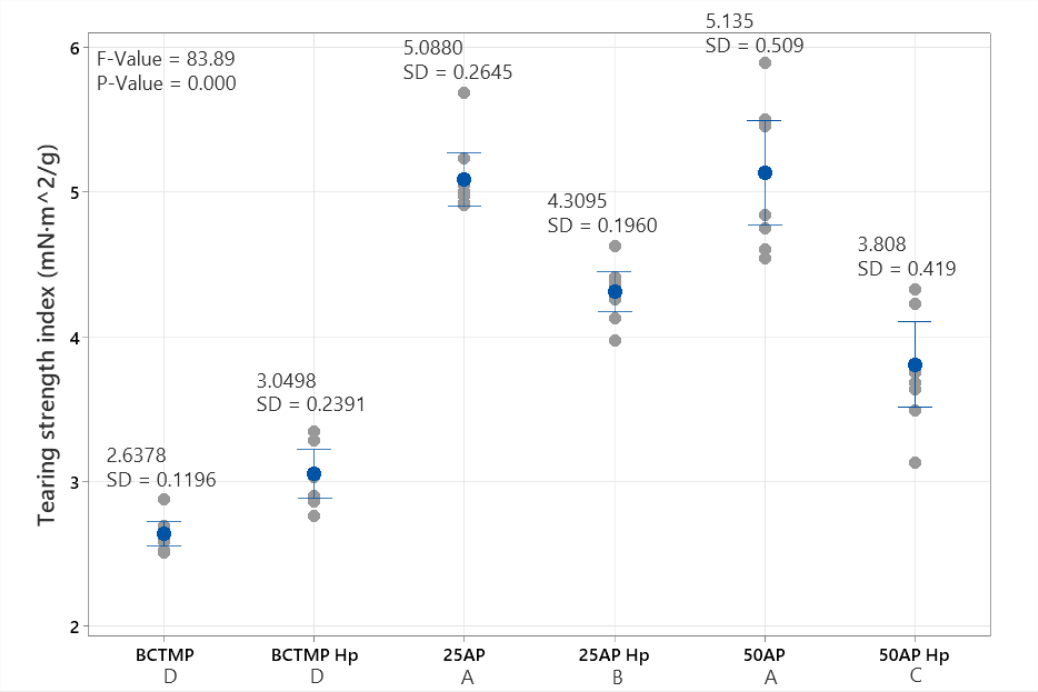

Figure 62. Tearing strength indexes of 25%, 50% apple pomace and 100% BCTMP standard- and hot-pressed handsheets.

The tearing strength indexes of 50AP, 25AP, and BCTMP was 5.135 mN·m^2/g, 5.088 mN·m^2/g, and 2.638 mN·m^2/g, respectively, showing an increase with higher apple pomace content and density, but not significant when apple pomace content was higher than 25%. However, after hot pressing, the tearing strength of 50AP -Hp and 25AP -Hp dropped to 3.808 mN·m^2/g and 4.309 mN·m^2/g, respectively. This decrease is likely due to the increased rigidity of apple pomace fibres and excessive strong fibrous bonding after hot pressing, as discussed in the "TEA" section 4.3.5, which also explained the insignificant increase from 25AP to 50AP. Additionally, the reduced TEA indicates a diminished ability to absorb energy and resist forces that propagate tears. While stronger fibre bonding typically enhances the energy required to resist rupture, excessive bonding can have the opposite effect. If bonding becomes so strong that fibres break instead of being pulled out of the sheet matrix, the tearing strength decreases because less work is needed to split the fibres than to pull them out (Lo et al., 2024).

Since shorter fibre length is negatively correlated with TEA (Larsson et al., 2018), it also impacts tearing strength. Similar results were reported by Agnihotri et al. (2010) and Robertsén and Joutsimo (2005), who observed a decrease in the tearing index with the reduction in fibre length in softwood materials.

4.3.9 Gurley test

Figure 63 illustrates the air resistance results of the handsheets. BCTMP exhibited the lowest air resistance at 0.15 sec/25 mL, highlighting its minimal ability to resist air passage. The Gurley values increased with higher apple pomace content and the application of hot pressing, correlating with the increase in density. 25AP and 50AP demonstrated air resistance values of 343.36 sec/25 mL and 23.89 sec/25 mL, respectively, which were significantly higher than BCTMP. This suggests that the fine apple pomace particles filled the pores between wood fibres that reduced the air permeability.

BCTMP -Hp showed a slight improvement over BCTMP with a value of 0.51 sec/25 mL, while 25AP -Hp and 50AP -Hp reached 61.43 sec/25 mL and 478.23 sec/25 mL, respectively. These values were all higher than their normal-pressed counterparts, which further proves the observation that hot pressing densifies the fibrous network, decreases porosity, and reduces air passage, as emphasised in previous sections.

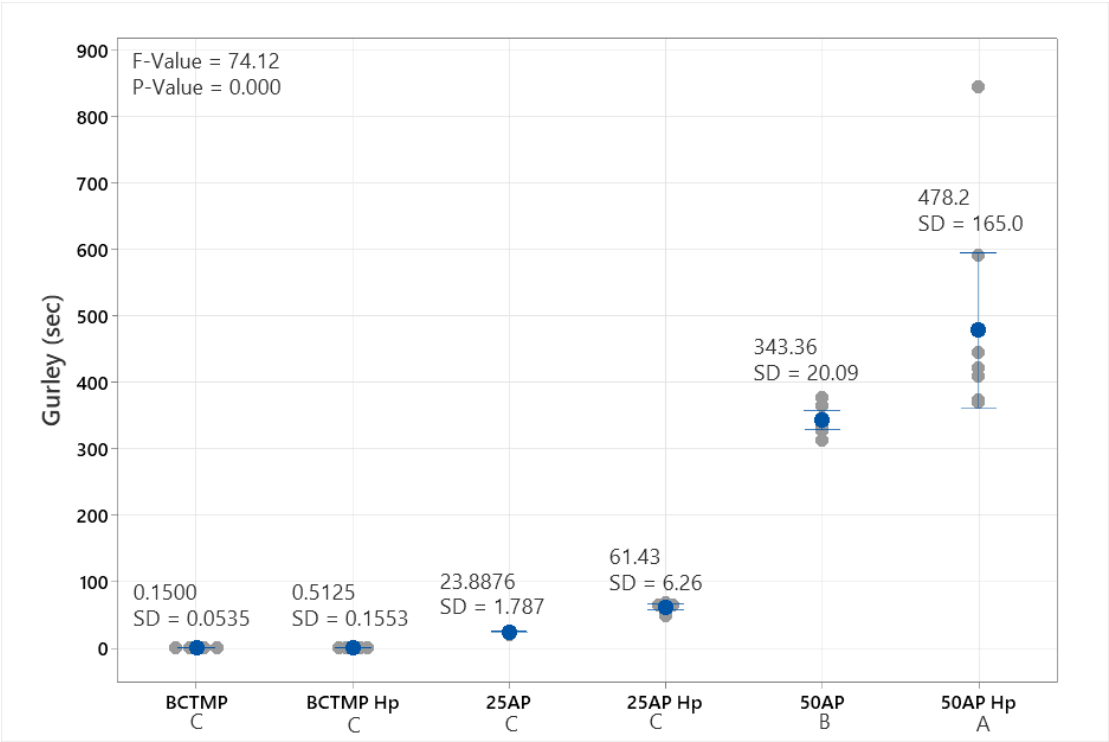

Figure 63. Gurley seconds (for 25 ml of air passage) of 25%, 50% apple pomace and 100% BCTMP standard- and hot-pressed handsheets.

4.3.10 Cobb testing results

Lower Cobb values reflect reduced water absorbability and improved water resistance (Li et al., 2020). **Figure 64** presents the Cobb values of the handsheets, showing a trend that Cobb values decrease with higher apple pomace content and the application of hot pressing. BCTMP showed the highest Cobb value at 773.14 g/m², nearly double that of 50AP at 400 g/m² and 45% higher than 25AP at 532.24 g/m². Hot-pressed sheets showed significantly improved water resistance, with Cobb values of 543.38, 392.93, and 257.73 g/m² for BCTMP -Hp, 25AP -Hp, and 50AP -Hp, respectively. This reduction is attributed to the apple pomace filling the pores and hot pressing further densifying the sheets that limiting the water penetration. Additionally, the phenomenon of lignin flow may be a potential attribution, as its mechanism involves the plastic flow of lignin after being softened by heat. As introduced in the literature, lignin's hydrophobic properties can create a surface layer that inhibits moisture penetration (Joelsson et al., 2022) while also filling voids and establishing a hydrophobic network (Sanchez-Salvador et al., 2024). Reiniati et al. (2015) further proposed that hot-pressing could induce lignin demethoxylation and cross-linking of free phenolic units to enhance resistance to water penetration into the cell wall.

These results contradict the findings of Gouw et al. (2017), as noted in the literature review, which suggested that increasing the apple pomace content reduces water resistance. This discrepancy is likely because of the methodological differences. In their study, wet sieving was not utilised to control particle sizes, resulting in higher porosity in the sheets. Among the specimens, only 50AP -Hp remained unsaturated after 60 seconds of absorption. This suggests that 50AP-Hp may not require waterproof coatings for applications withing several minutes but would still benefit from such coatings for prolonged exposure to water.

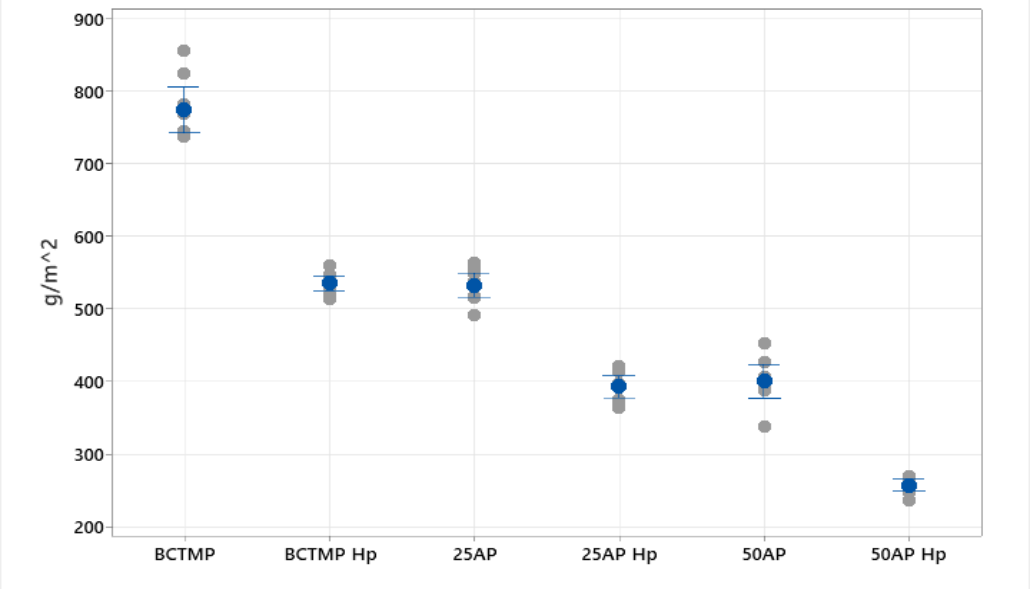

Figure 64. Cobb values of 25%, 50% apple pomace and 100% BCTMP standard- and hot-pressed handsheets.

4.3.11 Grease resistance test

Table 20 shows the results of grease resistance testing, including oil show-through time and break-through area. The data revealed that samples with higher density exhibited longer oil show-through times and smaller break-through areas, aligning with the trends observed in air and water resistance tests. This improvement was attributed to the low porosity, which effectively blocked the passage of oil molecules.

Among the normally pressed samples, 50AP showed the best performance, with an oil show-through time of approximately 5.5 hours and the smallest break-through area of 6.09 cm^2, which agreed with the results measured in screening trial. That of 25AP and BCTMP were 65 and 50 minutes, respectively. After hot pressing, 50AP-Hp achieved an extended show-through time exceeding six hours (the maximum measurable time) and a break-through area of 4.14 cm^2, with minimal staining on the copy paper. These results highlight a significant enhancement, with the resistance of 50AP-Hp being at least six times better than that of BCTMP-Hp at 65 minutes.

Table 20. The grease show-through time and break-through area of 25%, 50% apple pomace and 100% BCTMP standard- and hot-pressed handsheets.

	Show-through time (min)	Break-through area (cm^2)	Break-through Stain
BCTMP	50	17.70	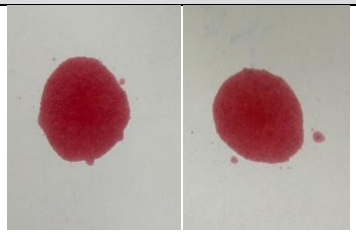
BCTMP-Hp	65	16.03	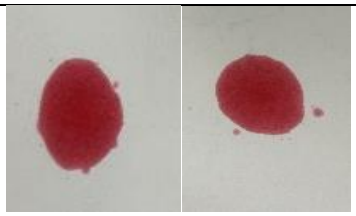
25AP	60	15.57	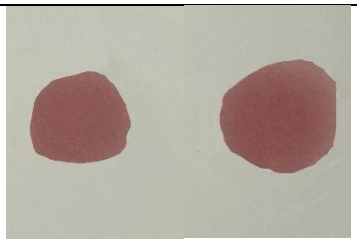
25AP-Hp	85	13.03	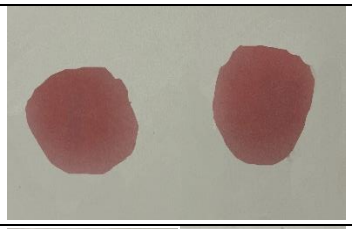
50AP	330 (5.5 hrs)	6.09	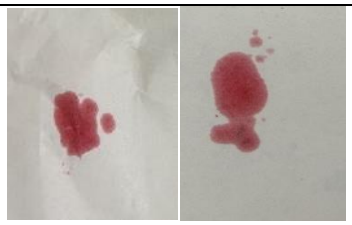
50AP-Hp	> 360 (6 hrs)	4.14	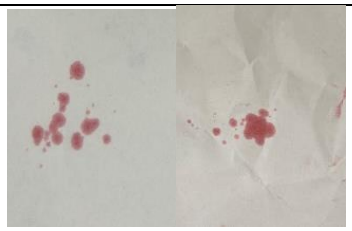

In summary, oil resistance improved with increased density, particularly after hot pressing. Thus, the 50AP-Hp does not require oil-resistant coating for usage less than six hours. However, for overnight storage, applying a coating agent is recommended to extend the oil and grease resistance time further.

4.3.12 Contact angle and roughness

The results for contact angle and surface roughness, including the mean values and SD of “Ra” and “Rz”, are presented in **Table 21**. The Ra and Rz values generated from fringe projection provide a general measure of surface roughness and the presence of peaks and valleys, with smaller values indicating smoother surface, as discussed earlier in Section 4.2.5. By analysing the Ra and Rz values of the specimens, the hot-pressed handsheets appeared to have a smoother surface compared to the standard sheets.

None of the specimens had a contact angle greater than 90°, which indicates that all surfaces were hydrophilic. The BCTMP and 25AP showed immediate absorption of water, making it difficult to capture the moment when the water droplet touched the surface, and BCTMP displayed the largest Ra and Rz values, indicating it had the roughest surface among the samples. This behaviour reflects their strongly hydrophilic nature, and based on the Wenzel Model, increased roughness results in more spreading effect on hydrophilic surfaces ($\theta < 90°$) (C. Li et al., 2021; Wenzel, 1949). Among the normal-pressed specimens, only the 50AP specimen was recorded a measurable contact angle of 54.8°. Although it has slightly higher roughness than 25AP, its high density slowed water penetration that made the water droplet could stay on the surface for longer period.

In contrast, all hot-pressed specimens exhibited larger contact angles at 79.4°, 81.5° and 85.3°, compared to their standard-pressed counterparts, and they had smoother surfaces (lower Ra and Rz values). This is likely attributed to their denser structure with lower porosity, which enables the surface to retain water droplets for a longer duration, and according to the Wenzel Model, a lower roughness can lead to higher contact angles for hydrophilic surfaces, as previously discussed. Lignin flow could also be a cause that the hydrophobic lignin layer reduced the surface roughness, and the additional compression from the hot-press reduce the portions of peaks and valleys that reduced the Rz values. Water droplets on the surface of BCTMP -Hp disappeared quickly, but remained slightly longer than BCTMP, so the moment when they in contact with the surface could be captured. This indicates that the surface of BCTMP -Hp is still

considerably hydrophilic compared to the other two specimens. Furthermore, the contact angle of 50AP-Hp was higher than that of 25AP-Hp, despite having greater roughness. This can be attributed to its higher density, which is similar to that of standard pressed sheets.

Table 21. Contact angles and roughness of the apple pomace and BCTMP standard- and hot-pressed handsheets.

	Contact angle	Image	Roughness
BCTMP	Instant absorption		Ra = 13.8 SD = 1.2 Rz = 169.8 SD = 17.1
BCTMP-Hp	79.4 (quickly absorption)		Ra = 8.0 SD = 0 Rz = 102.2 SD = 6.9
25AP	Instant absorption	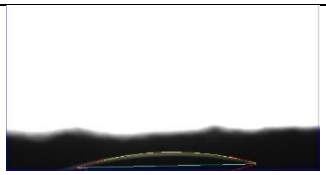	Ra = 8.6 SD = 0.8 Rz = 110.4 SD = 18.5
25AP-Hp	81.5		Ra = 7.6 SD = 0.8 Rz = 106.8 SD = 14.6
50AP	54.8		Ra = 11.4 SD = 1.02 Rz = 129.2 SD = 15.9
50AP-Hp	85.3	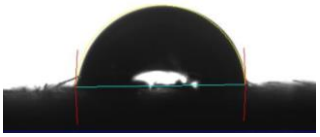	Ra = 8.8 SD = 0.4 Rz = 100.0 SD = 5.02

The results of the contact angle and roughness assessment suggest that the density, roughness and surface hydrophilicity are all important factors contributing to the wettability and water resistance.

4.4 Conclusion

According to the testing results, the formulation with 50% apple pomace exhibited the best mechanical and barrier performance among the tested formulations. This can be attributed to the small particle size of apple pomace fibres, which effectively filled the voids between longer wood fibres to form denser sheets. After hot pressing, the increased densification and lignin flow further enhanced the material's properties. However, due to the degradation of polysaccharides/pectin and lignin cross-linking reactions during hot-pressing, its flexibility was limited, which negatively impacted the tearing resistance and ductility of the handsheets. These findings demonstrate the great potential of apple pomace as an alternative material for single-use takeaway packaging. Nevertheless, the addition of a waterproof coating agent would be necessary if using liquid-containing foods, and grease-proof coating agent would be recommended for use exceeding six hours.

Chapter 5 Corn husk handsheets manufacturing and testing

5.1 Material Preparation

5.1.1 Corn husk fibre preparation

The corn husk (CH) utilised in this study was purchased from Tio Pablo and was in a dehydrated form. The treatment for CH was different from that for AP due to its longer and tougher fibre. The dehydrated husks were rehydrated with distilled water, and steam was applied for the softening process while being agitated, as shown in **Figure 65**. The pH of the liquid obtained from soaking the corn husk was measured to be 4.2, with an acidic nature, indicating the retention of fine additive would be low. After approximately two hours of rehydration, the corn husks were extruded using an extruder (LabTech Scientific LTE 26-40 Twin Screw) under high stress and temperature to break down their tough fibres. The extruded fibres were then chopped to produce smaller particles. Unlike apple pomace, the fine fibres from the corn husks were not sieved because the fibre dimensions, including length and width, varied significantly, with some fibres being curled.

Figure 65. Rehydration of dehydrated corn husks, involving soaking, agitating and softening by steam.

5.1.2 Blend of BCTMP and corn husk

Based on the results from the apple pomace handsheets chapter, a 1:1 blend (50% corn husk fibres) with BCTMP was chosen, while hemp seed husk powder was excluded due to its low effectiveness and retention by acidic environment. The pulp slurry was prepared followed by the TAPPI standard TAPPI 205 sp-02, using 4.5 g of material (dry basis) based on the planned ratio, and diluting to 0.3% consistency. The blend process was the same as that for apple pomace as illustrated in Section 4.1.1.

5.2 Corn husk standard handsheet making and testing

The standard methods and equipment for making corn husk handsheets were the same as those for apple pomace handsheets, which followed by the T205 sp-02 standard, which could be referred to Section 4.1.2 and 4.1.3.

The testing done on the corn husk handsheets were the same as those for the apple pomace sheets, which were grammage, thickness, density, tensile testing, Cobb testing, grease resistance testing, microscopic scanning, as well as contact angle and roughness referring to Section 4.2.1 to 4.2.12. These repetitive tests were done to ensure the repeatability in the method and approach by making the BCTMP in both trials.

5.3 Results and discussion

5.3.1 Handsheet formation

Figure 66 shows the standard (50CH) and hot-pressed (50CH-Hp) handsheets made with 50% corn husk. The colours of the normal- and hot-pressed sheets are similar, however, corn husk fibres could be easily peeled off the surface, indicating the poor bonding between the corn husk and BCTMP fibres during formation. This issue is likely due to the fibre entanglement because the latency of the corn husk pulp was not removed. Also, the uneven distribution of the corn husk in the handsheets is obvious, which might lead to variation in mechanical and barrier performance.

Because of the hydrophobic and light nature, the corn husk fibres tended to remain suspended on the slurry surface and settle on the top of the sheets during formation that

causes uneven distribution. Furthermore, the grammages of the handsheets were lower than planned, as some corn husk and BCTMP fibres adhering to the forming wire in the handsheet machine and the drying plates during the drying process, which caused some degree of material loss.

Figure 66. Standard (left) and hot-pressed (right) 50% Corn husk-50% BCTMP handsheets.

5.3.2 Thickness and Density

The physical properties, including weights, thickness, density and grammage, of the standard and hot-pressed corn husk handsheets are shown in
Table 22.

The mean density of handsheets made from corn husk was slightly lower than that of BCTMP sheets, measuring 242.43 kg/m³. The slightly lower density of the 50CH sheets is likely attributed to looser fibre packing and a higher number of pores. There was a lot more variation in the density of hot-pressed handsheets, this was likely caused by the same issue observed with apple pomace handsheets that the unparallel hot-press led to variability.

The density of corn husk sheets increased to 377.19 kg/m³ after hot pressing (50CH-Hp). Similarly, the mean density of 50CH-Hp remained lower than that of BCTMP-Hp, but with a p-value of 0.62, the difference is not statistically significant, suggesting the densities are similar when accounting for error. The lower mean density is likely due to limited densification caused by weak bonding. Although the high temperature (230°C) during hot pressing softened the corn husk fibres, the presence of a corn husk layer

between the press and the BCTMP fibres beneath prevented full compression of the sheets, resulting in restricted densification.

Table 22. The mean weight, thickness and density of standard and hot-pressed corn husk and BCTMP handsheets.

Formulation	50CH Hp (s)	50CH (s)	BCTMP Hp (Ins)	BCTMP (Ins)
Area (m^2)		All sheets were 0.02		
Weight (g)	4.089	4.155	5.012	5.255
SD	0.120	0.069	0.050	0.052
Thickness (μm)	551.16	886.81	657.73	1092.85
SD	49.95	19.66	54.70	40.21
Density (kg/m^3)	377.19	236.03	386.50	242.43
SD	40.85	3.58	32.64	7.54
Grammage	206.49	209.86	253.15	265.40
SD	6.06	3.47	2.52	2.63

In addition, it is noticeable that the grammage of 50CH and 50CH-Hp handsheets is significantly lower than that of the BCTMP handsheets and the planned grammage for their production. While the planned grammage was 225 gsm, based on dry basis, the actual grammage should have been higher if accounting for the moisture absorption. However, the grammage of 50CH and 50CH-Hp measured only 209.86 gsm and 206.5 gsm, respectively, which is likely due to material loss during the handsheet formation and drying processes. This could happen when the wet sheets were transferred from the forming wire, some corn husk fibres adhered to it, and it also happened that fibres stuck to the drying dishes when the dried sheets were removed from the drying rings. This loss of material demonstrated the ineffective/poor bonding between corn husk and BCTMP fibres, which made them easier to separate.

5.3.3 Surface observation and OCT results.

A representative B-scan and surface images generated by OCT at 10x magnification are presented in **Table 23**, with the rest are provided in Appendix E. The interpretation of the images has been explained in Section 4.3.3. By observing the B-scan images of corn husk and BCTMP handsheets, the light reflection slightly decreased after the addition of corn husk, indicating a less dense structure, while the surface of the corn husk sheets appears smoother than that of the BCTMP sheets. Unlike apple pomace that integrated and bonded with wood fibres, corn husk fibres stacked on top, which might cause the fibre entanglement, thereby no contribution to its density. Additionally, when comparing the B-scan images (in Appendix E) at various locations on the corn husk handsheets, the inconsistent porosity was revealed that each area displayed different porosity. This was likely due to the corn husk was not distributed uniformly across the sheets and led to uneven fibre packing.

Table 23. B-scan and surface images of 50% corn husk and 100% BCTMP standard and hot-pressed handsheets taken by the OCT at 10x magnification.

	B-scan images at 10x magnification	Surface image
50CH	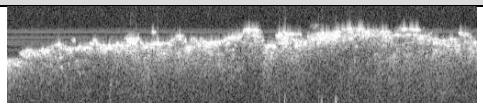	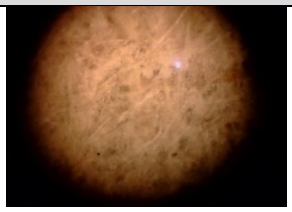
50CH -Hp	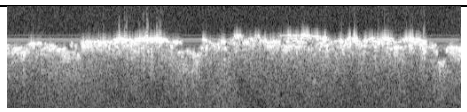	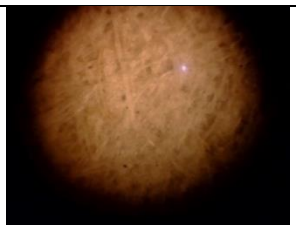
BCTMP	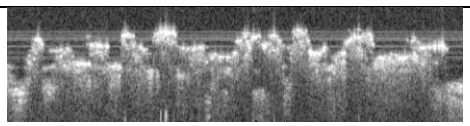	
BCTMP -Hp	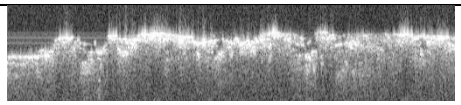	

The surface images show that the addition of corn husk introduced some dark substances on the surface, with long corn husk fibres visibly present, potentially increasing porosity. However, some of the dark material consisting of finely extruded corn husk particles could fill some voids. Hot pressing did not significantly darken the handsheets but resulted in a smoother surface compared to standard sheets. This was likely due to lignin flow and additional compression, which reduced surface roughness with fewer peaks and valleys, similar with the hot-pressed apple pomace sheets.

5.3.4 Tensile index

Figure 67 displays the tensile indexes of the handsheets. The mean tensile index of 50CH was higher than that of BCTMP, measuring 7.09 N·m/g compared to 6.66 N·m/g but not significant, and their results looked similar form the plot. Hot pressing increased the tensile indexes, but that of 50CH -Hp at 10.42 N·m/g, was significantly lower than BCTMP -Hp at 17.72 N·m/g. As expected, tensile index was closely related to density, and the poor bonding between corn husk and BCTMP fibres also likely contributed to the lower tensile performance, where the corn husk fibres did not contribute to the tensile strength enhancement, but their presence rose the overall grammage of the sheets, which ultimately reduced the tensile index. Additionally, the inconsistent distribution of CH fibres on the surface increased the variations of tensile stripe samples. Thus, some areas with more corn husk fibres might have higher tensile strength, while others were weaker and broke easily during testing, which caused the large variation among individual data points.

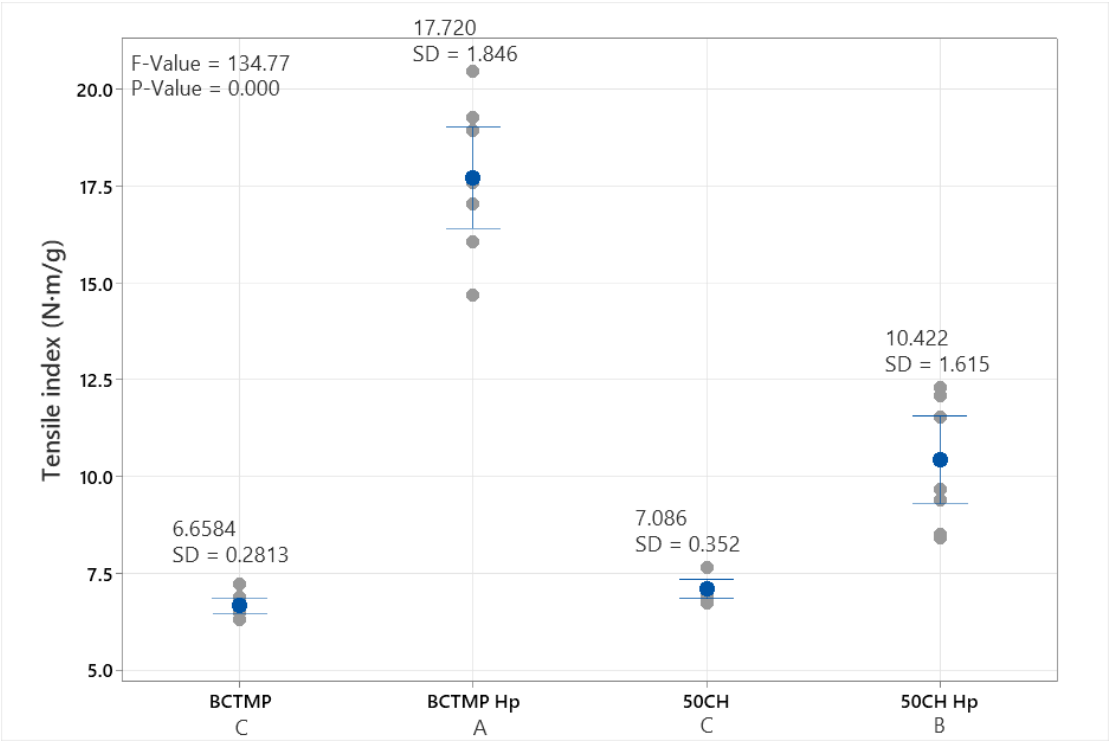

Figure 67. Tensile indexes of 50% corn husk and 100% BCTMP standard- and hot-pressed handsheets.

5.3.5 SCT

The SCT results for corn husk and BCTMP handsheets are displayed in **Figure 68**. Those for 50CH and 50CH-Hp were 8.96 N·m/g and 14.00 N·m/g, respectively, in contrast to the BCTMP sheets with values of 8.21 N·m/g and 15.85 N·m/g. Similarly, the SCT indexes between 50CH and BCTMP showed no significant difference, with slightly higher mean of SCT index for 50CH and overall results indicating that the SCT index was correlated with density. The reduction in grammage along with weak and ineffective fibre bonding are likely contributed to the lower SCT indexes. Notably, the significant variance in 50CH-Hp reflects the inconsistency of stripe samples, as previously discussed.

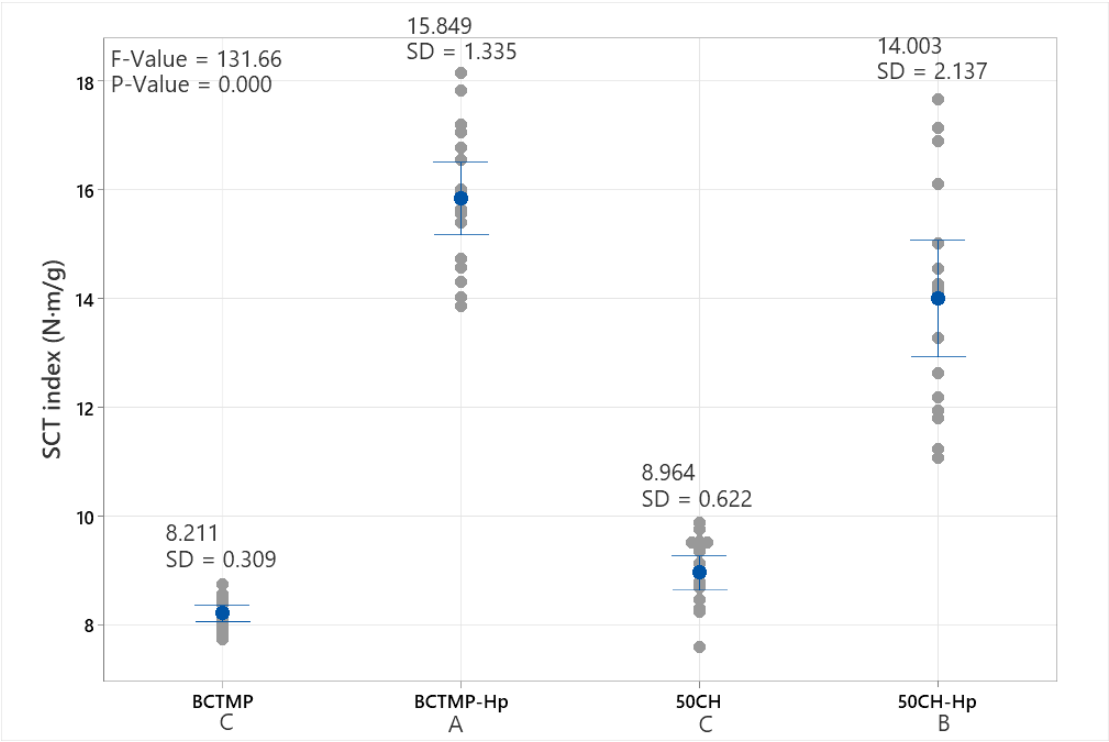

Figure 68. SCT indexes of standard- and hot-pressed 50% corn husk and 100% BCTMP handsheets.

5.3.6 Stiffness, elongation, and TEA

Figure 69 illustrates the tensile stiffness indexes of standard and hot-pressed corn husk and BCTMP handsheets. The tensile stiffness index of BCTMP was 1.234 kN·m/g, slightly higher than 50CH at 1.161 kN·m/g, but looked similar from the plot. That of BCTMP -Hp was 2.852 kN·m/g, higher than 50CH -Hp, measuring 1.769 kN·m/g. The results indicated that the addition proportion of corn husk fibres did not improve the tensile stiffness index, with the tensile stiffness index of 50CH -Hp being about 60% of BCTMP -Hp at 2.852 kN·m/g. This is likely due to lower density and grammage, and ineffective fibre bonding, similar with the tensile strength. Low grammage reflects smaller amounts of fibres within a unit area that provides less material to resist tensile stress.

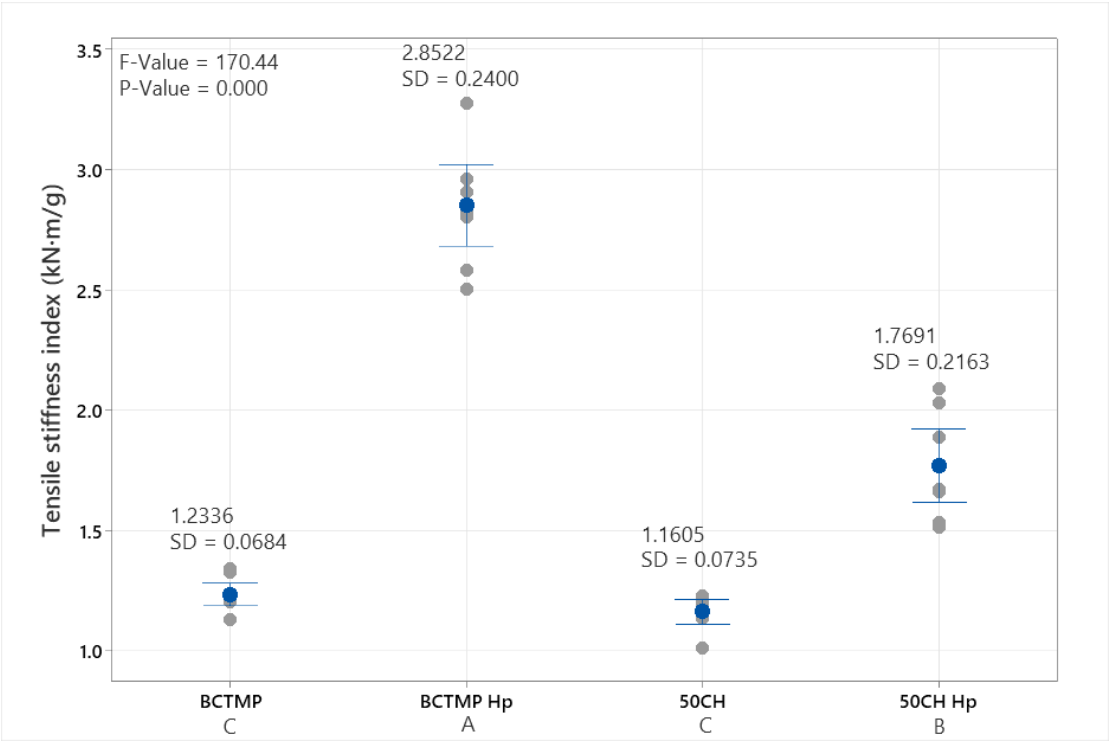

Figure 69. Tensile stiffness indexes of 50% corn husk and 100% BCTMP standard- and hot-pressed handsheets.

Figure 70 shows the TEA indexes, showing that the TEA indexes of 50CH were close to BCTMP, while those of 50CH-Hp were lower than BCTMP-Hp, which aligned with the correlation between density and TEA as discussed previously for apple pomace sheets. The mean TEA index of 50CH was 0.043 J/g was slightly higher than the 0.036 J/g recorded for BCTMP, but not significant due to the larger variance.

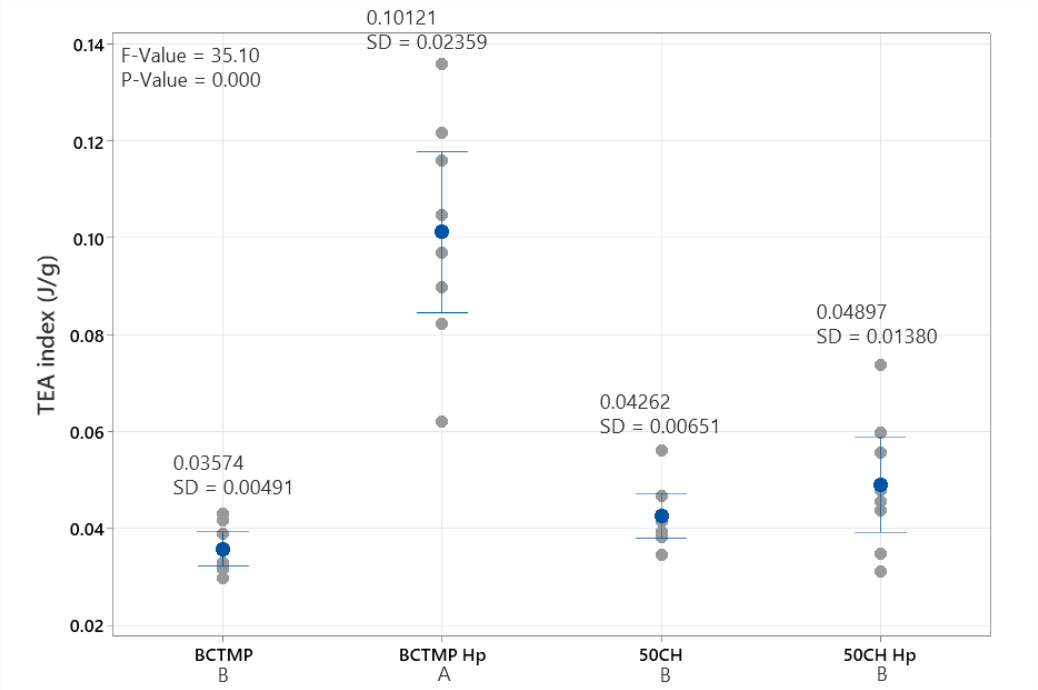

Figure 70. TEA (Tensile energy absorption) indexes of 50% corn husk and 100% BCTMP standard - and hot-pressed handsheets.

After hot pressing, the mean TEA index of 50CH -Hp increased slightly to 0.049 J/g, which was approximately half of the BCTMP -Hp, which reached 0.101 J/g. By analysing the variance, the TEA index of 50CH -Hp remained comparable to that of 50CH, indicating no significant increase, which was likely caused by the larger data variance. The variance was probably caused by the unparallel hot plate on the hot press as discussed for the apple pomace sheet. As noted by Lo et al. (2024), TEA generally correlates with density, except in cases of extremely high rigidity, such as with apple pomace fibres in this study, which explains the unchanged TEA index of 50CH-Hp.

It has been discussed that corn husk fibres exhibit high flexibility, which resulted in greater stretching indexes compared to BCTMP. The stretching indexes of 50CH was 0.0045 %·m^2/g, exceeding that of BCTMP at 0.0028 %·m^2/g. However, the elongation of corn husk sheets decreased, with 50CH-Hp showed a reduced stretching index of 0.0038 %·m^2/g compared to 50CH. This reduction was likely due to the degradation and dehydration of certain substances in the corn husk fibres or the reduced potential to develop bonding during the hot-pressing process that made the fibres rigid.

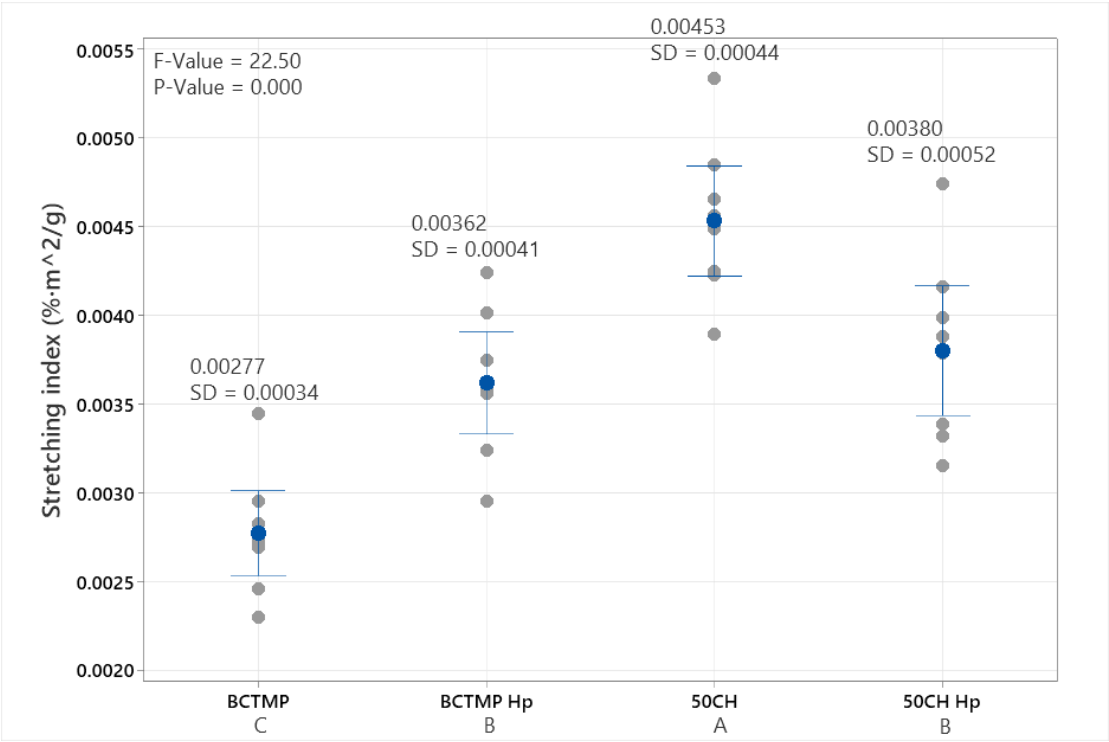

Figure 71. Stretching indexes of 50% corn husk and 100% BCTMP standard - and hot-pressed handsheets.

5.3.7 Bursting strength

Figure 72 highlights the differences in bursting strength indexes between corn husk and BCTMP handsheets. The bursting strength index of 50CH was higher than BCTMP, measuring 0.340 kN/g compared to 0.271 kN/g. However, 50CH -Hp exhibited obviously inferior mechanical properties compared to BCTMP -Hp, with an index of 0.478 kN/g. compared to 0.712 kN/g. Bursting strength is also linked to density as discussed earlier. The uneven distribution of corn husk fibres within individual sheets that areas with a higher concentration of corn husk fibres tended to have greater bursting strength, while locations on the surface with fewer fibres resulted in weaker performance, might contribute to variations in performance. This uneven distribution likely explains why the mean bursting strength index of 50CH was higher than that of BCTMP, despite their densities were close to each other. Additionally, the loose fibre packing between corn husk and BCTMP might have restricted densification during hot-pressing, resulting in not considerable increase in bursting strength, which made it lower than that of BCTMP-Hp.

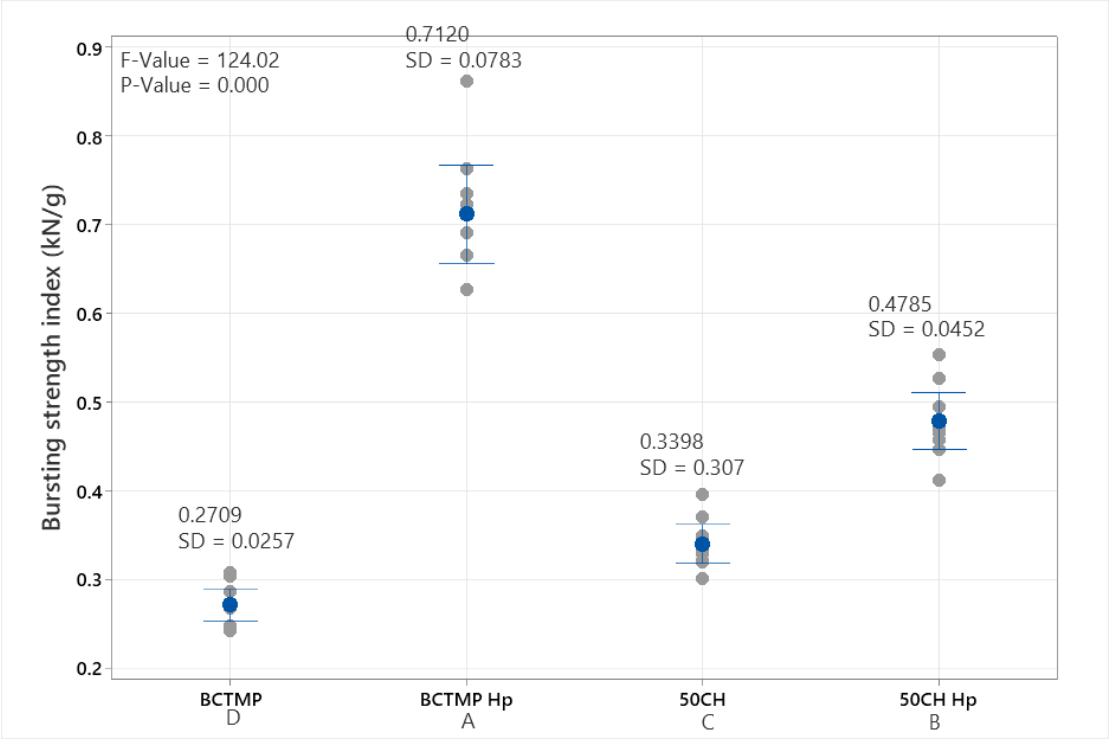

Figure 72. Bursting strength indexes of 50% corn husk and 100% BCTMP standard- and hot-pressed handsheets.

5.3.8 Tearing strength

Figure 73 presents the tearing strength indexes of corn husk and BCTMP handsheets. From the results of Tukey HSD analysis, the tearing indexes of all samples were not significantly different from each other, though the mean tearing strength indexes of the corn husk sheets were higher than those of the BCTMP sheets, with 50CH and 50CH-Hp measuring 3.074 mN·m²/g and 3.356 mN·m²/g, respectively. Hot-pressing slightly improved the mean tearing indexes of both BCTMP and 50CH hand sheets. The large variance in the 50CH samples was likely due to the uneven distribution of corn husk fibres on the sheet surface, as previously discussed. Specimens with more corn husks on the surface became tougher and more resistant to tearing. Since the force measurement is at the millinewton (mN) level, even small differences in fibre concentration on the surface could amplify the observed variation.

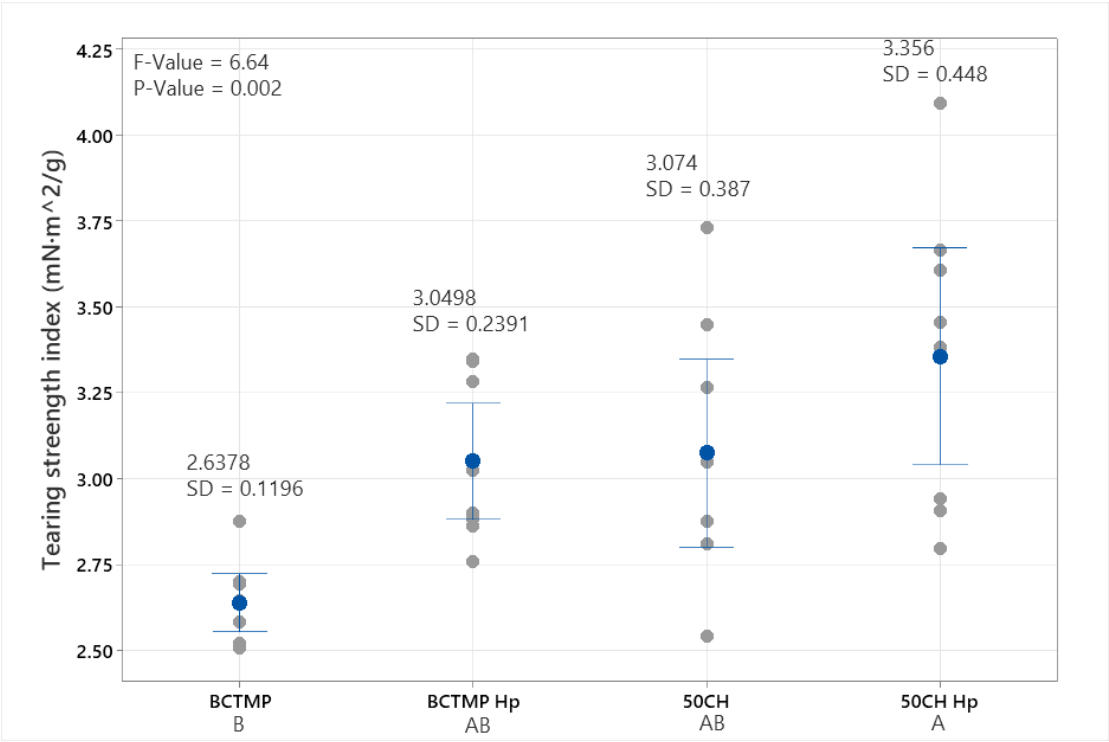

Figure 73. Tearing strength indexes of 50% corn husk and 100% BCTMP standard- and hot-pressed handsheets.

5.3.9 Gurley test

Figure 74 presents the Gurley second results for the 50CH and BCTMP handsheets, expressed in seconds per 25 mL of air. The Gurley second for 50CH was higher than that of BCTMP, recorded at 2.225 sec/25 mL, and further increased to 3.2375 sec/25 mL after hot-pressing. Despite having a lower density than BCTMP -Hp, the 50CH -Hp handsheets exhibited higher Gurley second values. This might be due to the presence of corn husk fibres, which could obstruct airflow through the sheet for sone extent. The uneven distribution of corn husk might have created areas (with more corn husks) with greater air resistance, acting as a barrier, even though the overall sheet density remained lower.

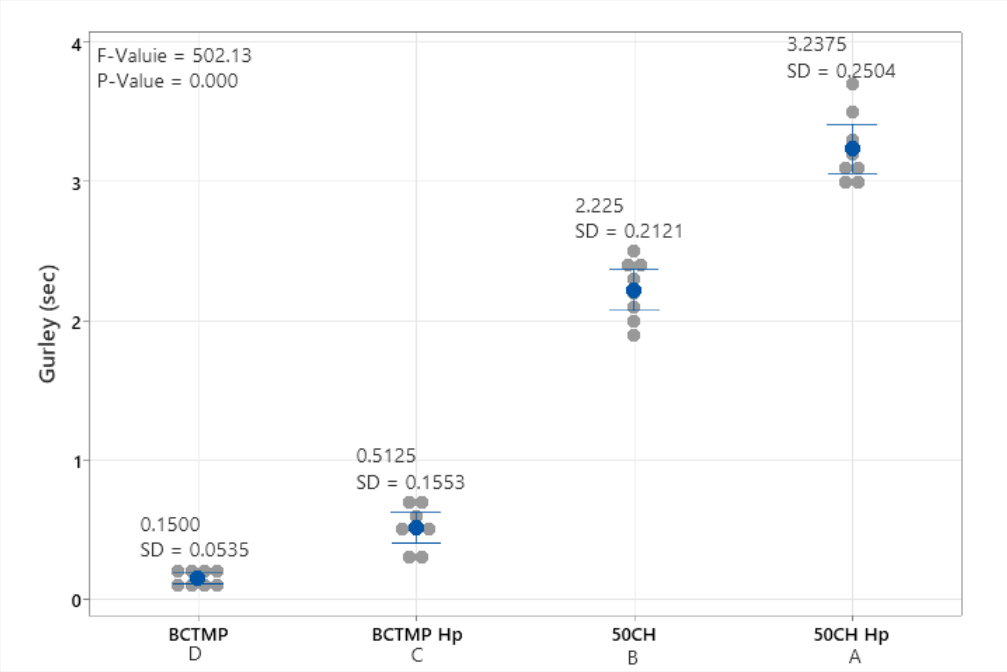

Figure 74. Gurley seconds of 50% corn husk and 100% BCTMP standard- and hot-pressed handsheets.

5.3.10 Cobb values

Figure 75 illustrates the Cobb values of corn husk and BCTMP handsheets. The Cobb values of the corn husk sheets were lower than those of the BCTMP sheets, with 50CH and 50CH-Hp measuring 548.3 g/m² and 407.4 g/m², respectively, although the density of 50CH and 50CH-Hp were close or lower than BCTMP sheets. This can be attributed to the hydrophobic properties of the corn husk, as introduced in literature review, and the lignin flow and hornification after hot-pressing, as discussed in the apple pomace section. The uneven distribution of corn husks on the sheet surface could also result in variations in water resistance, with areas containing more corn husk fibres exhibiting greater water resistance.

Generally, higher-density sheets have less water absorption because of fewer voids. However, when the material is greatly hydrophobic, sheets with lower density can still achieve reduced Cobb values due to the water-repellent properties of the fibres. Similarity was observed by Zawawi et al. (2013), which blended kenaf paper with polyethylene (PE) to significantly reduce water absorption. In their study, Cobb values

fell below 20 g/m² within 60 seconds because of the hydrophobic nature of PE (polyethylene) despite the high porosity of the paper matrix.

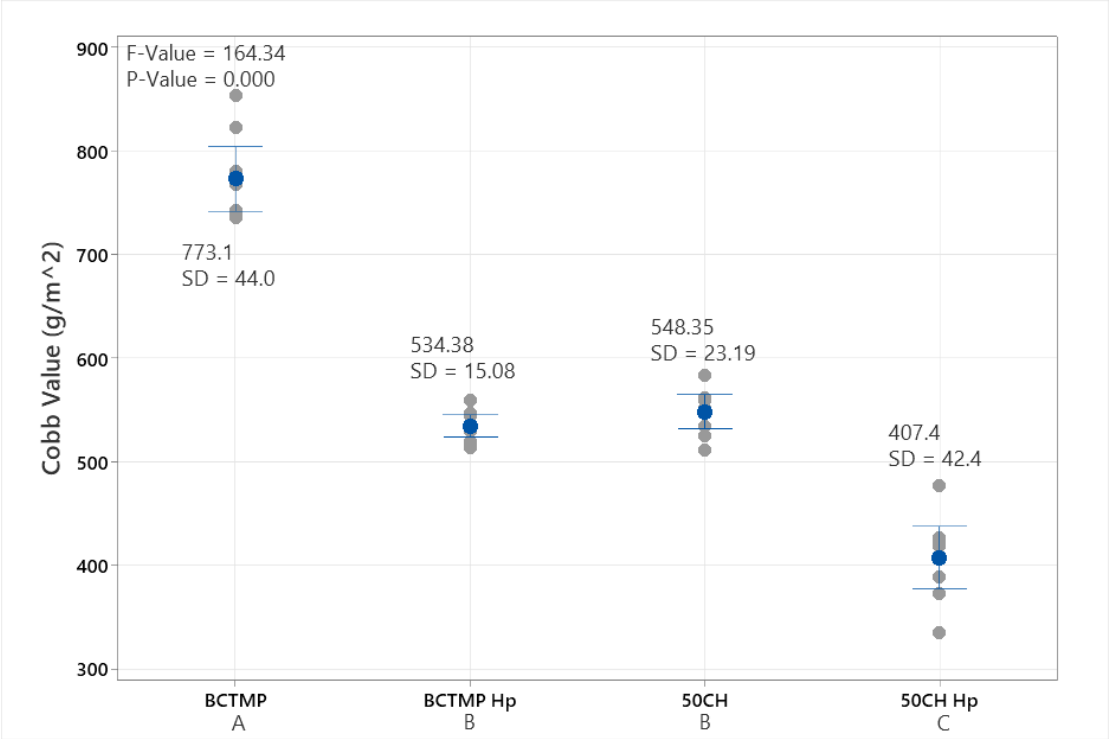

Figure 75. Cobb values of 50% corn husk and 100% BCTMP standard- and hot-pressed handsheets.

5.3.11 Grease resistance

Table 24 presents the results of grease resistance testing for corn husk and BCTMP handsheets. The show-through times for **50CH** and **50CH-Hp** were both shorter than those for BCTMP handsheets, measured at 20 minutes and 30 minutes, respectively. Additionally, the breakthrough areas after 24 hours were 20.82 cm² and 30.95 cm², respectively. The major cause of this reduced grease resistance appears to be weak fibre bonding, between corn husk and BCTMP, within the sheets, leading to lower density and higher porosity. These characteristics limited the ability of the corn husk fibres to prevent grease penetration, which left only the remaining 50% of BCTMP to contribute to oil resistance. Consequently, the performance of the 50% corn husk sheets was inferior to that of the 100% BCTMP handsheets. This suggests that handsheets containing 50% corn husk would require an oilproof coating to be suitable for use.

Table 24. Grease resistance testing results of 50% corn husk and 100% BCTMP standard- and hot-pressed handsheets, including the show-through time, break-through area and the image of the oil stain.

Formulation	Show-through time	Break-through area	Oil stain
50CH-Hp	30	20.82	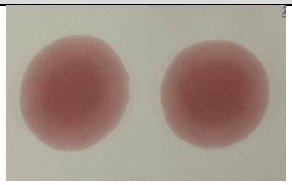
50CH	20	30.95	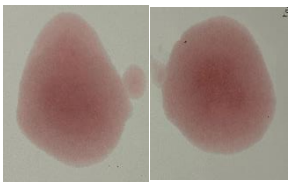
BCTMP-Hp	65	16.03	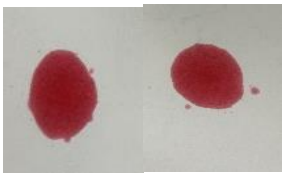
BCTMP	50	17.70	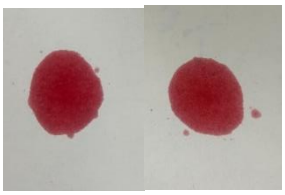

5.3.12 Contact angle and roughness

Table 25 displays the contact angle and surface roughness data for corn husk and BCTMP handsheets. The contact angles for both 50CH and 50CH-Hp were higher than 90°, measuring at 92.1° and 100.1°, respectively, which means hydrophobic surface. This increase was likely due to the greater roughness and hydrophobicity of the corn husk fibres than wood fibres, which was a result of weak fibre bonding that most of corn husks were on the surface. This assertion was supported by roughness measurements measured from fringe projection, showing Ra values of 16.8 and 10.8, and Rz values of 228.2 and 150.2, respectively. Similarly, the Ra and Rz values decreased after hot pressing, as discussed in the apple pomace sheets chapter, this reduction is attributed to lignin flow and additional compression during the process. It was mentioned previously that density, roughness and hydrophobicity are all the factors impact the contact angle. This explains the smoother surface of 50CH-Hp had larger

contact angles compared to 50CH, which was due to its denser and more hydrophobic structure.

Table 25. The contact angle and roughness data of 50% corn husk and 100% BCTMP standard- and hot-pressed handsheets.

Category	Contact angle	Image	Roughness
50CH	92.1	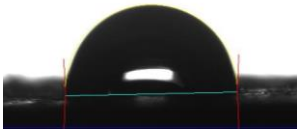	Ra = 16.8 SD = 0.98 Rz = 228.2 SD = 14.6
50CH-Hp	100.1	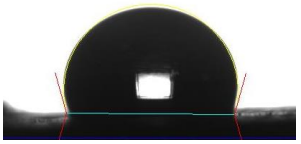	Ra = 10.8 SD = 1.2 Rz = 150.2 SD = 21.98
BCTMP	Instant absorption		Ra = 13.8 SD = 1.2 Rz = 169.8 SD = 17.1
BCTMP-Hp	79.4° (quickly disappearance)		Ra = 8.0 SD = 0 Rz = 102.2 SD = 6.97

5.4 Conclusion

The test results indicated that the inclusion of corn husk did not enhance, and in some cases, adversely affected the performance of handsheets compared to BCTMP. The ineffective bonding between corn husk fibres and BCTMP poses a challenge that requires further investigation. It is possible that conducting only mechanical pulping methods is not well-suited for such tough fibres like corn husk, which might need additional chemical such as an alkaline and cold soda to soften them followed by the refining to increase the bonding/collapse. Fresh corn husks would be recommended to replace the dehydrated husk as it would be easier to process them to avoid the rehydration. The inconsistent distribution of corn husk fibres also led to unpredictable

properties, varying with the concentration of corn husk used. However, a mixture of 50% corn husk and 50% BCTMP will still be tested in a moulded fibre thermoforming trial to explore any potential improvements which could come from scale-up.

Chapter 6 Consideration of the pathway to commercialisation

6.1 Introduction

As discussed in Chapter 2, thermoforming (hot-pressing) in a pre-formed mould of the desired design shape is the most advanced technique to produce moulded fibre products. The production stages for moulded fibre products includes vacuum forming, normal and hot pressing, and drying (Didone et al., 2017). One of the objectives of this study is to find a material that could be used to make food trays for takeaway food containers. A small scale of moulded fibre tray production trial was undertaken in this study to assess whether the improved properties observed in the AP handsheet samples would also translate to the moulded fibre thermo-forming process. To thermoform the tray, a moulded fibre thermo-former manufactured by Kiefel was employed, which was introduced in section 4.1.3, as shown in **Figure 76**.

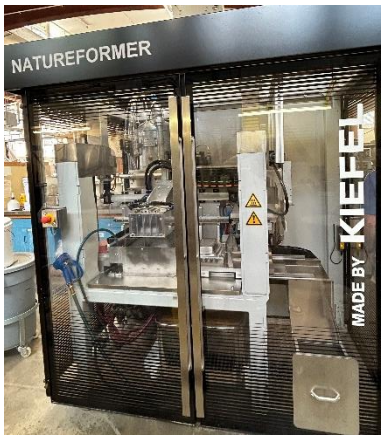

Figure 76. Pilot scale moulded fibre thermo-former manufactured by Keifel (KIEFEL Technologies® KFT Lab Natureformer KFT 90.1) for producing the trays.

6.2 Moulded fibre tray production

6.2.1 Tray moulding: thermo-forming

The preparation of the pulp utilised for tray formation was similar to that for making handsheets. It involved the same preprocessing steps for the biomass materials, measuring the consistency, and blending the materials according to the planned ratio. However, the consistency was adjusted to 0.6% to produce 100 L of pulp, which is the minimum requirement for operating the Kiefel moulded fibre thermo-former. The thermo-former was preheated to 230°C for 1.5 hours before use. The operated thermal moulding conditions of Kiefel were a temperature of 230 °C, with a pressing force of 393.94 kN/m^2, and a pressing time of 30 seconds, which were the suitable conditions that have been found to work best for BCTMP (Wade, 2023).

To ensure the proper operation of the thermo-former, the first few trays were made to calibrate the weight of the tray by adjusting the suction time, which controlled the amount of pulp sucked onto the mould. Once the weight and suction time was confirmed, the full trial run could proceed. Formulations involving 50% AP and 50% CH were selected for tray production.

During the tray formation, the suction for the 50% AP slurry was poor, potential from the mesh blocking, resulting in a much lower wet weight for the tray than expected. In addition, the water could not be fully removed by the vacuum in the thermo-former. This issue was likely caused by the small apple pomace particles formed via shearing into smaller sizes as they passed through the high shear rate pump, which exceeded the maximum suction capacity of the vacuum. To overcome this, the 50% AP slurry was diluted to create a 25% AP slurry with more BCTMP pulp. The leftover AP slurry was used to form sheets on the handsheet machine to prove whether the hypothesis that the particles were sheared by the pump. It was found that the drainage on the handsheet maker was much slower than usual, taking around 12 minutes to complete the dewatering process, which was five to ten minutes slower than the 50AP sheets found previously. This confirmed that the particle size of the apple pomace was significantly reduced during pumping through the Kiefel moulded fibre thermoformer. This may not be an issue for a commercial scale machine as there will be more options of equipment specified for the fine particles, but a possible solution would be to enlarge the sieve size during the apple pomace pre-processing stage specifically for thermoforming, which would allow the particle size to be closer to its original size for handsheet production

after being sheared. Alternatively, using a pump with a lower shear rate could also help mitigate this issue.

Ultimately, the 25% apple pomace (25AP) and 50% corn husk (50CH) trays were formed by the machine, as shown in the **Figure 77**. The outer edge shows some defects, which was caused by material sticking to the mould, possibly due to the material residue left on the mould from the previous trials. These defects would not happen in commercial moulding as the cause could be the issue from the individual thermal moulding machine, and they would not affect the testing result of the tray, as they the bottom of the tray would be cut for testing specimens.

The bottom of the trays were laser cut into strips using the GENESIS laser cutter (GENESIS® G640L) (see **Figure 78**) for testing purposes, including tensile strength with 12 replicates for widthwise and ten replicates for lengthwise stripes, and bursting strength with 4 replicates on each side of the tray. Barrier properties will be based on the results of handsheet testing.

(a).  (b). 

Figure 77. (a). The moulded fibre thermo-formed tray with 25% of apple pomace and 75% of BCTMP. (b). The moulded fibre thermo-formed tray with 50% of corn husk and 50% of BCTMP.

Figure 78. The GENESIS (G640L) laser cutting instrument with a moulded fibre tray for cutting,

6.2.2 Mechanics and barrier performance of thermoformed trays

The tensile results of widthwise and lengthwise stripes of the 25% apple pomace tray are presented in **Table 26**, and the tensile forced data was indexed with grammage. The tensile results for widthwise (WW) 25AP trays showed a tensile force index of 0.755 $N \cdot m^2/g$, a tensile displacement of 0.93 mm, and density of 484.57 kg/m^3, significantly higher than 25AP-Hp handsheets at 0.450 $N \cdot m^2/g$ and 458.65 kg/m^3. This increase in density was likely attributed to the thermo-former's standard-pressing part, which applied stronger compression of 5 bar and an additional 3.875 bar of pressure from the wall air than the 3.45 bar pressure used in the standard press for forming handsheets.

Lengthwise (LW) strips from the 25AP trays showed a tensile force index of 0.562 $N \cdot m^2/g$ and a displacement of 1.34 mm, with a density of 497.03 kg/m^3. The denser structure contributed to a higher tensile force, surpassing that of 25AP-Hp handsheets. The p-values of the densities of LW and WW were 0.137, which means slightly significant difference, and the variance could be due to the material's anisotropic properties, which was likely due to the fibre orientation in the direction of the flow. Safwa et al. (2024) observed that the damaged material occurred along the machine direction (MD) of the layers during thermoforming, which resulted in the tensile strength of MD being higher than that of cross-machine direction (CD).

Table 26. Tensile results of thermoformed trays with 25% apple pomace and 50% corn husk with BCTMP, including force at break, tensile displacement, grammage and density, including the means and standard deviations of 12 replicates for WW and 10 replicates for WW stripes.

Category		Index of tensile force ($N \cdot m^2/g$)	Tensile displacement (mm)	Grammage (gsm)	Density (kg/m^3)
25% AP tray	Widthwise	0.755	0.93	199.04	484.57
	SD	0.053	0.11	4.98	34.67
	Lengthwise	0.562	1.34	203.12	497.81
	SD	0.042	0.13	7.03	15.71
50% CH tray	Widthwise	0.177	0.52	339.89	394.08
	SD	0.040	0.12	15.79	55.05
	Lengthwise	0.151	0.73	322.14	382.99
	SD	0.026	0.07	17.81	22.12

Meanwhile, the tensile test results for the 50% corn husk trays displayed a similar trend where the WW stripes had greater tensile force, but less displacement compared to the LW stripes. The WW stripes demonstrated a tensile force index of 0.177 $N \cdot m^2/g$ and a displacement of 0.52 mm, whereas the LW stripes showed 0.151 $N \cdot m^2/g$ and 0.73 mm, respectively. The WW stripes surpassed the 0.156 $N \cdot m^2/g$ tensile force index of the 50CH-Hp handsheets, possibly due to the higher grammage and increased compression that increased the density, as previously noted. While the LW showed similar results (with SD), which was likely due to the similar densities. The increased density might be also attributed to improved tray formation on the thermo-former, which led to enhanced fibre bonding. Note, the 50% corn husk trays had significantly higher grammage than the 25% apple pomace trays, likely due to smaller particles blocking the mesh during tray formation. This resulted in less material in the tray for the same suction time. A similar issue arose with the 50% apple pomace trays as previously mentioned. Additionally, the 50% corn husk trays featured a significantly higher grammage but lower density than the 25% AP trays, indicating fibres are more loosely packed.

The bursting strength indexes for trays made from apple pomace and corn husk are detailed in **Table 27**. It has been mentioned in the TAPPI T403 standard that both sides of the specimen should be tested. The 25% apple pomace trays had an overall bursting

strength index more than three times higher than the 50% corn husk trays, at 1.859 kN·m^2/g compared with 0.509 kN·m^2/g, respectively. The front side (food-contact surface/moulded side) of each type of tray measured greater bursting strength than the back side (exterior side), which is likely because the front side was directly in contact with a heating mould that underwent more thermal treatment compared to the back side, resulting in a slightly denser and stiffer structure with smoother surface (Didone et al., 2017), and some mechanical properties, including bursting strength varies due to the different surface properties (Didone et al., 2017), manufacturing process, and material compositions (Dislaire et al., 2021).

Table 27. The bursting strength of thermoformed trays with 25% apple pomace and 50% corn husk with BCTMP, the results categorised by the strength for front side (food-contact surface/moulded side) and back side (exterior side).

Trays	Front side (kN·m^2/g)	Back side (kN·m^2/g)	Overall (kN·m^2/g)
25% apple pomace	1.890	1.828	1.859
SD	0.0410	0.0391	0.0507
50% corn husk	0.546	0.472	0.509
SD	0.0125	0.0160	0.0400

The mechanical results showed that the corn husk trays were significantly weaker than the 25% apple pomace trays. As previously explained that the barrier properties of handsheet would represent those of trays, the moisture and grease resistance of the corn husk handsheets was unsatisfactory, which meant that corn husk was not a proper choice as the food packaging in this study. Trays containing 25% apple pomace made after the failure of those with 50% AP might exhibit lower performance based on handsheet results. However, due to the technical constraints of the Kiefel, the 25% apple pomace tray was a more viable alternative.

6.3 Cost Feasibility of Manufacturing

It has been introduced previously that this study aims to develop moulded fibre materials which would be suitable for use as single-use food packaging and thus offer potential to reduce overall plastic consumption in the food takeaway area. It has been suggested by the Ministry of Environment (2020) and Office of the Prime Minister's

Chief Science Advisor (2023), approximately 40% of imported plastic in use of packaging (around 150,000 tonnes) is used for packaging, and 16% of these being single-use plastic food packaging made from PVC and polystyrene. However, the documentations do not specify the portions of different food packaging types (e.g. trays or tableware). Based on the assumption by Lo et al. (2024) that a 10% replacement could help reduce the environmental impact from those plastics and support New Zealand's recycling goals, this study would use the same assumption. As a result, it would be estimated 960 tonnes of single-use plastic could be replaced substituted by the trays made of apple pomace and BCTMP.

The market size for moulded fibre pulp packaging in Australia and New Zealand is estimated to be USD 227.3 million in 2024 and is expected to grow to USD 363.4 million by 2034, with a CAGR of 4.8% (Future Market Insights, 2024). The current cost of moulded fibre trays in the market varies depending on size, material, and application (e.g., food trays, cup carriers). For example, BioPak's natural plant-based moulded fibre takeaway base, with a 1000 mL volume, has a retail price of 0.445 NZD/tray including GST (NZ Safety Blackwoods, n.d.). Another takeaway dinner box made of recycled paper from Endura costs 0.43 NZD/tray (Products, n.d.). In contrast, Green Choice bagasse trays cost 0.581 NZD/tray (Disposable Tableware, n.d.). Therefore, the cost of apple pomace trays should be slightly lower or within this range to remain cost competitive.

The handsheet formulated with 50% AP had the best properties, although only 25% AP trays were moulded due to some issues discussed in section 6.2.1, a 50% AP formulation is assumed as mentioned previously that the small particles might not be an issue for manufacturing. The following estimated cost analysis includes the price of apple pomace sourced from manufacturers in New Zealand, as well as equipment, water and energy consumption required for production. These considerations ensure a comprehensive understanding of the economic feasibility of producing moulded trays using apple pomace as a sustainable alternative to conventional materials. The price of apple pomace, according to Profruit Juicing Company, is approximately 10 NZD/tonne, whereas BCTMP costs 600 USD/tonne (equivalent to 1060 NZD/tonne). However, it is necessary to consider the moisture content of the apple pomace. Based on the information from literature review, apple pomace typically contains around 70%

moisture, which makes the actual price for the dry basis become 33.33 NZD per tonne. Since the price of apple pomace is just around 3% of BCTMP (consider the moisture), substituting 50% of BCTMP with apple pomace could potentially reduce the overall raw material cost even taking account into the transportation and additional processing line setup.

6.3.1 Apple pomace fibre costs

Apples are one of the most widely grown fruits in New Zealand. The majority of apple production is in the Hawke's Bay region (65%), due to its fertile soil, abundant sunshine, and sheltered conditions (Hawke's Bay Fruitgrowers' Association, 2024). The process for producing apple pomace, illustrated in **Figure 79**, is based on the works of Bhushan et al. (2008) and Bates et al. (2001). As a byproduct of the pressing process, it can undergo enzymatic treatment and be reprocessed for additional juice extraction in some case.

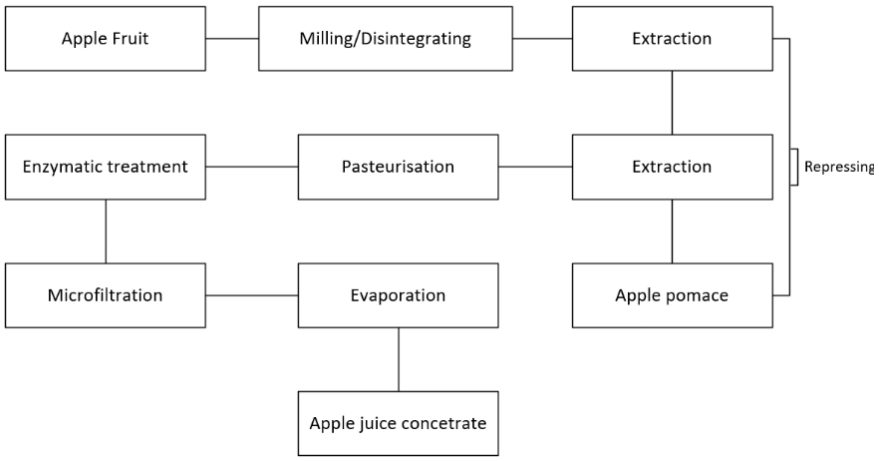

Figure 79. Processing diagram of the apple juicing, showing that the apple pomace is discharged after pressing.

The key manufacturers for apple juicing include Profruit (Hastings), Frupak (Hastings), and Juice Products New Zealand (JP-NZ) (South Canterbury), all of which serve as potential suppliers of apple pomace within New Zealand. Profruit supplied the apple pomace used in this study. In 2016, approximately 10,000–15,000 metric tonnes (MT) of apple pomace were produced from juicing (Archer et al., 2019), and this figure has been steadily increasing, as New Zealand's apple production is forecasted to reach

460,000 MT, according to the U.S. Department of Agriculture (USDA, 2023). With 22% of apples allocated for juice, concentrates, and other products, around 101,200 MT of apples are estimated to be processed for juicing. Based on a typical apple pomace yield of 30% of the original apple weight (Gowman et al., 2019; Lyu et al., 2020), this would result in more than 30,000 MT of pomace.

6.3.2 Process investment cost

To produce 960 tonnes of moulded fibre trays (over 27,000,000 trays based on 35 g/tray) from a blend of 50% apple pomace and 50% BCTMP, an annual production model is outlined. In this study, it is assumed that the BCTMP pulping process has already been existing. Therefore, the model will focus only on processing apple pomace and blending those two pulps to estimate the cost difference between moulded fibre trays made from traditional wood fibres and those incorporating apple pomace. It will require additional adjustments to accommodate the complexity of integrating it into scaled-up production.

Apple pomace suppliers are mostly distributed across the Hawkes Bay, transportation costs could be minimised if the pulping and moulding productions are available close to the sources. Such a plant would be particularly suited to this project's needs that ensures flexibility in operation, minimises logistical burdens, and makes the most of regionally available resources.

Transportation costs are excluded from this analysis because they are not part of the onsite processing, since the location has been assumed to be by the source, and the Hawk packaging in Hawkes Bay has moulded fibre thermo-forming capability. This evaluation only focuses on the pulping unit, while the cost for the thermoforming would be based on the power and cost for Kiefel moulding thermo-former.

A conceptual flow diagram was developed to illustrate the pulping and moulding processes. The diagram and associated mass balances are shown in the **Figure 80**, **Figure 81** and **Figure 82**. This includes the processing of apple pomace slurry (disintegration and wet sieving), and dispersion of BCTMP pulp. In the flow diagram, the apple pomace is firstly broken down in a disintegrator, then passed through a hydro-

cyclone to remove large particles such as seeds and skin residues, and this waste stream will be utilised as animal stock food. Then a rotary wet sieve further screens out particles smaller than 200 μm using flowing water. The water used for wet sieving can be recycled for subsequent batches to reduce water usage. The water will be filtered to remove apple pomace residues. Excessive water will be discharged as effluent (**Figure 81**). The filtered apple pomace with small particles ('Waste stream 3') will be combined with the waste stream from hydro-cyclone ('Waste stream 1') as stock food. The filter cake from waste stream 3 is assumed to have a moisture content of 50%. At the same time, dry BCTMP pulp is disintegrated with steam injected into the tank to maintain a constant temperature of 85°C. After 10 minutes of heating, the pulp is transferred to another tank, where cold water is added to cool the slurry and adjust its consistency. Once the slurry is cooled to room temperature (20°C), the BCTMP slurry is pumped into a blending tank equipped with an agitator, and in this study the BCTMP pulping processing is assuming to be existing. Then it is combined with screened apple pomace slurry (particle size 200 μm to 1 mm) while additional water is added to achieve the desired consistency (0.3%wt).

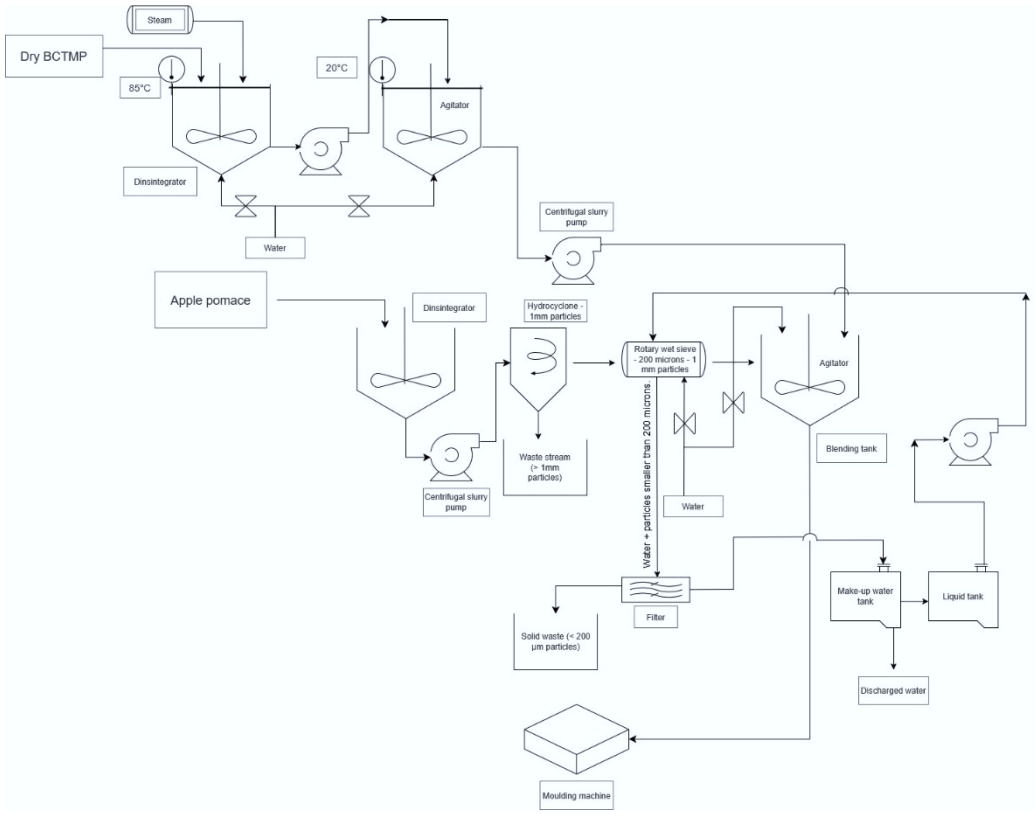

Figure 80. Flow diagram of pulping process, including the BCTMP latency removal, apple pomace processing (disintegration and wet-sieving, pulp blending, and thermo-moulding.

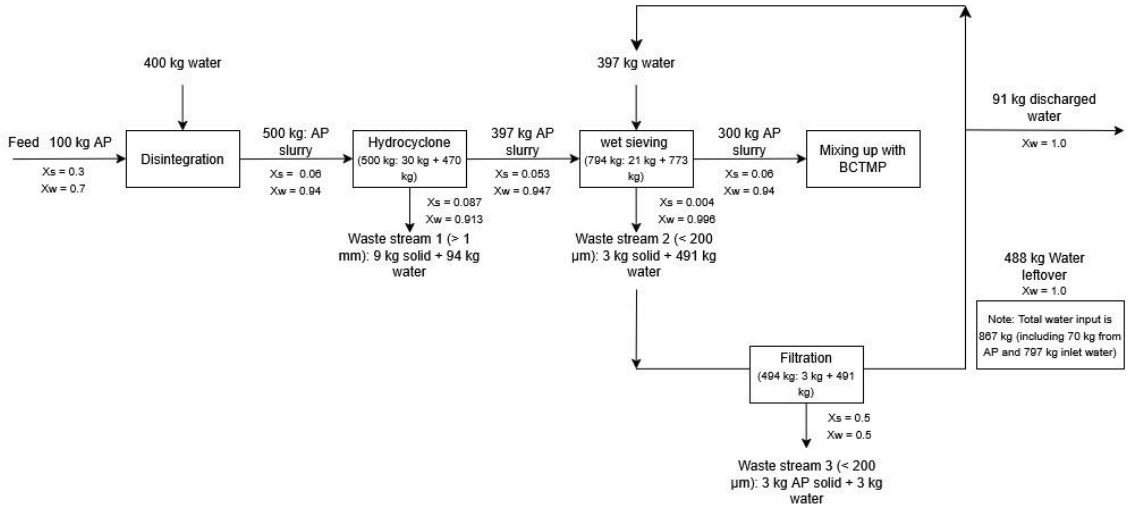

Figure 81. The mass balance of the apple pomace processing

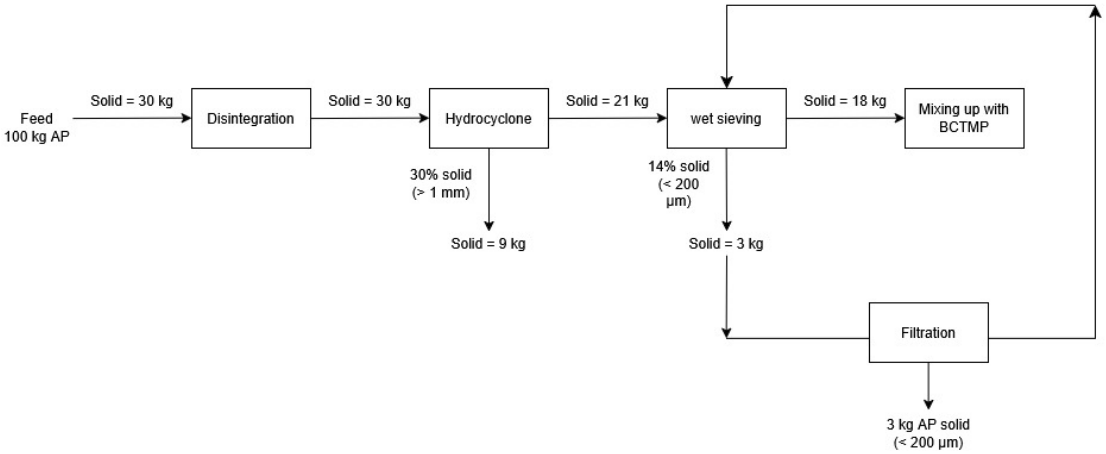

Figure 82. The solid balance of the apple pomace processing.

As mentioned previously, the BCTMP pulping process is assumed to be existing, associated equipment for processing apple pomace and pulp blending are presented in **Table 28** including their size and capacity details, which are from multiple suppliers and sources on the website "en.made-in-china.com" (Made-in-China, n.d.). The system was designed to suit batch production.

Table 28. The approximate cost of equipment involved, including their capacity and required loading estimation.

Component	Loading	Effectiveness/ Volume/Capacity	Estimated price (NZD)	Brand
Major equipment				
Disintegrator (Pulper)	AP: 47.6 kg of apple pomace + 119 kg of water. Disintegrate for around 10 min, at around 1 m^3/hr	1 m^3/hr 4000 rpm 15 kW	17,415	Shanghai Senfan machinery Co., Ltd.
Hydro-cyclone	4 m^3/hr disintegrated AP slurry	18 – 43 m^3/hr	4,500*1	Ganzhou Gelin Mining Machinery Co., Ltd.
Rotary wet sieve	2 m^3/hr 1 mm-sieving 4 m^3/hr water (keep rinsing the apple pomace to make it easily sieved)	1.5 – 100 t/hr 3 kW	14,000*1	Xinxiang Tianfeng Vibrating Machinery Co., Ltd.
Centrifugal slurry pump * 3		Up to 200 m^3/h 20 kW	2,600*3	Jiangsu haishi pump manufacturing Co., Ltd.
Agitator		Up to 2000 rpm 32 W	2,490	IKA
Parts and accessories				
Water valve			8.8*2	WOD Valve Group Co., Ltd.
Blending tank*2		1000 L	1,750*2	Wenzhou Rayen Machinery Co., Ltd.
Water tank*2		2000 L	7,500*2	Jinan Cassman Machinery Co., Ltd.
		Total:	64,722.6	

For the fixed- and total capital investments, shipping fees were estimated at five percent of the listed purchase price, and other additional expenses were calculated as percentages of the delivered-equipment cost for solid–fluid processing utilised in Lo et al. (2024), who did the economic analysis for hemp hurd tray manufacturing. However, since the objective of this cost analysis is to evaluate only the processing of apple pomace and pulp blending, with the BCTMP pulping process already in place, some elements in this capital investment model (**Table 29**) will not be applicable.

Table 29. Total capital investment, including the direct, indirect costs and working capacity.

	% Of delivered-equipment costs for solid-fluid processing plant	Equipment cost (NZD)
Direct cost		
Delivered equipment	5	3,236.13
Purchased-equipment installation	39	25,241.8
Instrumentation and control (installed)	26	16,827.9
Piping (installed)	10	6,472.3
Electrical systems (installed)	10	6,472.3
Buildings (including services)	0	0
Yard improvements	6	3,883.4
Service facilities (installed)	0	0
Total direct plant cost	96	62,133.7
Indirect cost		
Engineering and supervision	0	0
Construction expenses	0	0
Legal expenses	4	2,588.9
Contractor's fee	0	0
Contingency	10	6,472.3
Total indirect plant cost	126	9,061.2
Fixed-capital investment		71,194.9
Working capacity (15% of total capital investment)		10,679.2
Equipment		64,722.6
Total capital investment		146,596.7

Based on the assumption, the investment for buildings, service facilities (including water, compressed air, and vacuum systems, etc), and most indirect costs, except for legal expenses, are excluded, as they are assumed to be already established within the existing pulping plant. Therefore, the total capital investment, including the equipment, required for apple pomace processing and pulp blending is estimated to be NZ$146,596.7.

6.3.3 Operation cost

It is proposed that 960 tonnes of trays will be produced annually, with assuming 35 grams for each tray, the total number of the trays will be approximately 27,428,570. As detailed in Section 6.3, the cost of apple pomace is given NZ$10 per tonne by the Profruit. Based on the assumption that the apple pomace has a 70% moisture content and 60% of fine particles could be retained after wet-sieving. The annual requirement for apple pomace to make 50% apple pomace trays is calculated to be 2,666 tonnes, valued at NZ$ 266,600.

To run the equipment required for apple pomace processing, the actual power depends on motor capacity and loading during production. Based on the loading amount from **Table 28**, 285.6 kg of AP could be disintegrated by per hour, equivalent to around 3.5 hours per tonne. Thus, an estimated 273.112 kWh to process per tonne of AP is calculated, amounting to 728,116.6 kWh to process all AP, as displayed in **Table 30**. New Zealand's average industrial electricity price was 0.178 NZD/kWh in 2024 (Statista, 2024), this gives a cost of a NZ$ 48.61 per tonne and a total annual cost of NZ$ 129,605 are calculated. Additionally, the water expenses associated with apple pomace processing are also considered. Assuming that the water usage for disintegrating and wet sieving apple pomace is four times the volume of the pomace, based on the experiments conducted and consideration of water recycling from wet sieving, the water consumption would be approximately 10,664 tonnes. Considering that 60% of fine particles can be retained after wet sieving, equivalent to 480 tonnes on a dry basis, an additional 159,480 tonnes of water would be needed to achieve a 0.3% consistency. Water costs vary by location, but with an average rate of NZ$ 1.43 per

cubic meter, making the total water cost amounts to NZ$ 256,649. Additionally, wastewater treatment fees also differ by regions, with averaging around NZ$ 1.20 per cubic meter. Assuming that 90% of the water used requires treatment, this would result in an additional cost of NZ$ 193,833. The total cost of for additional apple pomace processing and pulp blending is illustrated in **Table 31**.

The additional operation cost of processing apple pomace per tray is estimated at NZ$ 0.0216. However, this should exclude the difference in material cost between trays made of 50% AP and 100% BCTMP, since the cheaper price of apple pomace that replaces 50% BCTMP can reduce the overall material cost, as shown in the Table **32**.

Table 30. Usage of electricity to process per tonne of apple pomace (3.5 hr/tones).

Equipment	Power (kW)	kWh
Disintegrator (Pulper)	15	52.5
Rotary wet sieve	3	10.5
Centrifugal slurry pump	20*3	210
Agitator	0.032	0.112
	Total	273.112

Based on the price of dry BCTMP pulp at NZ$ 1,060/tonne, the material cost difference, between 50% apple pomace tray and 100% BCTMP tray, amounts to NZ$ 482,140 for producing 960 tonnes of trays, equivalent to NZ$ 0.0176 per tray. As a result, the additional cost for making apple pomace trays compared to traditional BCTMP ones is NZ$ 0.0041 per tray, which means the overall cost might be almost the same. However, in real production scenarios, transportation costs cannot be ignored, and the cost of apple pomace tray may be higher compared to 100% BCTMP trays. Additionally, since the commonly used material for moulding food trays in the market might be most cost-effective than BCTMP pulp, the additional processing costs for adding apple pomace would increase due to the relatively smaller cost difference from the materials.

Table 31. Estimation of overall operating cost for pulping process of 50% apple pomace trays.

	Unit price (NZD)	Amount	Total price (NZD)
Apple pomace	10	2666 tonnes	266,60
Power	0.178	728116.6 kWh	129,604.8
Water	1.43	170,144 cubic	256,649
Wastewater treatment	1.2	161,528 cubic	193,833
		Total cost:	593,404.3
		Cost/tray:	0.0216

Table 32. Difference in the cost for materials for 960 tonnes of 50% apple pomace trays and 100% BCTMP trays.

Tray	Material cost (NZD)	Total (NZD)
100% BCTMP	1060*960	1,017,600
50% AP + 50% BCTMP	10*2666 + 1060*480	535,460
	Difference in cost	482,140

6.4 Legislation for Food Contact Material: Food compliance

Legislation for Food Contact Materials (FCMs) is designed to ensure that materials in direct contact with food, such as packaging, tableware, and containers, do not pose any risk to human health. These laws are designed to regulate the composition of FCMs and to limit the migration of substances from these materials into foodstuffs. While there are no stringent laws specifically regulating paper and board-based food packaging materials, the chemical composition of biomass blended with paper pulp and additives used during processing, as well as the chemical migration from paper and boards, must comply with existing regulatory standards (Baughan, 2022; Rijk & Veraart, 2010). Since the moulded fibre tray developed in this study is focused on the New Zealand local market, the FCM regulation of New Zealand will be introduced:

6.4.1 Australia and New Zealand

In Australia and New Zealand, FCMs are regulated under the framework provided by Food Standards Australia New Zealand (FSANZ) with the Australia New Zealand Food Standards Code, which was firstly published in 2000 (Baughan, 2022). While there are no specific regulations for FCMs, but the Standard 1.4.1, for addressing contaminants, and Standard 3.2.2, outlining food safety practices and general requirements, are applied. These standards ensure that chemicals migrating from packaging into food meet safety requirements to minimise risks such as contamination, the introduction of harmful microorganisms, and chemical transfer. Manufacturers are required to follow Good Manufacturing Practices (GMP) to ensure consistent quality and safety in materials used for packaging and processing.

According to Baughan (2022), FSANZ released the abandonment report for Proposal P1034: "Chemical Migration from Packaging into Food" in 2017, which provided an initial assessment of the risks associated with chemicals migrating from packaging into food. Meanwhile, New Zealand's Ministry for Primary Industries (MPI) conducted a study titled "Occurrence and Risk Characterisation of Migration of Packaging Chemicals in New Zealand Foods" (MPI Technical Paper No: 2017/61). This study focused on the migration of chemicals such as phthalates, printing inks, and photo-initiators, which could offer some valuable insights into the potential risks these substances pose. These efforts indicate the growing recognition of chemical migration as the key risk of FCMs.

Although there is no specific regulations for FCMs on food packaging, the regulated chemicals outlined by the European Union (EU) and listed by the Council of Europe (2002) can serve as a reference (**Table 33**):

Table 33. Quantitative migration (QM) restrictions of some substances in paper and board given by the EU (Council of Europe, 2002).

Substance	Restriction (QM limit) in mg/dm2 paper and board
Cadmium	0.002
Lead	0.003
Mercury	0.002
Pentachlorophenol	0.15 (mg/kg purity)

6.4.1.1 Composition in apple pomace

Based on the current studies, the apple pomace have been developed for functional food or supplementary foods, and there is not enough data yet to determine the potential risk associated with apple pomace (Lyu et al., 2020). However, there are still two concerns from the apple seeds and pesticide residues in the apple pomace (Skinner et al., 2018).

As the major material utilised in this study, whether the composition of apple pomace complies with FCM legislation when used in food packaging is important. As discussed in the previous section, New Zealand does not have specific regulations for FCMs but lists general migration restrictions. Current research indicates that apple pomace has been utilised in functional and supplementary foods, and there is insufficient data yet to support its potential risk (Lyu et al., 2020). However, there are two concerns from the presence of toxicity in apple seeds and pesticide residues in the pomace (Skinner et al., 2018).

Pesticide residues remain in the apple pomace, including chlorpyrifos and imidacloprid, may be a potential risk and must adhere to FSANZ's regulations. However, a review by Skinner et al. (2018) found that pesticide residues in apple pomace are generally within safety thresholds, which poses minimal risk to human health. A greater concern is the presence of natural toxins in apple seeds. Amygdalin released from apple seed can cause cyanide poisoning when disrupted (Lyu et al., 2020), leading to symptoms such as headaches and dizziness (Vogel et al., 1981). However, studies suggest that the poisoning would only occur with 800 g of apple pomace consumption, which is highly improbable (Gołębiewska et al., 2022; Lyu et al., 2020). In this study, only around 18 grams of sieved apple pomace will be used in each tray, which means the major amygdalin have already been removed with large seed residues, and the remaining amygdalin could bring a minimal concern. Additionally, the high temperature of thermal moulding process might degrade the remaining amygdalin as well. Despite the minimal risks associated with using apple pomace in FCMs, the essential migration testing for these specific chemicals is still recommended to ensure the material meets with safety standards.

6.4.1.2 Ban in PFAS

Per- and polyfluoroalkyl substances (PFAS), which are lipophobic and hydrophobic coating substances. These have been commonly used in packaging to provide resistance to water and oil, specifically in applications such as food takeaway containers and compostable fibre-based packaging. However, these substances are highly toxic that can cause severe health issues, such as liver damage, immune dysfunction, and cancer (The Packaging Forum, 2022a). The Environmental Protection Authority has announced a ban on the import and manufacture of cosmetics containing PFAS, effective from 31 December 2026 (Environmental Protection Authority, 2025). Although New Zealand currently lacks official documentation specifying class-based limits for PFAS in food packaging, New Zealand has agreed to restrict PFAS as part of the Stockholm Convention on Persistent Organic Pollutants in 2001 (The Packaging Forum, 2022b). Several global catering companies also have pledged to eliminate PFAS from their food packaging in 2020s, which is expected to impact New Zealand as well (Toxic-Free Future, n.d.).

Chapter 7 Conclusions and Recommendations

7.1 Conclusions

The objective of this thesis was to investigate the use of local New Zealand food processing waste as an alternative material for creating moulded fibre packaging, which could serve as a sustainable substitute for single-use plastic trays. Specifically, the research involved pulping apple pomace and corn husk, which were then mixed in various proportions with BCTMP pulp to create handsheets for evaluation. Some sheets were subsequently subjected to thermoforming conditions to assess their performance as potential formulations for food trays made via moulded fibre thermoforming process.

The assessment of the mechanical properties of control BCTMP and apple pomace/corn husk fibre-based handsheets indicated that increasing the apple pomace content enhanced the tensile properties. This improvement is attributed to the denser structure and stronger inter-fibre bonding, as the voids within the BCTMP were filled by the short fibres of apple pomace, which was proved by the surface images at 10x magnification. To maximise this effect, a hot-pressing process was implemented, which simulated the conditions of a thermoformer at 230°C, applying 7.8 kN per sheet for 30 seconds. The hot-pressed apple pomace sheets outperformed the hot-pressed BCTMP sheets, and generally, all hot-pressed sheets showed better performance than their standard-pressed counterparts, with the exception of reductions in TEA (total energy absorbed), elongation, and tearing strength of the apple pomace sheets due to the high rigidity caused by dehydrated apple pomace components and hornification.

The test results illustrated that an increase in corn husk content adversely affected the tensile properties of the handsheets. This reduction in performance was mainly due to poor bonding between the corn husk fibres and BCTMP, resulting in a loss of grammage, a lower density, a low percentage of effective fibres, and uneven fibre distribution across the surface. These factors contributed to variability in the tensile properties at different locations on the surface.

The improved water resistance was attributed to their increased density, lignin flow, surface roughness, hydrophobicity, and hornification, as demonstrated by the measurement of contact angle and roughness by fringe projection. The inclusion of apple pomace and corn husk fibres also enhanced all barrier properties, such as resistance to water, oil, and air. This enhancement was due to the high density provided by apple pomace and the hydrophobic surface characteristics of the corn husk sheets. The hot-pressing process further improved these properties, optimising the material's overall barrier effectiveness.

The manufacturing process and economic evaluation for tray production were carried out. The analysis indicated that using apple pomace in New Zealand could potentially substitute 10% of single-use plastic food trays, aligning with the Ministry of the Environment's objectives to phase out single-use plastics. A simulated pulping and moulding process was developed, and the cost analysis revealed that the total production cost for 960 tonnes of trays would be estimated 997,768 NZD (0.0364 NZD per tray), including materials, equipment, total capital investment, and energy costs. This would be considered to substitute about 10% of single-use plastics in food packaging use, resulting in reduced imported plastics and reducing the cost of disposing plastics. The compliance of apple pomace-based moulded pulp food trays with food contact standards was also assessed. It was found that New Zealand lacks specific directives or regulations for paper packaging, but stricter and more comprehensive regulations exist in China, which is a large potential overseas market. Furthermore, the materials and processing chemicals used must adhere to Good Manufacturing Practice (GMP).

7.2 Recommendations

1. Future studies could expand to analyse other aspects of pulps such as fibre coarseness, the impact of various pulp components like fines materials (whether fibrillar or particulate), fibre bonding levels, and refining intensity that will influence the fineness of pulp.
2. To enhance the mechanical and barrier properties further, it might be beneficial to incorporate agents like nano-cellulose and consider the use of cationic agents to

maintain pH levels and improve the retention of fine particles to allow for additional small-particle additives.

3. Chemical pulping or using green corn husks can be applied to explore the effectiveness of corn husks as this may overcome some of the difficulties encountered with using dried corn husks.
4. The impact of storage conditions on the fibres in this study should be investigated, considering it an important factor as manufacturers often store large quantities of fibres before being put into production in batches.
5. The suitability of the thermo-former and centrifugal pump utilised for producing trays with 50% apple pomace warrants investigating to ensure maximising the retention of particle size during moulding, so that trays with a higher apple pomace content could be produced.
6. A more rigorous economic and feasibility case study is required to determine if incorporating apple pomace into moulded thermos-formed food packaging will be commercially viable.

Reference

Abd Rahman, N. S., & Azahari, B. (2012). Effect of calcium hydroxide filler loading on the properties of banana stem handsheets. *BioResources Journal*, *7*(3), 4321-4340.

Agnihotri, S., Dutt, D., & Tyagi, C. (2010). Complete characterization of bagasse of early species of Saccharum officinerum-Co 89003 for pulp and paper making. *BioResources*, *5*(2), 1197-1214.

Ahmad Rassdi, N. H. (2013). Cellulosic-Based Packaging Material from Corn Husk.

Ahmadi, M., Latibari, A. J., Faezipour, M., & Hedjazi, S. (2010). Neutral sulfite semi-chemical pulping of rapeseed residues. *Turkish Journal of Agriculture and forestry*, *34*(1), 11-16.

Alghamdi, M. N. (2021). Effect of filler particle size on the recyclability of fly ash filled HDPE composites. *Polymers*, *13*(16), 2836.

Alince, B., Porubská, J., & Van de Ven, T. (2001). Effect of model and fractionated TMP fines on sheet properties. *The science of papermaking*, *2*, 343-1355.

Amode, N. S., & Jeetah, P. (2021). Paper production from Mauritian hemp fibres. *Waste and Biomass Valorization*, *12*, 1781-1802.

Anjos, O., Santos, A. J., Simões, R., & Pereira, H. (2014). Morphological, mechanical, and optical properties of cypress papers. *Holzforschung*, *68*(8), 867-874.

Archer, R., Eblaghi, M., Yedro, F. M., O'Donoghue, E., Huffman, L., & Bronlund, J. (2019). FIET project: Creamed pomace-a smooth-textured dietary fibre product from apple pomace. *Food New Zealand*, *19*(6), 26-27.

Bahreini, Z., Abedi, M., & Fateh, D. S. (2022). A Study on Preparation and Characterization of Microcrystalline Cellulose from Lucerne (alfalfa) Waste Fibers.

Bajpai, P. (2015). *Pulp and paper industry: Chemicals*. Elsevier.

Baley, C. (2002). Analysis of the flax fibres tensile behaviour and analysis of the tensile stiffness increase. *Composites Part A: Applied Science and Manufacturing*, *33*(7), 939-948.

Bates, R., Pierce, R., Morris, J., & Crandall, P. (2001). Tree fruit: Apple, pear, peach, plum, apricot and plums. *Principles and practices of small-and medium-scale fruit juice processing. FAO Agricultural Services Bulletin*, *146*, 151-169.

Baughan, J. S. (2022). *Global legislation for food contact materials*. Woodhead Publishing.

Bayatkashkoli, A. (2013). Evaluation of process variables effect on the bursting strength of newsprint, printing and writing paper. *Journal of the Indian Academy of Wood Science*, *10*, 55-61.

Behera, S., Patel, S., & Mishra, B. (2015). Effect of blending of sisal on pulp properties of waste papers in handmade papermaking.

Bell, J., & Keith, M. (1991). A survey of variation in the chemical composition of commercial canola meal produced in Western Canadian crushing plants. *Canadian journal of animal science*, *71*(2), 469-480.

Bhushan, S., Kalia, K., Sharma, M., Singh, B., & Ahuja, P. S. (2008). Processing of apple pomace for bioactive molecules. *Critical reviews in biotechnology*, *28*(4), 285-296.

Biermann, C. J. (1996). *Handbook of pulping and papermaking*. Elsevier.

Boufi, S., González, I., Delgado-Aguilar, M., Tarrès, Q., Pèlach, M. À., & Mutjé, P. (2016). Nanofibrillated cellulose as an additive in papermaking process: A review. *Carbohydrate polymers*, *154*, 151-166.

Branca, G., Resciniti, R., & Babin, B. J. (2024). Sustainable packaging design and the consumer perspective: a systematic literature review. *Italian Journal of Marketing*, *2024*(1), 77-111.

Buxoo, S., & Jeetah, P. (2020). Feasibility of producing biodegradable disposable paper cup from pineapple peels, orange peels and Mauritian hemp leaves with beeswax coating. *SN Applied Sciences*, *2*, 1-15.

Caulfield, D. F. (1987). *Dimensional stability of paper: papermaking methods and stabilization of cell walls*. Forest Products Laboratory Madison, WI.

Chemistry, L. T. (2024). *GENERAL, ORGANIC, AND BIOCHEMISTRY WITH PROBLEMS, CASE STUDIES, AND ACTIVITIES* (12.1: Carbohydrates Issue. https://chem.libretexts.org/Courses/Roosevelt_University/General_Organic_and_Biochemistry_with_Problems_Case_Studies_and_Activities/12%3A_Carbohydrates/12.01%3A_Carbohydrates

Chen, J.-H., Wang, K., Xu, F., & Sun, R.-C. (2015). Effect of hemicellulose removal on the structural and mechanical properties of regenerated fibers from bamboo. *Cellulose*, *22*, 63-72.

Cheng, H., Ford, C., Dowd, M. K., & He, Z. (2016). Use of additives to enhance the properties of cottonseed protein as wood adhesives. *International Journal of Adhesion and Adhesives*, *68*, 156-160.

Cheng, H., Villalpando, A., Easson, M. W., & Dowd, M. K. (2017). Characterization of cottonseed protein isolate as a paper additive. *International Journal of Polymer Analysis and Characterization*, *22*(8), 699-708.

Citrus New Zealand. (2020). *How big is NZs citrus industry?* https://www.citrus.co.nz/faq/how-big-is-the-citrus-industry-in-new-zealand/?utm_source=chatgpt.com

Council of Europe. (2002). *Resollution ResAP(2002)1 on paper and board materials and articles intended to come into contact with foodstuffs*. Retrieved from https://rm.coe.int/09000016804d82f8?utm_source=chatgpt.com

da Luz, F. S., Paciornik, S., Monteiro, S. N., da Silva, L. C., Tommasini, F. J., & Candido, V. S. (2017). Porosity assessment for different diameters of coir lignocellulosic fibers. *Jom*, *69*, 2045-2051.

Das, T. K., & Houtman, C. (2004). Evaluating chemical-, mechanical-, and bio-pulping processes and their sustainability characterization using life-cycle assessment. *Environmental Progress*, *23*(4), 347-357.

de Moraes Crizel, T., de Oliveira Rios, A., Alves, V. D., Bandarra, N., Moldão-Martins, M., & Flôres, S. H. (2018). Active food packaging prepared with chitosan and olive pomace. *Food Hydrocolloids*, *74*, 139-150.

Didone, M., Saxena, P., Brilhuis-Meijer, E., Tosello, G., Bissacco, G., Mcaloone, T. C., Pigosso, D. C. A., & Howard, T. J. (2017). Moulded pulp manufacturing: Overview and prospects for the process technology. *Packaging Technology and Science*, *30*(6), 231-249.

Didone, M., & Tosello, G. (2019). Moulded pulp products manufacturing with thermoforming. *Packaging Technology and Science*, *32*(1), 7-22.

Dislaire, C., Seantier, B., Muzy, M., & Grohens, Y. (2021). Mechanical and hygroscopic properties of molded pulp products using different wood-based cellulose fibers. *Polymers*, *13*(19), 3225.

Disposable Tableware. (n.d.). *Green Choice Large Square 3 Compartment Bio Food Pack*. https://disposabletableware.co.nz/product/green-choice-large-square-3-compartment-bio-food-

pack/?gad_source=1&gclid=Cj0KCQiA19e8BhCVARIsALpFMgF1qE232vaH77C-M4hcezu1bf-fhu_Htf1zTmN8r54HrxzulQoOMvQaAtctEALw_wcB

El-Sohaimy, S. A., Androsova, N. V., Toshev, A. D., & El Enshasy, H. A. (2022). Nutritional quality, chemical, and functional characteristics of hemp (Cannabis sativa ssp. sativa) protein Isolate. *Plants*, *11*(21), 2825.

Environmental Protection Authority. (2025). *PFAS are forever – a complicated chemical family*. https://www.epa.govt.nz/community-involvement/science-at-work/pfas/?utm_source=chatgpt.com

Farmahini-Farahani, M., Bedane, A. H., Pan, Y., Xiao, H., Eic, M., & Chibante, F. (2015). Cellulose/nanoclay composite films with high water vapor resistance and mechanical strength. *Cellulose*, *22*, 3941-3953.

FDA. (2024). *CFR - Code of Federal Regulations Title 21*. https://www.accessdata.fda.gov/scripts/cdrh/cfdocs/cfcfr/CFRSearch.cfm?fr=176.120

FMI. (2023). *Takeaway Containers Market Outlook (2023 to 2033)*. https://www.futuremarketinsights.com/reports/takeaway-containers-market

Fujimoto, J. G., Pitris, C., Boppart, S. A., & Brezinski, M. E. (2000). Optical coherence tomography: an emerging technology for biomedical imaging and optical biopsy. *Neoplasia*, *2*(1-2), 9-25.

Future Market Insights. (2024). *Molded Fibre Pulp Packaging Industry Analysis in Australia and New Zealand*. https://www.futuremarketinsights.com/reports/australia-and-new-zealand-molded-fiber-pulp-packaging-market

Galhano dos Santos, R., Ventura, P., Bordado, J. C., & Mateus, M. M. (2016). Valorizing potato peel waste: an overview of the latest publications. *Reviews in Environmental Science and Bio/Technology*, *15*, 585-592.

Gao, J. (2014). *Modelling latency removal in mechanical pulping processes* University of British Columbia].

Garcia-Amezquita, L. E., Tejada-Ortigoza, V., Pérez-Carrillo, E., Serna-Saldívar, S. O., Campanella, O. H., & Welti-Chanes, J. (2019). Functional and compositional changes of orange peel fiber thermally-treated in a twin extruder. *Lwt*, *111*, 673-681.

Gierer, J. (1980). Chemical aspects of kraft pulping. *Wood Science and Technology*, *14*(4), 241-266.

Giertz, H. W. (1958). The effects of beating on individual fibres. Transactions of Cambridge Symposium, British Paper and Board Association,

Gill, R. A. (1995). Fillers for papermaking. In *Applications of wet-end paper chemistry* (pp. 54-75). Springer.

Glenn, G., Shogren, R., Jin, X., Orts, W., Hart-Cooper, W., & Olson, L. (2021). Per-and polyfluoroalkyl substances and their alternatives in paper food packaging. *Comprehensive Reviews in Food Science and Food Safety*, *20*(3), 2596-2625.

Gołębiewska, E., Kalinowska, M., & Yildiz, G. (2022). Sustainable use of apple pomace (AP) in different industrial sectors. *Materials*, *15*(5), 1788.

Gouw, V. P., Jung, J., Simonsen, J., & Zhao, Y. (2017). Fruit pomace as a source of alternative fibers and cellulose nanofiber as reinforcement agent to create molded pulp packaging boards. *Composites Part A: Applied Science and Manufacturing*, *99*, 48-57.

Gowman, A. C., Picard, M. C., Rodriguez-Uribe, A., Misra, M., Khalil, H., Thimmanagari, M., & Mohanty, A. K. (2019). Physicochemical Analysis of Apple and Grape Pomaces. *BioResources*, *14*(2).

Grand View Research. (2023). *Molded Fiber Packaging Market Size, Share & Trends Analysis Report By Source (Wood Pulp, Non-Wood Pulp), By Molded Type (Thermoformed, Transfer), By Product, By End Use, By Region, And Segment Forecasts, 2024 - 2030*. https://www.grandviewresearch.com/industry-analysis/molded-fiber-packaging-market-report

Granucci, N., Harris, P. J., & Villas-Boas, S. G. (2023). Chemical Compositions of Fruit and Vegetable Pomaces from the Beverage Industries. *Waste and Biomass Valorization*, *14*(11), 3841-3856.

Han, J. H., & Krochta, J. M. (2001). Physical properties and oil absorption of whey-protein-coated paper. *Journal of Food Science*, *66*(2), 294-299.

Han, J. W., Ruiz-Garcia, L., Qian, J. P., & Yang, X. T. (2018). Food packaging: A comprehensive review and future trends. *Comprehensive Reviews in Food Science and Food Safety*, *17*(4), 860-877.

Hawke's Bay Fruitgrowers' Association. (2024). *New Zealand Apples and Pears October update*. https://hbfa.co.nz/new-zealand-apples-and-pears-october-update/?utm_source=chatgpt.com

Heinze, T. (2016). Cellulose: structure and properties. *Cellulose chemistry and properties: fibers, nanocelluloses and advanced materials*, 1-52.

Hejazi, S. M., Sheikhzadeh, M., Abtahi, S. M., & Zadhoush, A. (2012). A simple review of soil reinforcement by using natural and synthetic fibers. *Construction and building materials*, *30*, 100-116.

Heras-Ramírez, M. E., Quintero-Ramos, A., Camacho-Dávila, A. A., Barnard, J., Talamás-Abbud, R., Torres-Muñoz, J. V., & Salas-Muñoz, E. (2012). Effect of blanching and drying temperature on polyphenolic compound stability and antioxidant capacity of apple pomace. *Food and Bioprocess Technology*, *5*, 2201-2210.

Höglund, H. (2009). Mechanical pulping. *Pulping chemistry and technology*, 57-90.

Hsieh, C.-T., Chen, J.-M., Kuo, R.-R., Lin, T.-S., & Wu, C.-F. (2005). Influence of surface roughness on water-and oil-repellent surfaces coated with nanoparticles. *Applied Surface Science*, *240*(1-4), 318-326.

I'Anson, S., Sampson, W., & Savani, S. (2008). Density dependent influence of grammage on tensile properties of handsheets. *Journal of pulp and paper science*, *34*(3), 182.

Index mundi. (2024). *New Zealand Corn Production by Year*. https://www.indexmundi.com/agriculture/?country=nz&commodity=corn&graph=production

Jahangiri, F., Mohanty, A., Pal, A. K., Clemmer, R., Gregori, S., & Misra, M. (2024). Wax Coatings for Paper Packaging Applications: Study of the Coating Effect on Surface, Mechanical, and Barrier Properties. *ACS Environmental Au*.

Jajcinovic, M., Fischer, W. J., Hirn, U., & Bauer, W. (2016). Strength of individual hardwood fibres and fibre to fibre joints. *Cellulose*, *23*, 2049-2060.

Joelsson, T., Mattsson, A., Ketoja, J. A., Pettersson, G., & Engstrand, P. (2022). Lignin interdiffusion—A mechanism behind improved wet strength. Transactions of the 17th Fundamental Research Symposium, Cambridge, UK,

Joelsson, T., Pettersson, G., Norgren, S., Svedberg, A., Höglund, H., & Engstrand, P. (2020). High strength paper from high yield pulps by means of hot-pressing. *Nordic Pulp & Paper Research Journal*, *35*(2), 195-204.

Jones, D., Ormondroyd, G., Curling, S., Popescu, C.-M., & Popescu, M.-C. (2017). Chemical compositions of natural fibres. In *Advanced high strength natural fibre composites in construction* (pp. 23-58). Elsevier.

Joseleau, J.-P., Chevalier-Billosta, V., & Ruel, K. (2012). Interaction between microfibrillar cellulose fines and fibers: Influence on pulp qualities and paper sheet properties. *Cellulose*, *19*, 769-777.

Kabir, M. M., Alhaik, M. Y., Aldajah, S. H., Lau, K. T., Wang, H., & Islam, M. M. (2021). Effect of hemp fibre surface treatment on the fibre-matrix interface and the influence of cellulose, hemicellulose, and lignin contents on composite strength properties. *Advances in Materials Science and Engineering*, *2021*, 1-17.

Kan, M., & Miller, S. A. (2022). Environmental impacts of plastic packaging of food products. *Resources, Conservation and Recycling*, *180*, 106156.

Kang, H. J., & Min, S. C. (2010). Potato peel-based biopolymer film development using high-pressure homogenization, irradiation, and ultrasound. *LWT-Food Science and Technology*, *43*(6), 903-909.

Khwaldia, K., Attour, N., Matthes, J., Beck, L., & Schmid, M. (2022). Olive byproducts and their bioactive compounds as a valuable source for food packaging applications. *Comprehensive Reviews in Food Science and Food Safety*, *21*(2), 1218-1253.

Kiaei, M., & Samariha, A. (2011). Fiber dimensions, physical and mechanical properties of five important hardwood plants. *Indian Journal of Science and Technology*, 1460-1463.

Komuraiah, A., Kumar, N. S., & Prasad, B. D. (2014). Chemical composition of natural fibers and its influence on their mechanical properties. *Mechanics of composite materials*, *50*, 359-376.

Kumar, S., Chauhan, V. S., & Chakrabarti, S. K. (2016). Separation and analysis techniques for bound and unbound alkyl ketene dimer (AKD) in paper: A review. *Arabian Journal of Chemistry*, *9*, S1636-S1642.

Kuokkanen, M. J., Mäentausta, O. K., & Kuokkanen, T. J. (2018). Eco-and material-efficient utilization applications of biotechnologically modified fiber sludge. *BioResources*, *13*(1), 1457-1474.

Laftah, W. A., & Wan Abdul Rahman, W. A. (2016). Pulping process and the potential of using non-wood pineapple leaves fiber for pulp and paper production: A review. *Journal of Natural Fibers*, *13*(1), 85-102.

Lammi, S., Le Moigne, N., Djenane, D., Gontard, N., & Angellier-Coussy, H. (2018). Dry fractionation of olive pomace for the development of food packaging biocomposites. *Industrial Crops and Products*, *120*, 250-261.

Lang, C. V., Jung, J., Wang, T., & Zhao, Y. (2022). Investigation of mechanisms and approaches for improving hydrophobicity of molded pulp biocomposites produced from apple pomace. *Food and Bioproducts Processing*, *133*, 1-15.

Larsson, P. T., Lindström, T., Carlsson, L. A., & Fellers, C. (2018). Fiber length and bonding effects on tensile strength and toughness of kraft paper. *Journal of materials science*, *53*, 3006-3015.

Law, K.-Y. (2015). Water–surface interactions and definitions for hydrophilicity, hydrophobicity and superhydrophobicity. *Pure and Applied Chemistry*, *87*(8), 759-765.

Levlin, J.-E. (1980). *Some differences in the beating behaviour of softwood and hardwood pulps*. https://www.eucalyptus.com.br/artigos/1980_Differences+Beating+HWD+SWD+Pulps.pdf

Li, A., Xu, D., Luo, L., Zhou, Y., Yan, W., Leng, X., Dai, D., Zhou, Y., Ahmad, H., & Rao, J. (2021). Overview of nanocellulose as additives in paper processing and paper products. *Nanotechnology Reviews*, *10*(1), 264-281.

Li, C., Zhang, J., Han, J., & Yao, B. (2021). A numerical solution to the effects of surface roughness on water–coal contact angle. *Scientific reports*, *11*(1), 459.

Li, S., Ball, B., Donner, E., Thompson, M. R., Rempel, C., & Liu, Q. (2019). Mechanical properties of green canola meal composites and reinforcement with cellulose fibers. *Polymer Bulletin*, *76*, 1257-1275.

Li, Z., Rabnawaz, M., & Khan, B. (2020). Response surface methodology design for biobased and sustainable coatings for water-and oil-resistant paper. *ACS Applied Polymer Materials*, *2*(3), 1378-1387.

Liang, S., & McDonald, A. G. (2014). Chemical and thermal characterization of potato peel waste and its fermentation residue as potential resources for biofuel and bioproducts production. *Journal of agricultural and food chemistry*, *62*(33), 8421-8429.

Liu, C., Luan, P., Li, Q., Cheng, Z., Sun, X., Cao, D., & Zhu, H. (2020). Biodegradable, hygienic, and compostable tableware from hybrid sugarcane and bamboo fibers as plastic alternative. *Matter*, *3*(6), 2066-2079.

Liu, Y.-y., Liu, M.-r., Li, H.-l., Li, B.-y., & Zhang, C.-h. (2016). Characteristics of high yield pulp fibers by xylanase treatment. *Cellulose*, *23*, 3281-3289.

Liu, Y., & Daum, P. H. (2008). Relationship of refractive index to mass density and self-consistency of mixing rules for multicomponent mixtures like ambient aerosols. *Journal of Aerosol Science*, *39*(11), 974-986.

Lo, C. H., Wade, K. R., Parker, K. G., Mutukumira, A. N., & Sloane, M. (2024). Sustainable Paper-based Packaging from Hemp Hurd Fiber: A Potential Material for Thermoformed Molded Fiber Packaging. *BioResources*, *19*(1).

Lokantara, I., Suardana, N., Surata, I., & Winaya, I. (2020). A review on natural fibers: extraction process and properties of grass fibers. *International Journal of Mechanical Engineering and Technology (IJMET)*, *1*(11), 84-91.

Lyu, F., Luiz, S. F., Azeredo, D. R. P., Cruz, A. G., Ajlouni, S., & Ranadheera, C. S. (2020). Apple pomace as a functional and healthy ingredient in food products: A review. *Processes*, *8*(3), 319.

Macdonald, J. (2022). *Top of The South Organic Waste Mapping Report*.

Made-in-China. (n.d.). *GO SMART SOURCING*. https://en.made-in-china.com/

Marrot, L., Lefeuvre, A., Pontoire, B., Bourmaud, A., & Baley, C. (2013). Analysis of the hemp fiber mechanical properties and their scattering (Fedora 17). *Industrial Crops and Products*, *51*, 317-327.

Marsh, K., & Bugusu, B. (2007). Food packaging—roles, materials, and environmental issues. *Journal of Food Science*, *72*(3), R39-R55.

Mboowa, D. (2024). A review of the traditional pulping methods and the recent improvements in the pulping processes. *Biomass Conversion and Biorefinery*, *14*(1), 1-12.

Ministry of Environment. (2020). *Reducing the impact of plastic on our environment*. https://environment.govt.nz/assets/Publications/Files/Final-Reducing-the-impact-of-plastic-on-our-environment-December.pdf

Mo, W., Li, B., & Chen, K. (2024). The role of hornification in the deterioration mechanism of physical properties of unrefined eucalyptus fibers during paper recycling. *Tappi J*, *23*, 97-112.

Motamedian, H. R., Halilovic, A. E., & Kulachenko, A. (2019). Mechanisms of strength and stiffness improvement of paper after PFI refining with a focus on the effect of fines. *Cellulose*, *26*, 4099-4124.

Mustafa, A., Christensen, D., & McKinnon, J. (1996). Chemical characterization and nutrient availability of high and low fiber canola meal. *Canadian journal of animal science*, *76*(4), 579-586.

Nandkumar, P. (2009). Effects of pulp blending on strength properties of Ipomoea carnea Jacq. *Asian Journal of Chemistry*, *21*(6), 4571.

New Zealand Starch. (2020). *Production capacity*. https://www.nzstarch.co.nz/product/?utm_source=chatgpt.com

NZ Safety Blackwoods. (n.d.). *BioPak Natural Plant Fibre Takeaway Base-1000ml-50-Pack* https://nzsafetyblackwoods.co.nz/en/biopak-natural-plant-fibre-takeaway-base-1000ml-50-pack-424605?utm_term=&utm_campaign=SR%20-%20PMax%20-%20Tier%203%20-%20Remaining%20Categories&utm_source=adwords&utm_medium=ppc&hsa_acc=6884968864&hsa_cam=18134857366&hsa_grp=&hsa_ad=&hsa_src=x&hsa_tgt=&hsa_kw=&hsa_mt=&hsa_net=adwords&hsa_ver=3&gad_source=1&gclid=Cj0KCQiA19e8BhCVARIsALpFMgGDw-KCSRVioYpkc56qUU3hJ975Gt7zS-b9u5Sz8g_T10ZAWajKQicaAjvkEALw_wcB

Office of the Prime Minister's Chief Science Advisor. (2023). *To what extent can we quantify Aotearoa's plastic? New Zealand's data challenge*. https://www.pmcsa.ac.nz/topics/rethinking-plastics/quantifying-aotearoas-plastic/

Palonki, J. (2021). Refining energy and chemical savings in the BCTMP-process.

Petersson, M. (2011). The effect of pre-flocculation of fillers on paper strength.

Petroudy, S. D. (2017). Physical and mechanical properties of natural fibers. In *Advanced high strength natural fibre composites in construction* (pp. 59-83). Elsevier.

Pickering, K. L., Efendy, M. A., & Le, T. M. (2016). A review of recent developments in natural fibre composites and their mechanical performance. *Composites Part A: Applied Science and Manufacturing*, *83*, 98-112.

Pratley, H. (1965). Brightness Improvement During Cold Soda Pulping.

Preceden Research. (2025). *Molded Pulp Packaging Market Size, Share, and Trends 2025 to 2034*. https://www.precedenceresearch.com/molded-pulp-packaging-market

PrecedenceResearch. (2024). *Eco-friendly Food Packaging Market Size, Share, and Trends 2024 to 2034*. Precedence Research. https://www.precedenceresearch.com/eco-friendly-food-packaging-market

Products, P. (n.d.). *Endura Takeaway Dinner Box (Hot/Cold) - Carton/150*. https://packagingproducts.co.nz/products/food-service-and-catering/food-containers/endura-takeaway-dinner-box-carton150?gad_source=1&gclid=Cj0KCQiA19e8BhCVARIsALpFMgGjXHCHqTdlm8uKK50NGkDl6CV78BAE6m3WIer6s-NKm7Z0JrAZ_1caAjtWEALw_wcB

Qaseem, M. F., Shaheen, H., & Wu, A.-M. (2021). Cell wall hemicellulose for sustainable industrial utilization. *Renewable and Sustainable Energy Reviews*, *144*, 110996.

Rajala, H. (2012). The effect of size and structure of filler particles on paper properties.

Reiniati, I., Osman, N. B., Mc Donald, A. G., & Laborie, M.-P. (2015). Linear viscoelasticity of hot-pressed hybrid poplar relates to densification and to the in situ molecular parameters of cellulose. *Annals of forest science*, *72*, 693-703.

Retulainen, E., & Keränen, J. (2017). Changing Quality of Recycled Fiber Material–Part II. Characterization of the Strength Potential with Fiber Integrity Value and its Relationship with the Strength Properties of Paper. *BioResources*, *12*(3), 6109-6121.

Rijk, R., & Veraart, R. (2010). *Global legislation for food packaging materials*. John Wiley & Sons.

Robertsén, L., & Joutsimo, O. (2005). The effect of mechanical treatment on kraft pulps produced from different softwood raw materials. *Pap. Puu*, *87*(2), 111-115.

Rudi, H., & Resalati, H. (2015). Helianthus annus Waste Stalks, as a Substitute Raw Material for Mixed Hardwood Semi-Chemical Pulp.

Rudi, H., Resalati, H., Eshkiki, R. B., & Kermanian, H. (2016). Sunflower stalk neutral sulfite semi-chemical pulp: an alternative fiber source for production of fluting paper. *Journal of Cleaner Production*, *127*, 562-566.

Rui, Z., Yu, D., & Zhang, F. (2024). Novel cellulose nanocrystal/metal-organic framework composites: Transforming ASA-sized cellulose paper for innovative food packaging solutions. *Industrial Crops and Products*, *207*, 117771.

Sadrmanesh, V., & Chen, Y. (2019). Bast fibres: structure, processing, properties, and applications. *International Materials Reviews*, *64*(7), 381-406.

Safwa, M., Yeddu, H. K., & Leminen, V. (2024). Modeling of the Thermoforming Process of Paperboard Composites for Packaging. *BioResources*, *19*(2).

Sanchez-Salvador, J. L., Pettersson, G., Mattsson, A., Blanco, A., Engstrand, P., & Negro, C. (2024). Extending the limits of using chemithermomechanical pulp by combining lignin microparticles and hot-pressing technology. *Cellulose*, *31*(15), 9335-9348.

Santhosh, R., Nath, D., & Sarkar, P. (2021). Novel food packaging materials including plant-based byproducts: A review. *Trends in Food Science & Technology*, *118*, 471-489.

Schmid, V., Trabert, A., Schäfer, J., Bunzel, M., Karbstein, H. P., & Emin, M. A. (2020). Modification of apple pomace by extrusion processing: Studies on the composition, polymer structures, and functional properties. *Foods*, *9*(10), 1385.

Semple, K. E., Zhou, C., Rojas, O. J., Nkeuwa, W. N., & Dai, C. (2022). Moulded pulp fibers for disposable food packaging: A state-of-the-art review. *Food Packaging and Shelf Life*, *33*, 100908.

Sfiligoj Smole, M., Hribernik, S., Stana Kleinschek, K., & Kreže, T. (2013). Plant fibres for textile and technical applications. *Advances in agrophysical research*, 369-398.

Sharma, P., Gupta, A., & Issar, K. (2017). Effect of packaging and storage on dried apple pomace and fiber extracted from pomace. *Journal of food processing and preservation*, *41*(3), e12913.

Shuvo, I. I. (2020). Fibre attributes and mapping the cultivar influence of different industrial cellulosic crops (cotton, hemp, flax, and canola) on textile properties. *Bioresources and Bioprocessing*, *7*, 1-28.

Sitholé, B., Shirin, S., Zhang, X., Lapierre, L., Pimentel, J., & Paice, M. (2010). DERESINATION OPTIONS IN SULPHITE PULPING. *BioResources*, *5*(1).

Sixta, H., Potthast, A., & Krotschek, A. W. (2006). Chemical pulping processes. *Handbook of pulp*, *1*.

Skinner, R. C., Gigliotti, J. C., Ku, K.-M., & Tou, J. C. (2018). A comprehensive analysis of the composition, health benefits, and safety of apple pomace. *Nutrition reviews*, *76*(12), 893-909.

Stark, N. M., & Berger, M. J. (1997). Effect of particle size on properties of wood-flour reinforced polypropylene composites. Proceedings of the fourth international conference on woodfibre–plastic composites,

Statista. (2024). *Average cost of electricity for industrial consumers in New Zealand from 2013 to 2024 (in New Zealand cents per kilowatt hour)*. https://www.statista.com/statistics/988214/new-zealand-industrial-electricity-costs/

Stevulova, N., Cigasova, J., Purcz, P., Schwarzova, I., Kacik, F., & Geffert, A. (2015). Water absorption behavior of hemp hurds composites. *Materials*, *8*(5), 2243-2257.

Strand, A., Kouko, J., Oksanen, A., Salminen, K., Ketola, A., Retulainen, E., & Sundberg, A. (2019). Enhanced strength, stiffness and elongation potential of paper by spray addition of polysaccharides. *Cellulose*, *26*, 3473-3487.

Tanpichai, S., Witayakran, S., Srimarut, Y., Woraprayote, W., & Malila, Y. (2019). Porosity, density and mechanical properties of the paper of steam exploded bamboo microfibers controlled by nanofibrillated cellulose. *Journal of Materials Research and Technology*, *8*(4), 3612-3622.

The Packaging Forum. (2022a). *PFAS in food packaging*. https://www.packagingforum.org.nz/wp-content/uploads/2022/03/PFAS-IN-FOOD-PACKAGING_FINAL.pdf#:~:text=The%20Stockholm%20Convention%20on%20Persistent%20Organic%20Pollutants,(including%20New%20Zealand)%20have%20agreed%20to%20restrict.

The Packaging Forum. (2022b). *PFAS in food packaging: A Literature Summary*.

Toxic-Free Future. (n.d.). *Retailers committing to phase out PFAS as a class in food packaging and products*. https://toxicfreefuture.org/mind-the-store/retailers-committing-to-phase-out-pfas-as-a-class-in-food-packaging-and-products/#:~:text=Restaurant%20Brands%20International%20(RBI)%20announced%20in%20March,PFAS%20in%20food%20packaging%20globally%20by%202025.

USDA. (2023). *Fresh Deciduous Fruit Annual*. https://apps.fas.usda.gov/newgainapi/api/Report/DownloadReportByFileName?fileName=Fresh%20Deciduous%20Fruit%20Annual_Wellington_New%20Zealand_NZ2023-0018.pdf

Vainio, A., & Paulapuro, H. (2007). Interfiber bonding and fiber segment activation in paper. *BioResources*, *2*(3), 442-458.

Vasile, C., & Baican, M. (2021). Progresses in food packaging, food quality, and safety—controlled-release antioxidant and/or antimicrobial packaging. *Molecules*, *26*(5), 1263.

Versino, F., Ortega, F., Monroy, Y., Rivero, S., López, O. V., & García, M. A. (2023). Sustainable and bio-based food packaging: A review on past and current design innovations. *Foods*, *12*(5), 1057.

Vogel, S. N., Sultan, T. R., & Ten Eyck, R. P. (1981). Cyanide poisoning. *Clinical toxicology*, *18*(3), 367-383.

Vries, B. d. (2024). *Development of a single-use moulded fibre food packaging, made from New Zealand resources*.

Wade, K. (2023). Can a moulded fibre thermoformer help support sustainable packaging innovation? *Appita Magazine*(1), 58-60.

Wang, Y., Chen, X., Liang, Y., & Yu, C. (2021). Fabrication of super-hydrophobic filter paper via mixed wax phase separation for efficient oil/water separatio. *BioResources*, *16*(3), 5794.

WasteMINZ. (2018). *What is known about food waste in New Zealand.* https://lovefoodhatewaste.co.nz/wp-content/uploads/2020/09/What-is-known-about-food-waste-in-New-Zealand.pdf

Wenzel, R. N. (1949). Surface roughness and contact angle. *The Journal of Physical Chemistry*, *53*(9), 1466-1467.

Yadav, M. P., Hicks, K. B., Johnston, D. B., Hotchkiss Jr, A. T., Chau, H. K., & Hanah, K. (2016). Production of bio-based fiber gums from the waste streams resulting from the commercial processing of corn bran and oat hulls. *Food Hydrocolloids*, *53*, 125-133.

Yang, J., Ching, Y. C., & Chuah, C. H. (2019). Applications of lignocellulosic fibers and lignin in bioplastics: A review. *Polymers*, *11*(5), 751.

Yaradoddi, J. S., Banapurmath, N. R., Ganachari, S. V., Soudagar, M. E. M., Sajjan, A. M., Kamat, S., Mujtaba, M., Shettar, A. S., Anqi, A. E., & Safaei, M. R. (2022). Bio-based material from fruit waste of orange peel for industrial applications. *Journal of Materials Research and Technology*, *17*, 3186-3197.

Yue, Z., Sun, L.-L., Sun, S.-N., Cao, X.-F., Wen, J.-L., & Zhu, M.-Q. (2022). Structure of corn bran hemicelluloses isolated with aqueous ethanol solutions and their potential to produce furfural. *Carbohydrate polymers*, *288*, 119420.

Zawawi, N. I. M., Asa'ari, A. Z. M., Abdullah, L. C., Abdullah, H. H., Harun, J., & Jawaid, M. (2013). Water Absorbency and Mechanical Properties of Kenaf Paper Blended via a Disintegration Technique. *BioResources*, *8*(4).

Zdunek, A., Kozioł, A., Pieczywek, P., & Cybulska, J. (2014). Evaluation of the nanostructure of pectin, hemicellulose and cellulose in the cell walls of pears of different texture and firmness. *Food and Bioprocess Technology*, *7*, 3525-3535.

Zhang, R., Ma, S., Li, L., Zhang, M., Tian, S., Wang, D., Liu, K., Liu, H., Zhu, W., & Wang, X. (2021). Comprehensive utilization of corn starch processing by-products: A review. *Grain & Oil Science and Technology*, *4*(3), 89-107.

Zhang, Y., Duan, C., Bokka, S. K., He, Z., & Ni, Y. (2022). Molded fiber and pulp products as green and sustainable alternatives to plastics: A mini review. *Journal of Bioresources and Bioproducts*, *7*(1), 14-25.

Zhuo, Y., He, J., Li, W., Deng, J., & Lin, Q. (2023). A review on takeaway packaging waste: Types, ecological impact, and disposal route. *Environmental Pollution*, 122518.

Appendix

Appendix A Raw data of physical and mechanical properties of the handsheets.

A.1 Weight (in gram) of the standard and hot-pressed handsheets.

Table 34. Weight of the standard and hot-pressed handsheets in this study.

Sheet No.	BCTMP	BCTMP-Hp	50AP	50AP-Hp	25AP	25AP-Hp	50CH	50CH-Hp
1	5.333	4.968	4.951	4.813	4.937	4.882	4.127	4.116
2	5.254	5.016	4.910	4.856	4.881	4.636	4.103	4.172
3	5.282	4.981	4.885	4.827	5.033	4.660	4.007	4.134
4	5.230	4.954	4.977	4.836	4.911	4.661	4.167	4.125
5	5.226	5.088	4.956	4.851	5.093	4.971	4.204	3.920
6	5.232	5.094	4.883	4.811	4.470	4.718	4.198	4.205
7	5.321	5.018	5.005	4.819	4.856	4.666	4.224	4.180
8	5.162	4.981	4.929	4.901	4.907	4.523	4.212	3.857

A.2 Thickness data (in μm) of the standard and hot-pressed handsheets.

Table 35. Thickness of the standard and hot-pressed handsheets in this study.

Sheet No.	BCTMP	BCTMP-Hp	50AP	50AP-Hp	25AP	25AP-Hp	50CH	50CH-Hp
1	1146.5	583.4	487.7	432.7	651.2	580.1	878.8	455.7
2	1056.5	700.4	481.9	466.6	640.7	455.6	898.8	549.3
3	1137.7	627.6	489.6	514.4	643.6	585.1	844.6	502.2
4	1115.0	757.8	495.2	434.7	622.8	445.1	885.5	532.4
5	1026.9	599.5	491.9	409.5	641.2	516.8	885.2	611.5
6	1079.7	638	483.8	414.8	581.0	468.1	917.9	570.4
7	1119.4	701	484.9	427.0	575.8	587.4	898.2	608.6
8	1061.1	654.1	498.8	467.1	625.7	552.7	885.5	579.2

A.3 Tensile properties of the standard and hot-pressed handsheets.

Table 36. Tensile properties of the BCTMP handsheets.

Sheet No.	Tensile Force (N)	Elongation (%)	Tensile Stiffness (kN/m)	TEA (J/m^2)	Tensile Strength (kN/m)
1	27.3	0.76	326.1	10.45	1.823
2	26.0	0.61	327.4	7.85	1.734
3	26.4	0.74	322	8.78	1.761
4	26.3	0.71	353.6	8.31	1.673
5	25.1	0.91	297.9	10.98	1.916
6	28.7	0.78	350	11.34	1.780
7	26.7	0.66	329	8.78	1.729
8	25.9	0.71	313.1	9.38	1.721

Table 37. Tensile properties of the BCTMP-Hp handsheets.

Sheet No.	Tensile Force (N)	Elongation (%)	Tensile Stiffness (kN/m)	TEA (J/m^2)	Tensile Strength (kN/m)
1	55.8	0.74	628.4	15.56	3.720
2	64.7	0.82	709.8	20.86	4.312
3	72	1.01	745.5	30.63	4.797
4	67.2	0.89	727	24.25	4.481
5	73.2	1.09	760.8	34.92	4.877
6	77.7	0.92	843	29.85	5.181
7	66.8	0.95	714.8	26.57	4.454
8	60.1	0.91	650	22.6	4.065

Table 38. Tensile properties of the 50AP handsheets.

Sheet No.	Tensile Force (N)	Elongation (%)	Tensile Stiffness (kN/m)	TEA (J/m^2)	Tensile Strength (kN/m)
1	132.4	1.5	1030	85.97	8.827
2	117.8	1.82	860.7	96.46	7.853
3	127.3	1.85	939.1	106.9	8.487
4	134.8	1.6	1040	94.63	8.987
5	130.7	1.98	956.4	118.4	8.713
6	140.8	1.94	1020	124.5	9.387
7	132	2.03	941.4	122.8	8.800
8	125.5	1.71	947.6	85.74	8.367

Table 39. Tensile properties of the 50AP-Hp handsheets.

Sheet No.	Tensile Force (N)	Elongation (%)	Tensile Stiffness (kN/m)	TEA (J/m^2)	Tensile Strength (kN/m)
1	168.8	1.35	1270	93.33	11.253
2	161.7	1.14	1289	72.61	10.78
3	162.4	1.41	1167	94.61	10.827
4	163	1.23	1243	80.26	10.867
5	166.9	1.16	1284	75.29	11.127
6	165.8	1.11	1336	72.25	11.053
7	170.7	1.31	1266	90.8	11.38
8	148	1.06	1233	61.14	9.867

Table 40. Tensile properties of the 25AP handsheets.

Sheet No.	Tensile Force (N)	Elongation (%)	Tensile Stiffness (kN/m)	TEA (J/m^2)	Tensile Strength (kN/m)
1	78.4	2.04	613.6	74.64	5.225
2	86.9	2.04	684.7	83.06	5.795
3	81.1	1.64	687.9	60.19	5.405
4	84.6	1.47	747.8	55.01	5.624
5	79.5	1.46	698.5	51.59	5.298
6	71.4	1.52	628.3	49.07	4.759
7	79.3	1.00	781.3	32.15	5.284
8	85.5	1.72	702.2	67.02	5.699

Table 41. Tensile properties of the 25AP-Hp handsheets.

Sheet No.	Tensile Force (N)	Elongation (%)	Tensile Stiffness (kN/m)	TEA (J/m^2)	Tensile Strength (kN/m)
1	106.60	1.26	895.7	56.39	7.107
2	127.00	1.26	1044.0	67.19	8.467
3	93.90	0.94	901.0	34.59	6.600
4	124.70	1.10	1072.0	55	8.313
5	100.90	1.09	910.2	45.16	8.727
6	106.50	1.35	880.5	60.59	7.100
7	99.70	1.32	840.0	56.46	6.647
8	96.87	1.42	788.9	59.42	6.458

Table 42. Tensile properties of the 50CH handsheets.

Sheet No.	Tensile Force (N)	Elongation (%)	Tensile Stiffness (kN/m)	TEA (J/m^2)	Tensile Strength (kN/m)
1	21.55	0.97	236.5	8.87	1.437
2	21.73	0.93	253.8	8.57	1.449
3	24.04	1.08	246.5	11.36	1.603
4	21.63	0.96	212.7	8.92	1.600
5	22.30	1.03	241.2	9.89	1.486
6	22.00	0.90	254.2	8.34	1.469
7	21.20	0.83	261.8	7.37	1.414
8	21.60	0.90	241.2	8.10	1.438

Table 43. Tensile properties of the 50CH-Hp handsheets.

Sheet No.	Tensile Force (N)	Elongation (%)	Tensile Stiffness (kN/m)	TEA (J/m^2)	Tensile Strength (kN/m)
1	35.70	0.69	434.2	9.44	2.379
2	38.10	1	373.1	15.53	2.541
3	35.80	0.81	394.5	11.6	2.384
4	37.40	0.83	422.5	12.44	2.494
5	26.30	0.67	330.9	6.88	1.752
6	26.00	0.67	321.1	6.6	1.735
7	29.93	0.8	323.4	9.24	1.995
8	29.05	0.81	323.4	9.31	1.937

A.4 SCT strength of standard and hot-pressed handsheets.

Table 44. SCT strength of the standard- and hot-pressed handsheets.

BCTMP							
2081	2144	2203	2125	2227	2071	2134	2061
2295	2071	2286	2232	2183	2217	2256	2279
BCTMP-Hp							
3478	3551	3932	4303	4308	4386	3734	4025
3654	3624	4484	3996	4000	4670	3901	4165
50AP							
5504	5519	5602	5221	5729	5807	5784	5502
5524	5597	5299	5192	5656	5983	5834	5632
50AP-Hp							
8203	8124	8098	8165	8098	8076	8096	8034
8398	8256	8104	8324	8108	8133	8136	8235

25AP							
3909	3939	3860	3992	4183	3768	3753	3939
4075	4063	4163	4232	4295	3997	3821	3699
25AP-Hp							
5792	5768	5661	4962	5245	4879	5060	4991
5455	6012	5563	5150	5284	5250	4894	4762
50CH							
1729	1861	1924	1851	1846	2095	1993	1863
1582	1753	1924	1885	2071	1748	2034	1942
50CH-Hp							
2623	3609	2491	2764	2823	2505	3170	2755
2300	2369	3038	2540	3189	3751	3565	2761

A.5 Tearing strength and bursting strength of standard and hot-pressed handsheets.

Table 45. Tearing strength (in mN) of the standard and hot-pressed handsheets.

Sheet No.	BCTMP	BCTMP-Hp	50AP	50AP-Hp	25AP	25AP-Hp	50CH	50CH-Hp
1	725	759	1365	1027	1259	1141	599	718
2	665	699	1365	1037	1225	930	582	760
3	767	826	1172	1054	1250	1023	582	607
4	682	725	1482	852	1242	972	726	853
5	682	860	1373	767	1267	1098	539	726
6	699	860	1121	911	1284	1014	692	718
7	725	725	1163	885	1284	1039	650	590
8	657	725	1205	911	1217	997	794	573

Table 46. Bursting strength (in kN) of the standard and hot-pressed handsheets.

Sheet No.	BCTMP	BCTMP-Hp	50AP	50AP-Hp	25AP	25AP-Hp	50CH	50CH-Hp
1	66	167	376	381	241	347	70	115
2	71	175	382	431	298	313	68	98
3	66	192	393	370	291	387	80	110
4	64	157	385	446	259	392	78	93
5	81	189	389	452	291	385	74	98
6	71	186	391	431	236	307	68	97
7	77	159	394	397	278	375	68	87
8	79	217	371	368	250	367	64	92

Appendix B Barrier properties of standard and hot-pressed handsheets

B.1 Gurley seconds of the standard and hot-pressed handsheets.

Table 47. Gurley seconds (sec/25 mL air) of the standard and hot-pressed handsheets.

Sheet No.	BCTMP	BCTMP-Hp	50AP	50AP-Hp	25AP	25AP-Hp	50CH	50CH-Hp
1	0.2	0.7	326.8	370.4	24.2	59.6	2.3	3.2
2	0.2	0.5	346.5	373.6	25.2	63.8	2.4	3.0
3	0.1	0.7	334.1	369.8	24.7	68.2	2.5	3.3
4	0.1	0.3	313.3	422.0	20.7	65.9	2.0	3.7
5	0.2	0.6	363.7	844.6	23.7	48.0	2.2	3.0
6	0.1	0.5	376.6	445.2	21.7	63.6	2.4	3.5
7	0.1	0.5	338.9	408.4	25.5	58.5	1.9	3.1
8	0.2	0.3	347.0	591.8	25.4	63.8	2.1	3.1

B.2 Cobb values of the of the standard and hot-pressed handsheets.

Table 48. Initial, final weights and Cobb values of the standard and hot-pressed BCTMP handsheets.

Sheet No.	BCTMP			BCTMP-Hp		
	Initial weight (g)	Final weight (g)	Cobb value (g/m^2)	Initial weight (g)	Final weight (g)	Cobb value (g/m^2)
1	2.5346	4.4296	743.14	2.4178	3.7419	519.25
2	2.6235	4.5152	741.84	2.4352	3.7446	513.49
3	2.5779	4.5366	768.12	2.4601	3.8536	546.47
4	2.6084	4.4856	736.16	2.5096	3.8695	533.29
5	2.6428	4.7418	823.14	2.481	3.8323	529.92
6	2.5893	4.5786	780.12	2.4885	3.8756	543.96
7	2.5657	4.7437	854.12	2.4588	3.8859	559.65
8	2.596	4.4792	738.51	2.4684	3.8173	528.98

Table 49. Initial, final weights and Cobb values of the standard and hot-pressed 50% AP handsheets.

Sheet No.	50AP			50AP-Hp		
	Initial weight (g)	Final weight (g)	Cobb value (g/m^2)	Initial weight (g)	Final weight (g)	Cobb value (g/m^2)
1	2.4493	3.4648	398.24	2.4221	3.0554	248.35
2	2.5307	3.5276	390.94	2.4726	3.0776	237.25
3	2.6132	3.765	451.69	2.3471	3.0326	268.82
4	2.4665	3.492	402.16	2.417	3.0988	267.37
5	2.4516	3.4856	405.49	2.375	3.0444	262.51
6	2.498	3.4852	387.14	2.4218	3.0917	262.71
7	2.4791	3.3398	337.53	2.4477	3.0917	252.55
8	2.4635	3.552	426.86	2.4074	3.0761	262.24

Table 50. Initial, final weights and Cobb values of the standard and hot-pressed 25% AP handsheets.

Sheet No.	25AP			25AP-Hp		
	Initial weight (g)	Final weight (g)	Cobb value (g/m^2)	Initial weight (g)	Final weight (g)	Cobb value (g/m^2)
1	2.1927	3.561	536.59	2.3218	3.3319	396.12
2	2.3718	3.6833	514.31	2.0853	3.0298	370.39
3	2.3303	3.7648	562.55	2.2456	3.2421	390.78
4	2.4995	3.8173	516.78	2.2301	3.2834	413.06
5	2.402	3.7653	534.63	2.2895	3.3645	421.57
6	2.4136	3.6673	491.65	2.3224	3.2487	363.25
7	2.4981	3.9121	554.51	2.2282	3.1846	375.06
8	2.6911	4.0878	547.73	2.3571	3.4107	413.18

Table 51. Initial, final weights and Cobb values of the standard and hot-pressed 50% CH handsheets.

Sheet No.	50CH			50CH-Hp		
	Initial weight (g)	Final weight (g)	Cobb value (g/m^2)	Initial weight (g)	Final weight (g)	Cobb value (g/m^2)
1	2.0052	3.4381	561.92	1.938	3.016	422.59
2	2.0864	3.4484	534.12	1.990	3.056	418.20
3	2.024	3.5103	582.86	2.012	3.100	426.82

4	2.0054	3.3438	524.86	1.510	2.363	334.63
5	2.0896	3.5151	559.02	1.868	3.084	477.06
6	2.1904	3.6208	560.94	1.966	3.034	418.78
7	2.0693	3.4756	551.49	2.042	2.991	372.27
8	2.0489	3.3534	511.57	1.972	2.963	388.63

B.3 Grease resistance of standard and hot-pressed handsheets.

Table 52. Grease resistance of standard and hot-pressed handsheets, including show-through time (in minutes), and breakthrough area (in cm^2).

Sheet No.	BCTMP	BCTMP-Hp	50AP	50AP-Hp	25AP	25AP-Hp	50CH	50CH-Hp
1	50	65	330	>360	65	85	20	30
2	50	65	330	>360	65	85	20	30
a =	4.5	4.3	3.0	2.0	4.4	4.2	6.2	5.1
b =	5.0	4.9	2.5	2.8	4.1	3.8	6.0	5.5
Area	17.67	16.55	5.89	4.40	14.17	12.53	29.21	22.03
a =	4.7	4.2	3.2	2.6	4.8	4.2	6.5	4.8
b =	4.8	4.7	2.5	1.9	4.5	4.1	6.4	5.2
Area	17.72	15.50	6.28	3.88	16.96	13.52	32.67	19.60

B.4 Contact angle and roughness of the standard and hot-pressed handsheets.

Table 53. Contact angle of the of the standard and hot-pressed handsheets.

Sheet No.	BCTMP	BCTMP-Hp	50AP	50AP-Hp	25AP	25AP-Hp	50CH	50CH-Hp
1	Instant absorption	78.85	54.9	87.15	Instant absorption	80.75	92.36	86.82
2		79.12	52.62	86.22		83.1	94.55	105.1
3		80.12	56.8	82.64		80.54	89.35	108.37

Table 54. Roughness of the of the standard and hot-pressed handsheets.

Roughness data: Ra and Rz values						
BCTMP	Ra	14	16	13	13	13
	Rz	167	202	152	168	160
BCTMP - Hp	Ra	8	8	8	8	8
	Rz	99	109	106	107	90
25AP	Ra	8	9	8	10	8

	Rz	95	102	99	146	110
25AP - Hp	Ra	7	7	8	9	7
	Rz	94	95	109	134	102
50AP	Ra	12	11	13	10	11
	Rz	129	108	139	117	153
50AP - Hp	Ra	9	9	9	8	9
	Rz	99	102	102	91	106
50CH	Ra	16	18	16	18	16
	Rz	238	245	202	227	229
50CH - Hp	Ra	10	10	13	10	11
	Rz	130	143	193	141	144

Appendix C Physical, mechanical and barrier properties of standard handsheets for preliminary formulation screening.

C.1. Weight, thickness, density and grammage of the handsheets made for formulation screening.

Table 55. Weights (g) of the handsheets made for formulation screening.

Sheet No.	BCTMP	BCTMP + 10F	20AP	20AP + 10F	35 AP	35AP + 15F	50AP	50AP + 20F
1	4.1505	3.8333	3.9181	3.8836	3.975	3.7263	3.8781	3.7085
2	3.8622	3.8335	3.9329	3.8196	3.9883	3.7184	3.8976	3.698
3	4.0764	4.0086	3.9238	3.8712	3.9704	3.7547	3.8601	3.6786
4	3.9322	3.8797	3.8543	3.8636	4.0052	3.7528	3.8136	3.6396
5	3.8894	3.9570	3.8743	3.7916	3.9465	3.7998	3.8478	3.6962
6	4.0060	3.8647	3.9	3.8412	3.9279	3.7634	3.8582	3.6368
7	3.8226	3.9336	3.8692	3.8551	3.994	3.7556	3.864	3.7065
8	3.9340	4.1432	3.8931	3.8334	3.9308	3.7596	3.8195	3.7037

Table 56. Thickness (mm) of the handsheets made for formulation screening.

Sheet No.	BCTMP	BCTMP + 10F	20AP	20AP + 10F	35 AP	35AP + 15F	50AP	50AP + 20F
1	0.74	0.66	0.65	0.6	0.58	0.5	0.51	0.45
2	0.72	0.73	0.68	0.66	0.52	0.54	0.51	0.44
3	0.75	0.7	0.66	0.67	0.55	0.53	0.52	0.48
4	0.74	0.73	0.65	0.65	0.58	0.55	0.48	0.5
5	0.75	0.68	0.66	0.63	0.54	0.53	0.53	0.42
6	0.73	0.69	0.62	0.65	0.62	0.48	0.52	0.52
7	0.72	0.74	0.64	0.62	0.6	0.52	0.5	0.42
8	0.76	0.71	0.68	0.65	0.54	0.53	0.5	0.43
9	0.79	0.68	0.66	0.64	0.56	0.47	0.51	0.47
10	0.71	0.69	0.65	0.65	0.53	0.5	0.52	0.43

Table 57. Density (kg/m^3) of the handsheets made for formulation screening.

Sheet No.	BCTMP	BCTMP + 10F	20AP	20AP + 10F	35 AP	35AP + 15F	50AP	50AP + 20F
1	316.99	309.47	338.53	342.34	400.28	409.48	426.67	460.25
2	294.97	309.49	339.81	336.70	401.62	408.61	428.82	458.95
3	311.33	323.62	339.02	341.25	399.82	412.60	424.69	456.54
4	300.32	313.22	333.02	340.58	403.32	412.39	419.58	451.70
5	297.05	319.46	334.75	334.23	397.41	417.56	423.34	458.73
6	305.95	312.00	338.31	338.61	395.54	413.56	424.48	451.35
7	291.95	317.57	334.31	339.83	402.19	412.70	425.12	460.01
8	300.46	334.49	336.37	337.92	395.83	413.14	420.23	459.66

Table 58. Grammage (g/m^2) of the handsheets made for formulation screening.

Sheet No.	BCTMP	BCTMP + 10F	20AP	20AP + 10F	35 AP	35AP + 15F	50AP	50AP + 20F
1	234.89	216.94	221.74	219.78	224.96	210.88	219.47	209.88
2	218.57	216.95	222.57	216.16	225.71	210.44	220.58	209.28
3	230.70	226.86	222.06	219.08	224.70	212.49	218.46	208.18
4	222.54	219.56	218.13	218.65	226.67	212.38	215.82	205.98
5	220.11	223.94	219.26	214.58	223.34	215.04	217.76	209.18
6	226.71	218.72	221.59	217.39	222.29	212.98	218.35	205.82
7	216.33	222.61	218.97	218.17	226.03	212.54	218.68	209.76
8	222.64	234.48	220.32	216.94	222.46	212.77	216.16	209.60

C.2 Tensile force (force at break) in N of the standard handsheets made for formulation screening.

Table 59. Tensile force of the standard handsheets made for formulation screening.

Sheet No.	BCTMP	BCTMP + 10F	20AP	20AP + 10F	35 AP	35AP + 15F	50AP	50AP + 20F
1	22.4	16.3	66.6	54.3	77.5	64.0	101.0	95.7
2	23.6	15.4	62.9	51.0	92.4	66.1	102.6	82.6
3	22.3	16.2	66.5	53.8	95.9	76.3	104.0	99.3
4	18.4	17.2	65.3	55.1	95.3	70.0	104.0	86.4
5	20.5	13.3	61.4	55.6	84.3	67.2	101.2	92.5
6	18.9	18.7	67.2	56.6	89.4	71.1	95.6	93.5
7	19.3	15.3	59.0	52.8	76.0	70.2	91.1	88.6
8	20.6	16.9	62.3	55.0	82.2	66.9	107.2	94.5

C.3 Cobb values of the standard handsheets made for formulation screening.

Table 60. Initial, final weights and Cobb values of the standard BCTMP handsheets BCTMP with 10% fillers.

Sheet No.	BCTMP			BCTMP + 10F		
	Initial weight (g)	Final weight (g)	Cobb value (g/m^2)	Initial weight (g)	Final weight (g)	Cobb value (g/m^2)
1	3.8346	12.3737	853.91	3.8510	11.1634	731.24
2	3.8439	12.5632	871.93	3.8515	11.1929	734.14
3	3.8592	12.6912	883.2	3.7293	11.0045	727.52
4	3.8680	12.8534	898.54	3.8429	11.1361	729.32
5	3.8518	12.6342	878.24	3.8537	11.2208	736.71

Table 61. Initial, final weights and Cobb values of the standard 20% AP handsheets 20% AP with 10% fillers.

Sheet No.	20AP			20AP + 10F		
	Initial weight (g)	Final weight (g)	Cobb value (g/m^2)	Initial weight (g)	Final weight (g)	Cobb value (g/m^2)
1	3.7845	10.1664	638.19	3.8079	9.4154	560.75
2	3.8784	10.0596	618.12	3.8225	9.2778	545.53
3	3.9640	10.3586	639.46	3.8523	9.4330	558.07
4	3.8946	10.2857	639.11	3.8756	9.3364	546.08
5	3.8856	10.1637	627.81	3.8645	9.0863	522.18

Table 62. Initial, final weights and Cobb values of the standard 35% AP handsheets 35%AP with 15% fillers.

Sheet No.	35AP			35AP + 15F		
	Initial weight (g)	Final weight (g)	Cobb value (g/m^2)	Initial weight (g)	Final weight (g)	Cobb value (g/m^2)
1	4.0015	8.9773	497.58	3.8595	8.2216	436.21
2	4.0322	9.0831	505.09	3.8382	8.1758	433.76
3	3.9212	9.3352	541.4	3.7731	7.7996	402.65
4	3.9642	9.2213	525.71	3.8942	8.2524	435.82
5	3.9523	9.2146	526.23	3.8582	8.1946	433.64

Table 63. Initial, final weights and Cobb values of the standard 50% AP handsheets 50%AP with 20% fillers.

Sheet No.	50AP			50AP + 20F		
	Initial weight (g)	Final weight (g)	Cobb value (g/m^2)	Initial weight (g)	Final weight (g)	Cobb value (g/m^2)
1	3.7071	7.2113	350.42	3.5358	6.7986	326.28
2	3.8064	7.3701	356.37	3.5642	6.9367	337.25
3	3.7838	6.9903	320.65	3.5276	6.5435	301.59
4	3.7627	7.0223	325.96	3.5134	6.5248	301.14
5	3.7469	7.2811	353.42	3.5378	6.8279	329.01

C.4 Oil penetration time (in min) of the standard handsheets made for formulation screening.

Table 64. Oil penetration time of the standard handsheets made for formulation screening.

Sheet No.	BCTMP	BCTMP + 10F	20AP	20AP + 10F	35 AP	35AP + 15F	50AP	50AP + 20F
1	0.3336	0.3336	10	45	180	240	300	330
2	0.3336	0.3498	11	46.02	180	240	300	330
3	0.3336	0.3498	10	48	180	240	300	330
4	0.3336	0.3336	12	48	180	240	300	330

Appendix D The Fibre quality analysis (FQA) of apple pomace

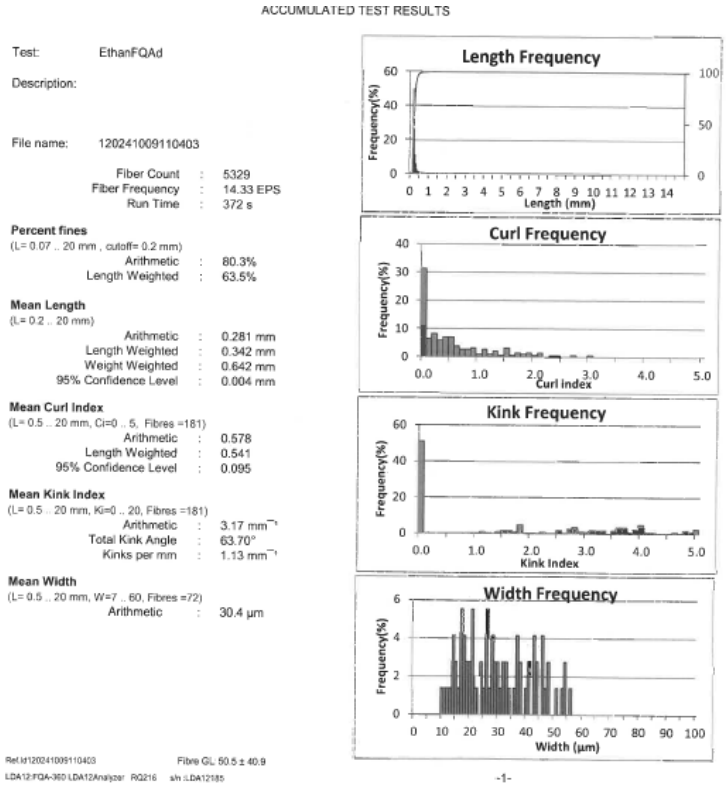

Figure 83. FQA of apple pomace 1

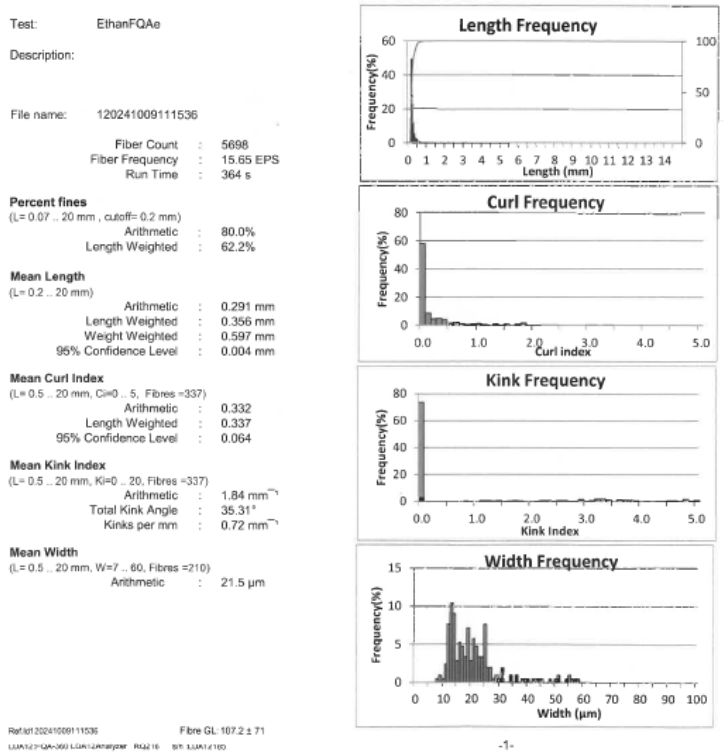

Figure 84. FQA of apple pomace 2.

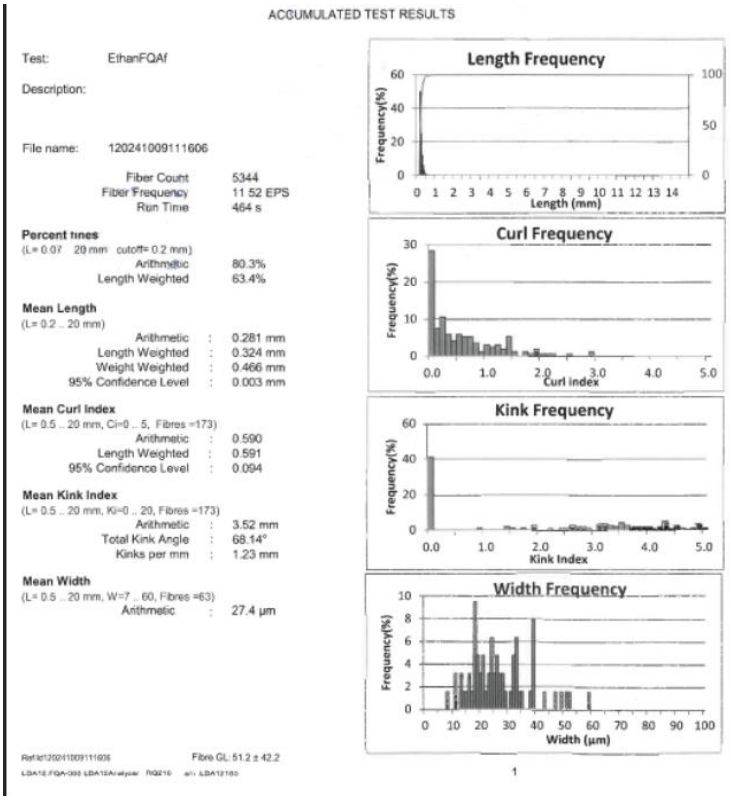

Figure 85. FQA of apple pomace 3.

Appendix E B-scan and surface images of standard and hot-pressed handsheets generated by OCT.

Table 65. B-scan and surface images of the standard and hot-pressed handsheets taken by OCT at 10x magnification.

Formulation	B-scam image	Surface image
BCTMP	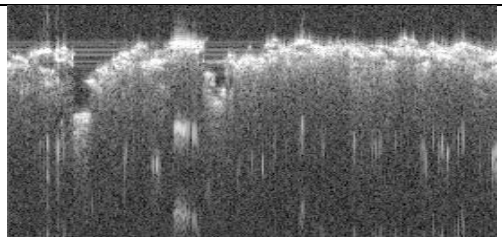 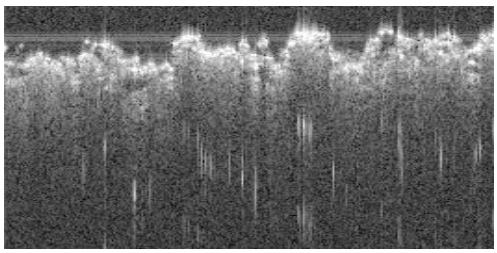	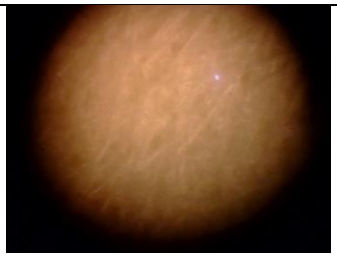 

	 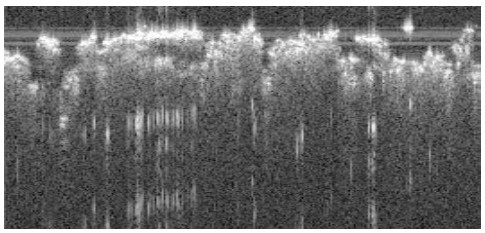	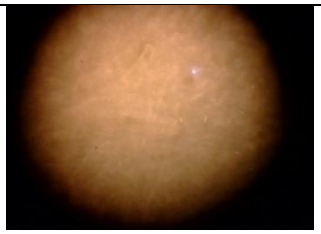 
BCTMP -Hp	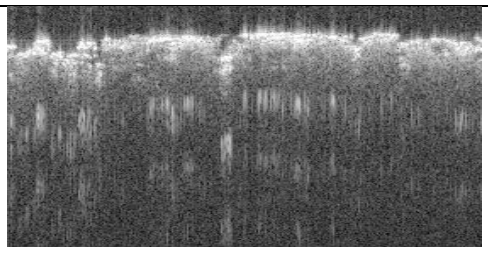 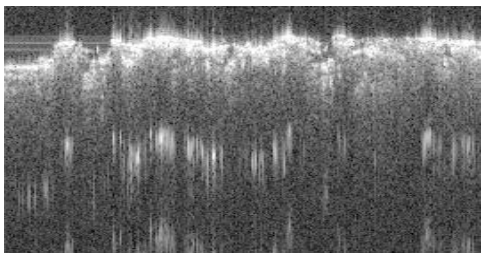	 
	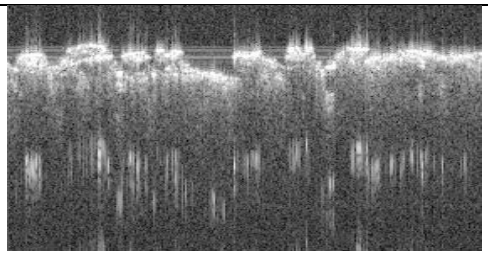 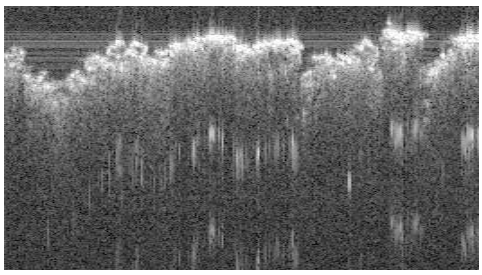	 

25AP	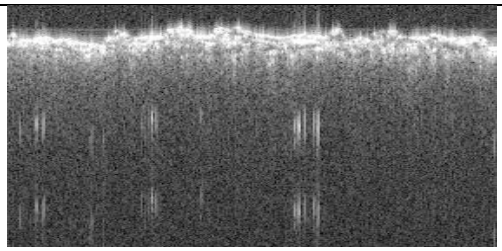 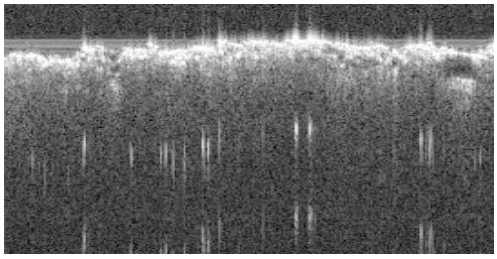	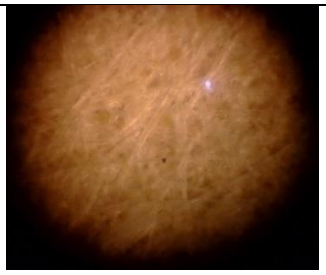 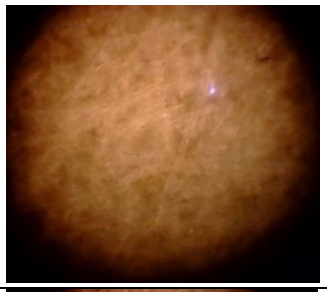
	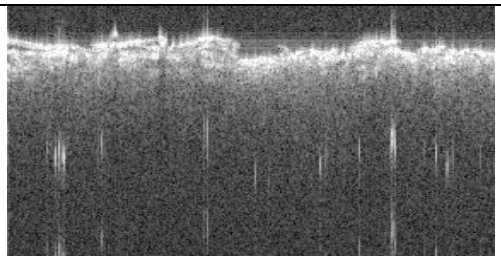 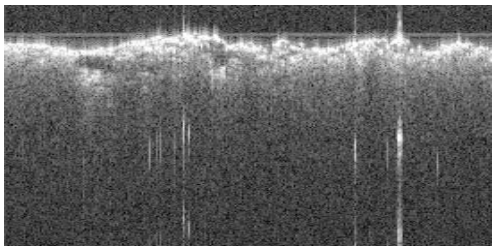	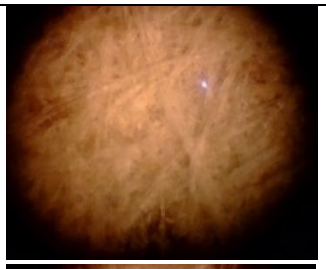 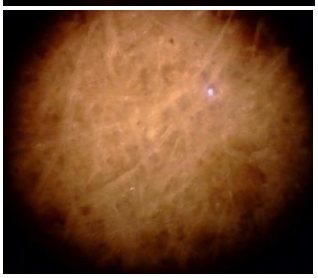
25AP -Hp	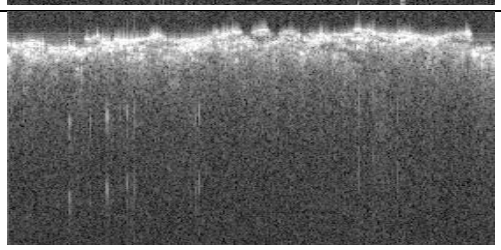 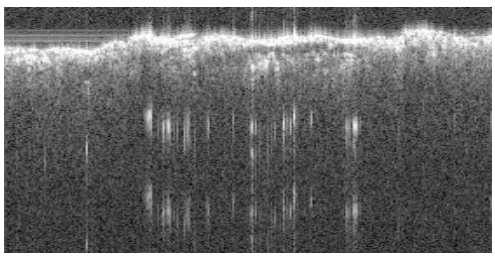	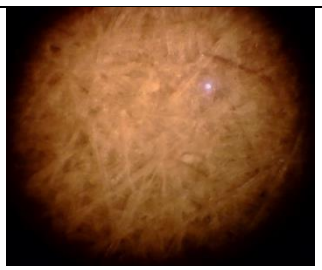 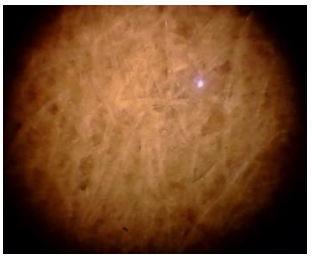

	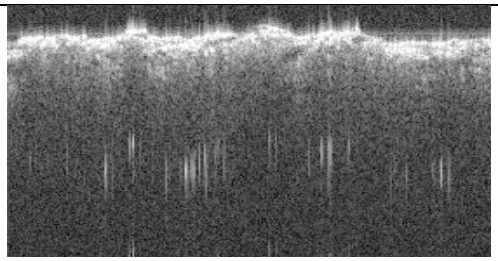 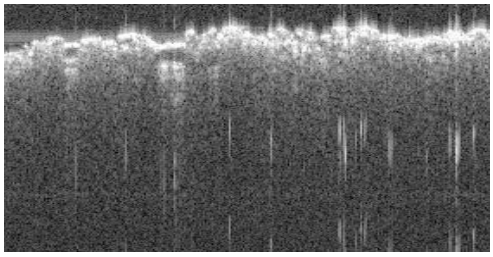	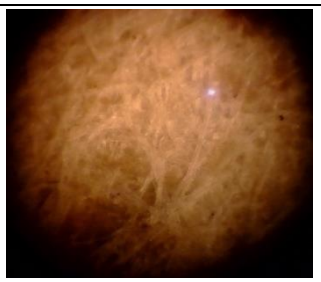 
50AP	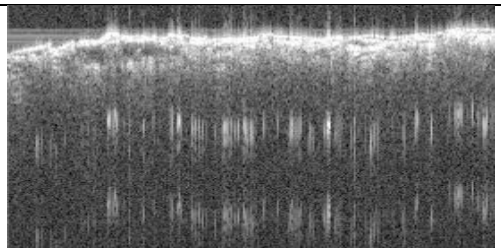 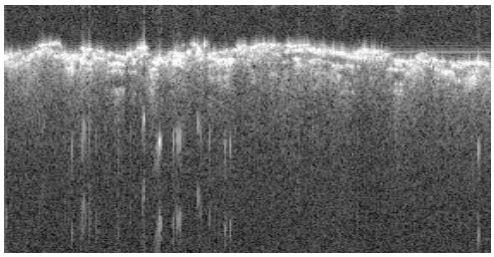	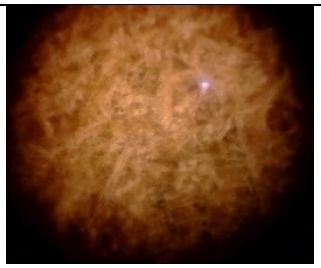 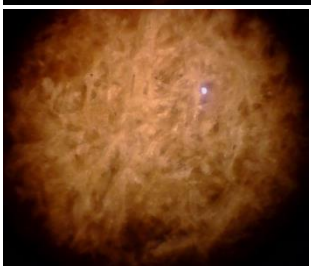
	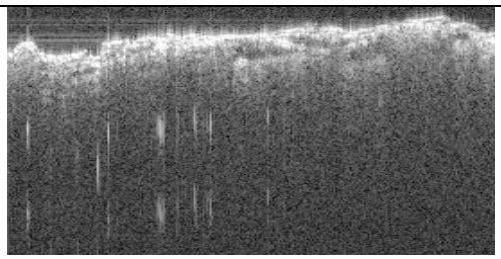 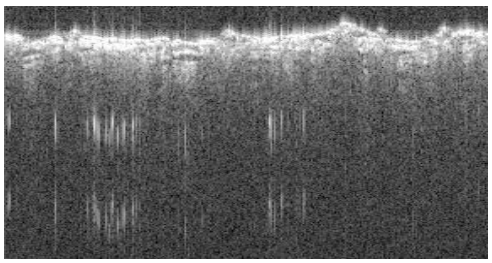	 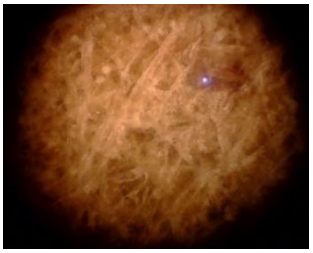

50AP -Hp	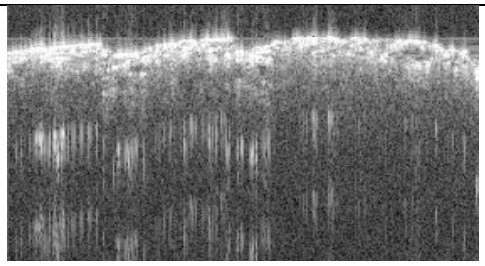 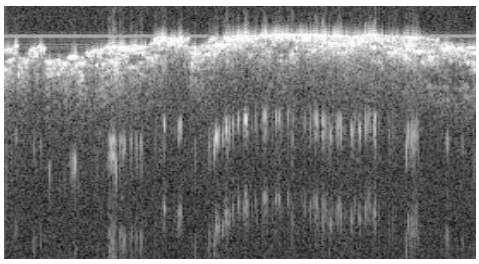	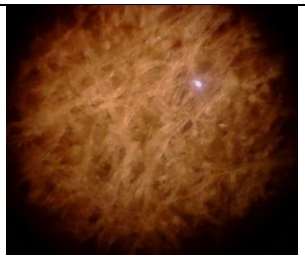 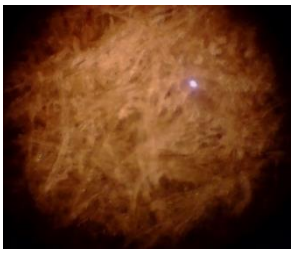
	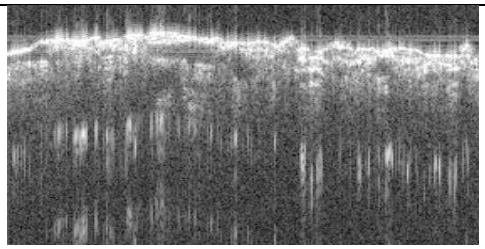 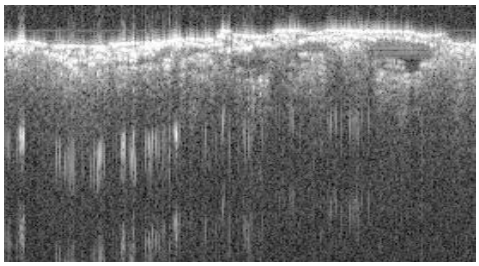	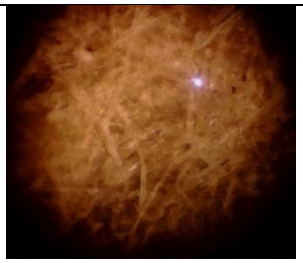 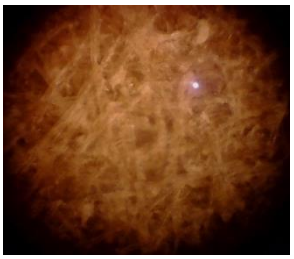
50CH	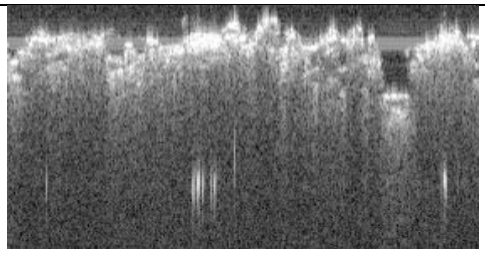 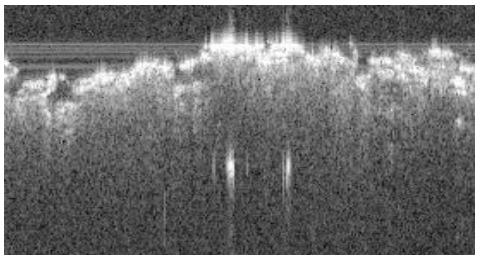	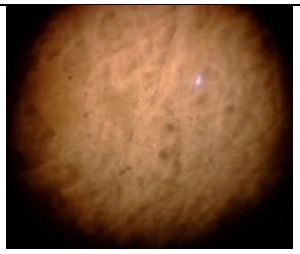 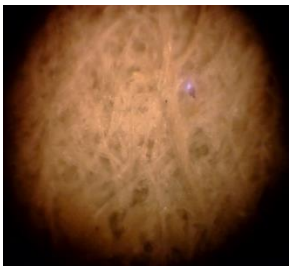

	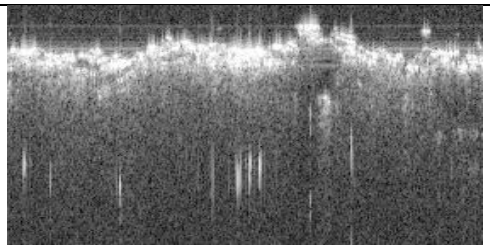 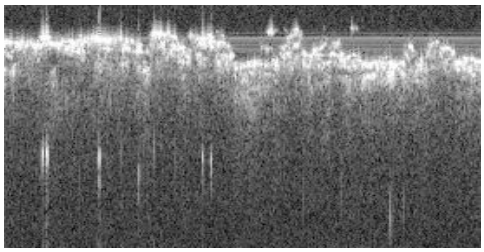	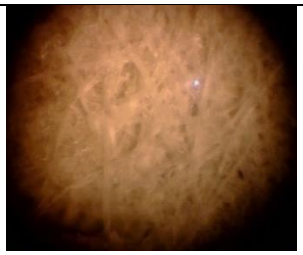 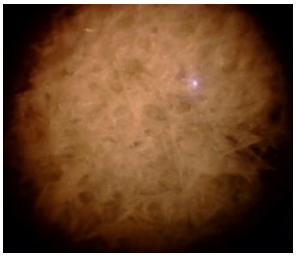
50CH -Hp	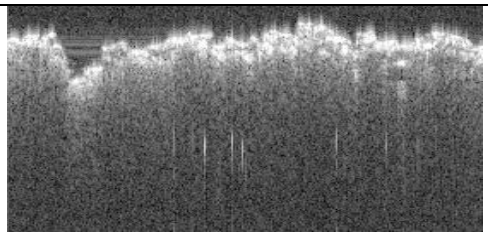 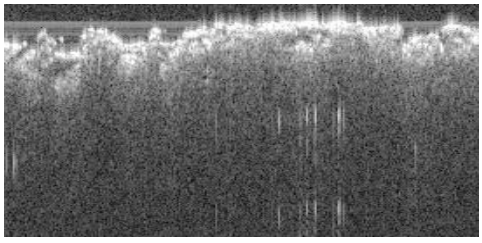	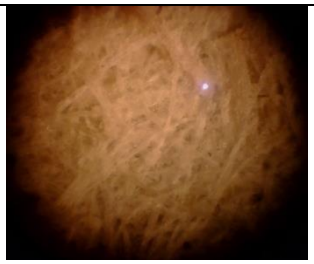 
	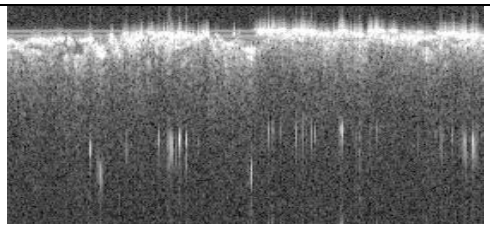 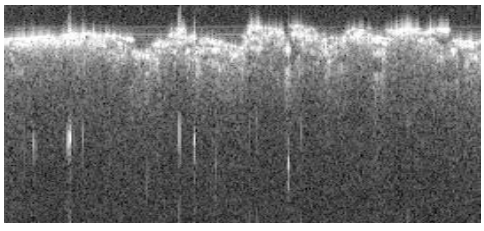	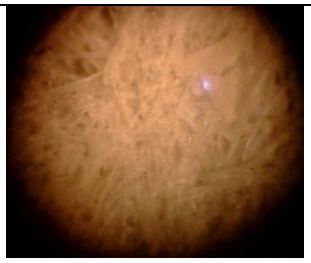 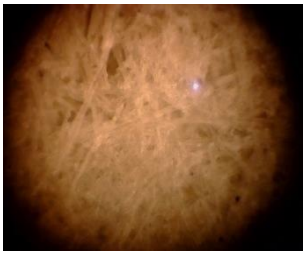

Appendix F Mechanical data of apple pomace/corn husk moulded fibre trays

Table 66. Tensile force of 25AP moulded fibre trays in widthwise dimension.

	Thickness (mm)	Grammage (g/m^2)	Density (kg/m^3)	Maximum Force (N)	Tensile displacement at Maximum Force (mm)
1	0.417	211.40	507.35	180.68	1.14
2	0.377	199.27	529.03	137.66	0.73
3	0.430	200.47	466.21	155.61	0.86
4	0.447	205.20	459.40	164.36	0.98
5	0.410	200.26	488.45	135.85	0.94
6	0.413	199.15	481.80	147.45	1.04
7	0.363	194.58	535.54	140.73	0.83
8	0.373	191.24	512.24	152.33	0.93
9	0.393	195.99	498.27	158.68	0.96
10	0.490	197.71	403.49	138.01	0.79
11	0.413	196.55	475.53	151.82	0.98
12	0.430	196.73	457.51	141.94	0.98

Table 67. Tensile force of 25AP moulded fibre trays in lengthwise dimension.

	Thickness (mm)	Grammage (g/m^2)	Density (kg/m^3)	Maximum Force (N)	Tensile displacement at Maximum Force (mm)
1	0.417	202.38	485.72	113.16	1.27
2	0.397	202.91	511.53	113.74	1.32
3	0.400	198.75	496.89	112.81	1.45
4	0.397	195.15	491.97	103.39	1.32
5	0.400	200.98	502.45	97.78	1.16
6	0.397	206.90	521.59	121.08	1.44
7	0.400	198.31	495.78	115.9	1.38
8	0.420	196.47	467.78	111.89	1.35
9	0.403	209.35	519.06	109.69	1.14
10	0.453	220.04	485.38	143.32	1.56

Table 68. Tensile force of 50CH moulded fibre trays in widthwise dimension.

	Thickness (mm)	Grammage (g/m^2)	Density (kg/m^3)	Maximum Force (N)	Tensile displacement at Maximum Force (mm)
1	0.937	324.65	346.60	51.32	0.51
2	0.873	328.59	376.25	60.77	0.6

3	0.810	346.52	427.80	36.33	0.25
4	0.777	328.50	422.96	74.07	0.65
5	0.703	339.92	483.30	73.62	0.51
6	1.050	329.05	313.38	42.58	0.43
7	0.950	321.52	338.44	41.84	0.53
8	0.890	328.06	368.61	51.08	0.59
9	0.880	369.27	419.62	79.1	0.63
10	0.840	370.23	440.75	79.95	0.59
11	0.737	345.46	468.96	74.83	0.56
12	1.077	346.94	322.23	58.43	0.37

Table 69. Tensile force of 50CH moulded fibre trays in lengthwise dimension.

	Thickness (mm)	Grammage (g/m^2)	Density (kg/m^3)	Maximum Force (N)	Tensile displacement at Maximum Force (mm)
1	0.830	345.56	416.34	44.19	0.71
2	0.833	333.96	400.75	44.17	0.64
3	0.860	298.12	346.65	50.65	0.78
4	0.827	300.11	363.03	57.11	0.85
5	0.843	298.74	354.24	56.6	0.79
6	0.830	312.99	377.09	54.36	0.77
7	0.833	320.98	385.18	49.93	0.67
8	0.857	336.51	392.81	41.31	0.68
9	0.840	345.22	410.97	42.06	0.72
10	0.860	329.23	382.82	42.41	0.66